University of Kerbala

College of Science

Department of Chemistry

Preparation of Iraqi Clay- Biomaterials as an Efficient Adsorbent for Some Toxic Metal Ions from Aqueous Solution

A Thesis

Submitted to the Council of the College of Science, University of Kerbala in Partial Fulfillment of the Requirements for the Degree of Master of Science in Chemistry

By

Rihab Hatem Brej AL – Shammary

B.Sc. Chemistry (Thi-Qar University)

(2004)

Supervised by

Asst. prof.
Dr. Ihsan Mahdi Shaheed
2025 A.D

Prof.
Dr. Eman Talib Kareem
1447 AH

بسم الله الرحمــن الرحيــم

الَّذِي أَحْسَنَ كُلَّ شَيْءٍ خَلَقَهُ ۖ وَبَدَأَ خَلْقَ الْإِنسَانِ مِن طِينٍ

صدق الله العلي العظيم

سورة السجدة

الاية 7

الاهــداء

الى.....

من خط للوفاء قيما سيدي أبي الفضل العباس عليه السلام

من كانت للاباء عنوانا مولاتي زينب عليها السلام

بلسم الروح ونبع الحنان الدافئ والدي والدتي ...

اخوتي .. عرفانا واحتراما

Acknowledgement

First and foremost, I sincerely thank Allah Almighty for granting me strength, patience, and guidance throughout this journey.I also extend my heartfelt gratitude and blessings to His noble Messenger, Prophet Muhammad (peace be upon him and his family), and to the pure Ahlulbayt (peace be upon them), whose light and inspiration have guided my path.

I would like to express my deep thanks, gratefulness and appreciation to my supervisors Asst. prof. Dr. Ihsan M. Shaheed and prof. Dr. Eman.T.Kareem for them suggestion of the project, supervision, support, guidance and assistance throughout the work of this study.

Also, I wish to express my thanks to the dean of the college of science, the Head of the chemistry department, and to all chemistry staff members for all the assistance they offered. I am particularly grateful to my colleagues in the chemistry department. I would like to extend my sincere thanks and deep appreciation to Dr. Abbas H. Mohammed, Asst. Prof. Bassam Ashour, and Asst. Prof. Zuheir Ali from the Marine Science Center, University of Basrah, for their valuable assistance, guidance, and continuous support, which greatly contributed to the successful completion of my thesis.

Many thanks to my family who sustained and encouraged me throughout the work.

Certificate

We certify that this thesis, ***Preparation of Iraqi Clay- Biomaterials as an Efficient Adsorbent for Some Toxic Metal Ions from Aqueous Solution*** by **Rihab Hatem Brej** my Supervision at the Chemistry Department, College of Science , University of Kerbala as a partial requirements for the Master degree of science in Chemistry.

Signature

Name: Dr.Ihsan Mahdi Shaheed

Title: Assistant Professor

Address: University of Kerbala

College of Science

Department of Chemistry

Date:

Signature:

Name: Dr. Eman Talib Kareem

Title: Professor

Address: University of Kerbala

College of Science

Department of Chemistry

Date:

Deport of the Head of the Chemistry Department

According to the recommendation presented by the Chairman of the Postgraduate MSC Studies Committee, forward this" **Preparation of Iraqi Clay- Biomaterials as an Efficient Adsorbent for Some Toxic Metal Ions from Aqueous Solution.**

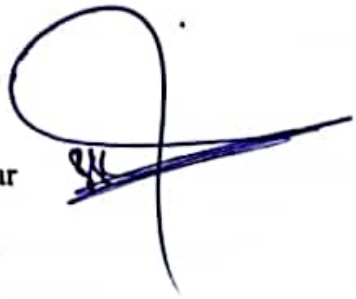

Name: Dr. Sajid Hassan Guzar

Title: Professor

The Head of Department of Chemistry

College of Science

Date:

Examination Committee Certification

We certify that we have read this entitled " **Preparation of Iraqi Clay-Biomaterials as an Efficient Adsorbent for Some Toxic Metal Ions from Aqueous Solution** " as the examining committee, examined the student" Rihab Hatem Brej " on its contents and that in our opinion, its adequate for the Degree of Master in science of Chemistry.

Signature:
Name: Dr. Sajid Hassan Guzar
Title: Professor
Address: University of Kerbala, College of Science, Department of Chemistry
Date: / /2025
(Chairman)

Signature:
Name: Dr. Sundus Hadi Merza
Title: Assist. Professor
Address: Baghdad University, Education for Pure Science Ibn -AL- Haitham
Date: / /2025
(Member)

Signature:
Name: Shaymaa Ibrahim Saeed
Title: Professor
Address: University of Kerbala, College of Science, Department of Chemistry
Date: ٩/ ٩/2025
(Member)

Signature:
Name: Dr. Ihsan Mahdi Shaheed
Title: Assist. Professor
Address: University of Kerbala, College of Science, Department of Chemistry
Date: ٩/٩/2025
(Member &supervisor)

Signature:
Name: Dr. Eman Talib Kareem
Title: Professor
Address: University of Kerbala, College of Science, Department of Chemistry
Date: / /2025
(Member &supervisor)

Approved by the council of the College of Science
Signature:
Name: Dr. Hassan Jameel Al-Fatlawy
Title: Professor
Address: Dean of College of science, University of Kerbala.
Date: / /2025

Abstract

This thesis investigated the use of Iraqi clay Ca-bentonite and modified clay (Ca-bentonite-chitosan) as cheap and environmentally friendly adsorbent surfaces for removal of pb (II) and Cr(III) ions from aqueous solutions. The influence of clay amount, temperature, equilibrium time, and solution pH on adsorb of pb(II) and Cr (III) ions onto Ca-bentonite and Ca-bentonite-chitosan clays from their synthetic solutions in mono-system were studied by batch method. The results showed that the removal efficiency and the maximum capacity of adsorption of pb(II), Cr (III) ions on the modified clay higher than natural clay. The contact times were 50 and 45 min. for adsorption pb(II) ion on natural and modified clay respectively, but when adsorption Cr(III), the contact times were 35 and 15 min. The optimum dosages of natural and modified clay were 0.1 and 0.07 g for pb(II) ion adsorption, but when adsorption Cr(III) ion, the optimum dosages were 0.3 and 0.1g for natural and modified clay respectively. pH had a major effect upon adsorption of pb(II) and Cr(III) ions in both systems, with the best adsorption of two ions occurred at pH = 5.

The experimental results for adsorption of pb(II) and Cr (III) ions onto natural clay were achieved with Freundlich isotherms at three temperatures (298, 308 and 318) K. The adsorption process results of pb(II) were agreed with the Langmuir and Freundlich isotherm models on modified clay ,but the Cr (III) ion on modified clay, which is fitted to the Langmuir isotherm model only. Thermodynamic functions, for instance, (ΔG, ΔH, and ΔS) were calculated from Van't Hoff equations for adsorption of pb (II) and Cr (III) ions on natural and modified clays. The values of (ΔG) of both ions adsorption on two surfaces were negative, suggesting a spontaneous adsorption process. The enthalpy values (ΔH) of pb(II) and Cr (III) ions adsorption on natural and modified clays were positive, suggesting an endothermic adsorption process. The entropy values (ΔS) of pb(II) and Cr (III) ions adsorption on two surfaces were positive, suggesting an increase in randomness.

List of contents

List of Tables

List of Figures

List of Symbols and Abbreviations

Abbreviation	***Definition***
AAS	**Atomic absorption spectrophotometer**
AES	**Atomic emission spectroscopy**
AFS	**Atomic fluorescence spectroscopy**
Ca-Bt	**Calcium-bentonite**
Ca-Bt-CS	**Calcium-bentonite-chitosan**

C_e	Equilibrium concentration of adsorbate
C_0	Initial concentration of adsorbate
DDA	degree of deacetylation
EDX	Energy Dispersive X-ray
FE-SEM	Field-emission Scanning Electron Microscopy
FT-IR	Fourier Transform Infrared (FTIR)
GSMGC	General Company for Geological Survey and Mining
H	Hour
Keq	Thermodynamic equilibrium constant
K_f	Freundlich constant related to adsorption capacity
K_L	Langmuir equilibrium constant related to energy of adsorption (L/mg)
L.O.I	Loss on ignition
L	Liter
min	Minute
MS	Mass spectroscopy
n	Freundlich constant related with adsorption intensity
ppm	Part per million
ppb	Part per billion
q_{max}	Adsorption capacity of the adsorbent at equilibrium time
q_e	Amount of adsorbate per weight of adsorbent at Equilibrium

R	**Gas constant**
R^2	**Correlation coefficient**
%R	**Percentage removal of adsorbate**
rpm	**Revolution per minute**
R_L	**Equilibrium factor**
SSA	**Specific surface area**
T	**Temperature**
V	**Volume of solution**
Wt %	**Weight percentage**
XRD	**X-Ray Diffraction**
XRF	**X-ray fluorescence**
µm	**Micrometer**
ΔG^o	**Gibbs free energy change**
ΔH^o	**Enthalpy change**
ΔS^o	**Entropy change**
λmax	**Maximum wave length**
%A	**The ratio of atoms of a given element to the total number of atoms in the sample**
Int	**Signal intensity**

Chapter One

Introduction

1. General Introduction:

Nowadays, human is facing several types of environmental stresses and ecological crisis among which environmental pollution which is one of the major problem. Environmental pollution is the undesirable physical, chemical or biological alterations in the physical, chemical and biological characteristics of different environmental constituents namely air, water and land leading to deterioration of environment and makes it harmful for humans, other living organisms[1].

The substance that causes pollution is known as a pollutant. Pollutants can exist as liquids, solids or gases. A substance becomes a pollutant when its concentration exceeds its natural abundance, and this increase in concentration is caused either by human activities or by natural phenomena[2]. Sometimes, certain valuable materials may also pollute the environment due to overuse or misuse or mismanagement e.g., fertilizers improve the soil fertility but pollute soil due to overuse and pollute water due to misuse and mismanagement[3]. Therefore, environmental pollution may also be defined as an addition of undesirable materials or excessive addition of useful materials in the environment beyond the threshold limits where the usefulness of that material is damaged and resulting in the degradation of environmental quality thereby making it unfit for life[4].

The majority of pollution types are imperceptible to the naked eye and manifest in various ways .There are essentially seven types of pollution: air pollution, water pollution, soil pollution, noise pollution, thermal pollution, light pollution, and radiation pollution[5]. Pollution is a problem that affects organisms, especially the developing ones, such as embryos and children, in consideration of the vulnerability of their status. Prolonged exposure to minimal quantities of pollutants can progressively alter the functioning of cells, tissues, and organs, essentially interfering

with deoxyribonucleic acid (DNA) expression. Unfortunately, the absolute limits of toxicity and tolerability of many pollutants are not yet known.

The World Health Organization (WHO), indeed, has recognized that environmental factors cause around 24% of diseases worldwide, and more than 33% of diseases in children under the age of 5 years are due to environmental factors[6].

1.1 Water pollution

Water pollution is defined as the presence of substances in water bodies that change their chemical, physical, or biological properties and can have adverse effects on living organisms and their environment[7].It occurs when contaminants, such as chemicals, microorganisms, or waste are introduced into water systems beyond a level that is safe for consumption by humans and the health of any ecosystem .Water pollution is caused by various contaminants, such as chemical pollutants (pesticides and heavy metals), microbiological pollutants (bacteria and viruses), nutrient pollutants (nitrogen and phosphorus) , thermal pollution and waste products (sewage and industrial waste) [8]. The measurement of water pollution is typically expressed as the concentration of the contaminant in milligrams per litre (mg/L) or parts per million (ppm)[9]. Water pollution can have both natural and anthropogenic causes. Natural causes include algae blooms and runoff from agricultural felds ,while anthropogenic causes include discharge from factories and sewage treatment plants, as well as waste products such as sewage and industrial waste [10]. These pollutants can harm aquatic species, disrupt food webs, and cause harm to human health[11].

1.2 Wastewater Treatment Processes

When water is polluted and decontamination becomes necessary, the best purification approach should be chosen to reach the decontamination objectives .A purification process generally consists of five successive steps[13]:

- preliminary treatment or pre-treatment (physical and mechanical): Pre-treatment consists of eliminating the (floating) solid particles and all suspended substances from the effluent. This pre-treatment stage, which can be carried out using mechanical or physical means is indispensable[12].
- Primary (sedimentation) treatment: the first major stage of treatment, which usually involves the uptake of settleable solids, which are separated as mud.
- Secondary (biological) treatment: the dissolved and colloidal organic compounds are oxidized in the presence of microorganisms.
- Tertiary treatment: further treatment of a biologically treated effluent to remove bacteria, suspended solids, specific toxic compounds or nutrients to enable the final effluent to comply with a standard more stringent before discharge.
- Sludge treatment: the dewatering, stabilization, and disposal of mud[13].

1.3 Heavy Metals

1.3.1 Definition of heavy metals

The term "heavy metals", have been generally used to describe metals with atomic weight greater than iron (56). Also, the term "heavy metals", have been used to describe metals having density greater than 5 g cm^{-3}. The actual definition of heavy metals is any metallic element that has a proportionally high density and is poisonous at low concentrations such as, Pb, Cd, Hg and Cr [14]. Generally, heavy metals are non-biodegradable in natural environment and are categorized in two groups. The first group is toxic metals (i.e. Pb, Cd and As) which are undesirable, don't have biological benefits for human health and toxic at any concentrations. The second group is essential metals (i.e. Cu, Zn, Mn, Fe, Ni and Cr etc.) which are desirable and have biological benefits for human health at low concentrations, but it become toxic at high concentrations[15].

Table 1-1 depicts the maximum concentration of some heavy metals that may be absorbed in the human body and the associated health conditions and disorders[16].

Table 1-1: Adverse Health Impacts of some Heavy Metals.

No.	Heavy Metals	WHO Allowed Permissible Limits (mg/L)	Adverse Effects on Human Health
1.	Nickel (Ni)	0.07	Lung scarring, lung cancer, renal disease, and cardiovascular illness disorders the lungs
2.	Silver (Ag)	0.1	Argyriasis, liver and kidney dysfunction, and blood cell abnormalities
3.	Iron (Fe)	3.0	At high amounts, hemochromatosis and liver cell destruction occur.
4.	Cadmium (Cd)	0.003	Acute toxic effects include headaches, skin ulcers, eczema, vomiting, diarrhea, and malignancies.
5.	Arsenic (As)	0.05	All possible side effects are eczema, skin ulcers, reproductive infection, genotoxicity,
6.	Chromium (Cr)	0.05	All possible side effects are eczema, skin ulcers, reproductive infection, genotoxicity, embryotoxicity, and lung cancer
7.	Cobalt (Co)	0.05	Allergic erythema, asthma, bronchitis, and carcinoma
8.	Lead (Pb)	0.05	Alzheimer's syndrome, senile impairment, kidney dysfunction, cancer and neurodegenerative disorders

1.3.2 Sources of Heavy Metals

The releasing sources of heavy metals to the different environmental media such as soil, air and water are divided to the natural and anthropogenic sources[17].The natural sources such as volcanic eruptions, sea-salt sprays, forest fires, rock weathering, biogenic sources and wind-borne soil particles. The anthropogenic sources such as industries processes, agriculture processes, discharge of wastewater, mining processes, metallurgical processes, as well as emissions of chimneys and motors. The main sources of metals are pesticides, paint productions, printing of textiles, earth's crust, hair dyes and Polyvinyl chloride (PVC) pipes for lead

(Pb); rechargeable batteries, tobacco, phosphate fertilizers, pigments, industrial wastes and agrochemical wastes for cadmium (Cd); stainless steel, alloy production, wood saving, textile dyes, leather tanning and electroplating for chromium (Cr); kitchen utensils, machine parts, batteries, earth's crust, cigarette and stainless steel for nickel (Ni); volcanic activities, pyrolysis of biomass, mining, paint of ships, wastewater discharges and forest fires for mercury (Hg); volcanic activities, disposal of arsenical chemicals, mining of gold and copper, arsenical pesticides, smelting and fertilizers for arsenic (As)[14].

1.3.3 Heavy metals under the study

1.3.3.1 Lead

It is a heavy, transition metal element, with symbol pb and atomic number 82. It is one of the elements in the carbon group of the periodic table. Lead (Pb) is a naturally occurring metal and generally form lead compounds by combining with two or more elements. Lead reacts with air and water to form lead sulfate, lead carbonates or lead oxide. These compounds act as a protective barrier to prevent corrosion. Lead can also interact with both acid as well as base. It has a low melting point and located above hydrogen in the electromotive series[18].

Although the existence of lead is indicated in nature but human activities has been found as the main reason for increasing lead content in the environment. Lead is released in air from mining of lead, factories utilizing lead compounds, alloys, vehicle exhaust and burning of fossil fuels[19].

The lead is removed from atmosphere by rain and transferred to soil or comes in contact with surface water. Moreover, lead is used as pesticide during vegetable and fruit cultivation. .Disposal of lead containing waste products, uptake of lead based paints from bridges, buildings and damaged battery from industries further results into the accumulation of lead in municipal landfills.

Lead combines very strongly with the soil particles and present in the top layer of soil. Lead enters water bodies or lakes when these soil particles are washed away by rain water. Thus, lead is transferred to animals and plants from air, water, soil and this cycle continues[20].

1.3.3.2 Chromium

Chromium (Cr) is classified as a Group 1, a transition element that is carcinogenic to living organisms, is a great risk to the environment, and is ranked fifth of the potentially worst toxic elements Chromium (Cr) exists in aqueous solution as trivalent (Cr^{3+}) and hexavalent (Cr^{6+}) forms. Cr^{3+} is an essential trace element while Cr^{6+} is a dangerous and carcinogenic element, which is of great concern globally due to its extensive applications in various industrial processes such as textiles, manufacturing of inks, dyes, paints, and pigments, electroplating, stainless steel, leather, tanning, and wood preservation, among others[21]. Cr^{3+} in wastewater can be transformed into Cr^{6+} when it enters the environment. Therefore, the United States Environmental Protection Agency (US EPA) has classified Cr as one of the 17 chemicals that pose a threat to human and research on Cr remediation from water has attracted much attention recently[22] .Chromium is a silvery metal, hard, lustrous metal, tasteless and odorless, malleable, and highly resistant to corrosion. Toxic effect due to human contact with chromium compounds were known a few years right after its isolation. The well-known toxic effects caused by chromium compounds, such as perforation of the nasal septum, chrome holes in the skin, hepatotoxic and nephrotoxic effects, and gastrointestinal bleeding[23].

1.4 Adsorption

Adsorption is basically a process of mass transfer in which solute or removable species are transported from a liquid phase onto the surface of a solid phase. By physiochemical interactions, adsorbed species are bounded to the solid surface. In

this process, generally, adsorbate migration occurs in three sequential steps: (1) migration of adsorbate to the border shell of the adsorbent, (2) intraparticle diffusion into pores, and (3) adsorption and desorption of solute. The characteristics of adsorbate, adsorbent, and matrix control the rate of all these steps[24]. Adsorption uptake by the adsorbent is heavily influenced by its surface properties, such as surface area and pore volume. Throughout the adsorption process, adsorbate molecules encircle the active sites of porous adsorbents [25] .

Adsorption is among the most commonly used techniques in wastewater treatment because of its major benefits, cheap cost, simple design, high efficiency, and ease of maintenance[26] . The adsorbate is the solute that participates in the adsorption process such as heavy metals, organic pollutants, radioactive elements and the adsorbent is the material that provides the surface such as clay, activated carbon and nanomaterials[27].

1.4.1 Adsorption types

Physical and chemical adsorption are the two types of adsorption[28]

1-**Physical adsorption:** is caused by the interaction of intermolecular forces (van der Waals forces), such as adsorption of gas by activated carbon.Physical adsorption is typically performed at a low temperature, low adsorption heat, fast adsorption rate, and is nonselective. Because the effect of intermolecular attractions are weak, changing the structure of adsorbate molecules is difficult, separating adsorbed material is simple, and the energy of adsorption is low(also called physisorption), as shown in Figure 1-1.

2-**Chemical adsorption:** this type of adsorption occurs on electronically unsaturated active surfaces and known as active adsorption. The chemical adsorption results from chemical forces (greater than Vander Waals forces)[29], leads to the creation and destruction of chemical bonds. The

adsorption heat of uptake or release is greater, as is the activation energy required (also called chemisorption). Chemical adsorption and physical adsorption are not separated and frequently occur together, as shown in Figure 1-1

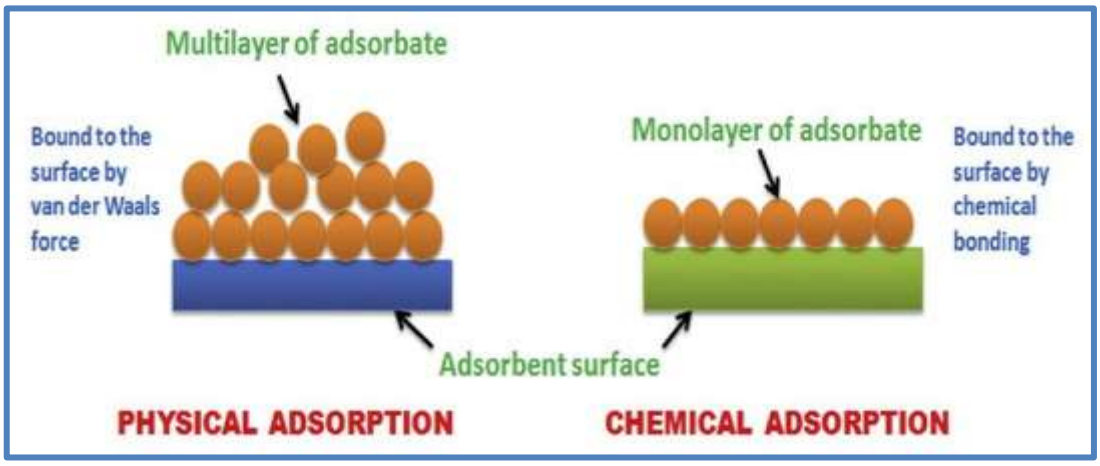

Figure 1-1: Chemical and physical adsorption[30]

1.4.2 Factors affecting the adsorption process:

The amounts which are adsorbed from solution on solid is on the basis of some aspects such as process used for system, allowed time duration, adsorbent's porosity, adsorbate's concentration, system's temperature, interfacial tensions between adsorbent and solution, adsorbate and solvent, nature of adsorbent, pH solution, existence of foreign material[31]. The major significant aspects are provided in the following way:

1. **Nature of adsorbent:** Majorly, the adsorbent's nature is depending on adsorbent's chemical composition, the surface that cause adsorption is impacted because of the existence related to cracks edges, pores, and corners. It has been indicated that the adsorbate was adsorbed on various solid surface at same temperatures, the more the adsorbent's surface area, the more amounts of adsorbate will be adsorbed on it. Thus, the substances such as

charcoal and silica are extremely efficient adsorbents since they were very porous structures, thus the surface area is large[29].

2. **Nature of adsorbate:** The adsorption of soluble substance from its solutions depends upon several factors such as its solubility in experimental solvents, physical state in solution, chemical nature, the size, shape, presence of polar groups, and concentration of the adsorbate material all affect the reaction between adsorbent surface and the adsorbate molecules. The adsorption process can be selective of one of the components with the increase in molecular weight and solubility of polar group and charges the interference between the surface adsorbent and adsorbate molecules and so on[32].
3. **Nature of solvent:** The solvents have significant impact in the adsorption study because adsorption is depending upon of interactions related to solvent with solute existing in adsorbed layer. The solvent effect is indicated for being significant in adsorption on the polar surfaces, majorly in the case when solvent has been polar and/or containing aromatic ring. The solute's adsorption has been inversely relative to its solubility in the solvent. For certain solvent, less or slightly soluble adsorbate is more adsorbed in comparison to much soluble ones[33].
4. **Temperature:** The temperature is a factor of high importance in studying the adsorption. Typically, low temperatures are needed to large adsorption, common process of adsorption is exothermic. In certain conditions, the high temperatures are enhancing the adsorption. Variations are depending on the nature related to adsorbate-adsorbent interactions[29].
5. **Influence of pH**: pH of a solution is specified as a major factor impacting the adsorbent's capacity in wastewater treatment. The adsorption's efficiency is depending upon of pH solution, as the changes in pH result in changing the

ionization degree related to adsorptive molecular as well as the adsorbent's surface characteristic. There is a requirement for adjusting the value of the pH solution for evaluating the mechanism of adsorption. The existence regarding certain functional group, like hydroxide (-OH), the cationic dye adsorption happens at elevated pH value, while for the anionic dye adsorption is required at low pH due to the fact that surface become positively charged[34].

6. **Contact time**

The adsorption processes are influenced by contact time, where time needed for adsorption systems to achieve equilibrium differs depending on surface nature and unfilled adsorption sites[35]. It is the longest period of time when adsorption process is finished and the equilibrium or change is minor[36].

7. Ionic Strength

The neutral molecules are adsorbed to a larger degree than more highly ionized molecules[37]. Soluble electrolytes typically exhibit their action by influencing adsorbate solubility or physical properties (surface potential and surface charge). When electrolyte used to increase ionic strength is also more soluble in solvent than adsorbate, ionic strength increases the extent of adsorption.[38]

1.4.3. Adsorption isotherms

Adsorption isotherms are useful in describing the interaction between adsorbate and adsorbent.They play important roles in determining the optimum adsorption capacity of adsorbent and indicate how efficient an adsorbent can adsorb, and also allows an estimation of the validity of adsorbent's application. Isotherms also represent the amount of adsorbate that binds on the surface of adsorbent depending on the material available in the solution and are important requirements in designing a system

for adsorption.[39]. The shape of an isotherm provides information on the stability of the interactions between adsorbent and adsorbate and on the adsorption affinity of molecules. Adsorption isotherms are described in many mathematical forms, some are based on simplified physical description of adsorption, while others are empirical and have to correlate experimental data[40]

Adsorption isotherm can be graphically represented by plotting the adsorbate quantity on the solid surface (qe (mg/g)) against the concentration of adsorbate in solution (Ce(mg/L)) at equilibrium [41].There is a wide range of adsorption isotherm forms for chemisorption, with an primary sharply increasing curve that steadily flattens. The initial increase is related to the greater trend of surface to bind the adsorbed particles, and the adjustment off is related to the saturation of these forces. On the other hand, physical adsorption is characterized by an adsorption isotherm that appears to have a progressively positive slope with rising adsorbed concentration (for adsorption from solute) and gas pressure (for gas adsorption)[42].

1.4.4 Adsorption Isotherms Models

Adsorption equilibrium results are typically defined by adsorption isotherms that are critical for optimizing adsorption process design parameters. They are indeed useful in providing enough physical and chemical data to know the adsorption mechanism. These isotherms connect to the quantity of solute adsorbed at equilibrium per mass of adsorbent, qe, to a concentration of adsorbate at equilibrium, Ce. To fit experimental data in this study, two main isotherm models were chosen: Langmuir and Freundlich[43].

1.4.4.1. Langmuir isotherm

Langmuir isotherm explains monolayer adsorption under the assumption that all adsorption sites provide equal adsorbate affinities (the surface is homogeneous) so

this adsorption at one site has no effect on adsorption at another[44]. In his model, he assumed that[45]:

- There are fixed adsorption sites on the surface of each adsorbent and a fraction of these sites could be occupied by adsorbates at a given temperature and pressure
- Each adsorption site on the surface of adsorbent can accommodate one entry
- Heat of adsorption for each adsorption site is the same and independent of the fraction of sites occupied by adsorbate.
- Interaction does not exist between adsorbates occupying different adsorption sites. The equation for the Langmuir isotherm is as follows[46]:

$$\frac{C_e}{q_e} = \frac{1}{K_L\ q_{max}} + \frac{C_e}{q_{max}} \qquad (1.1)$$

Where qe represents the quantity of adsorbed for unit weight of adsorbent (mg / g), Ce represents equilibrium concentration of adsorbate (mg/L), q_{max} represents adsorption capacity (mg /g), or monolayer capacity, and K_L represents the Langmuir equilibrium constant related to energy of adsorption and binding site affinity (L /mg).

The slope and intercept of linear plot of experimental results of Ce/qe vs Ce, equation (1.1), can be used to calculate the values of q_{max} and K_L. One of key traits of Langmuir model could be described in term of the dimensionless constant known as the equilibrium factor R_L, which is described as [47]:

$$R_L = \frac{1}{1+K_L\ C_0} \qquad (1.2)$$

Where C_o represents initial concentration in (mg /L). Value of R_L suggests whether isotherm is unfavorable adsorption (R_L > 1), linear adsorption (RL=1), favorable adsorption (0< R_L <1), or irreversible adsorption (RL =0)[48]. The linear form to linearize experimental results by plotting Ce/qe against Ce. The slope =($1/q_{max}$)

and intercept =$(1/K_L q_{max})$ of the linear equation are used to calculate the Langmuir constants K_L and q_{max} [49],as shown in Figure 1-2

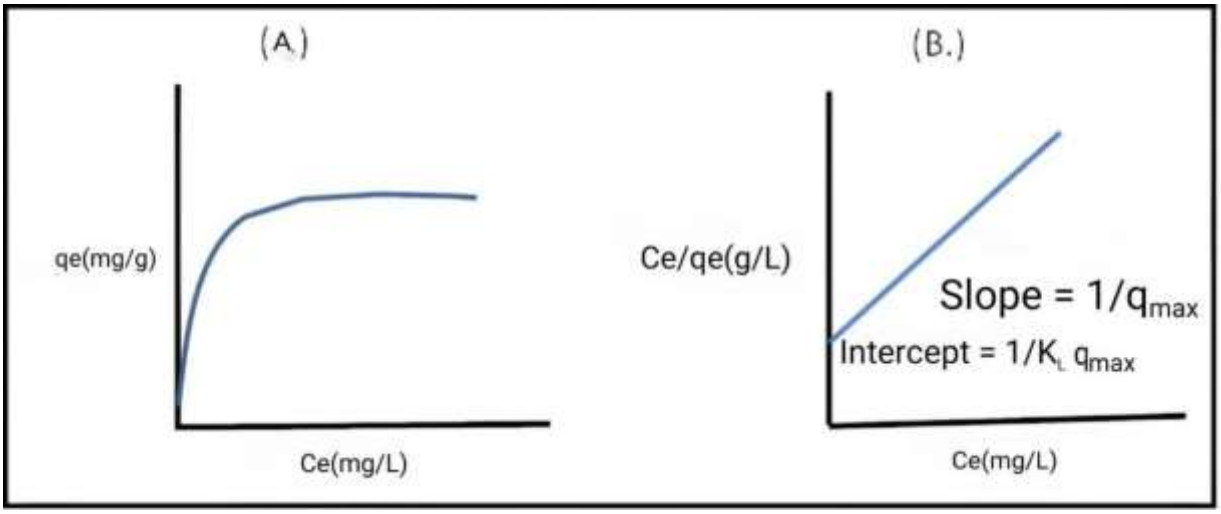

Figure 1-2 :(A.)The Langmuir isotherm (B.) The Langmuir isotherm in linear form[33]

1.4.4.2 Freunlich isotherm

Freundlich isotherm is a common relationship used to describe the sorption equation. It is concerned with heterogeneous adsorption on surfaces and the interaction of adsorbate molecules. The Freundlich equation predicts that the sorption energy decreases exponentially as an adsorbent of the sorption centers is completed. It is used to explain heterogeneous systems and is expressed by below equations [34].

$$\boldsymbol{\log q_e = \log K_F + \frac{1}{n} \log C_e} \qquad (1.3)$$

Where K_F represents capacity factor or experimental Freundlich constant (mg/g), (1/n) represents heterogeneity factor. The intercept = log KF and the slope = (1/n) have been calculated using the log qe vs log Ce plot, as shown in Figure 1-3. The constants (KF and n) are linked to the strength and distribution of the adsorptive bond, respectively[34]. Mathematically, it has been indicated that n can be classified as an indicator of adsorption site heterogeneity. For example, as n approaches zero, surface sites heterogeneity increases. When n is greater than one, bond energies raise with

surface density, when n is less than one, bond energies reduce with surface density, and when n equals one, all surface sites are equivalent[35].

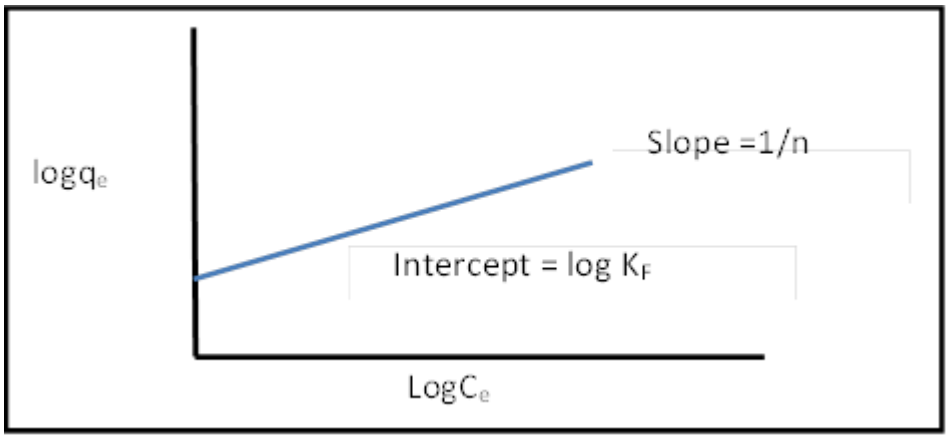

Figure 1-3: The Freundlich isotherm in linear form(33).

1.5 The clays:

Clay is a mineral mixture of crystalline hydrated aluminum silicates with a divers composition. The grain diameter of these fine components of sediments resulting from the weathering of rocks, their transport, and deposition of weathering products is less than 20 micrometers. Clays are classified according to their grain size (particle size) in to coarse clays(20 to 2 micrometers) and fine clays(2 to 0.2 micrometers) and colloidal clays (< 0.2 micrometers)[50]. When clays are adequately crushed and washed, hydrated alumina or iron oxide play a large role in colloidal or near-colloidal particles, which leads to plasticity. Clays are distinguished from many other soil particles by their plasticity [49].

1.6 Clay Minerals

Clay minerals are known as a complex silicate composed of different ions. Based on arrangement of these ions, the crystal units are divided in to two types:

a. silicon – oxygen tetrahedron consists of silicon surrounding by four oxygen atoms and unite to form the silica sheet.

b. aluminum or magnesium octahedron consists of aluminum surrounding by six hydroxyl units and combine to form gibbsite sheet (If aluminum is main dominating atom) or brucite sheet (If magnesium is main dominating atom)[50].

1.7 Properties of mineral clays

These properties depend largely on proportion of their plates, their ability to exchange ions and absorb. The most important of these properties are:

1. a layer structure with one dimension in the nanometer range; the thickness of the 1:1 (TO) layer is about 0.7 nm, and that of the 2:1 (TOT) layer is about 1 nm,

2. The anisotropy of the layers or particles.

3. The existence of several types of surfaces: external basal (planar) and edge surfaces as well as internal (interlayer) surfaces.

4. The ease with which the external, and often also the internal, surface can be modified (by adsorption, ion exchange, or grafting).

5. Plasticity.

6. Hardening on drying or firing; this applies to most (but not all) clay minerals

Because of its characteristics, the clays carry a main role in many fields by acting as a healthy scavenger of contaminants by absorbing anions and cations via ion adsorption, exchange, or both [51].

As a result, clay usually contains substitutable cations and anions that are carried onto the surface. Na^{+}, Ca^{2+}, Mg^{2+}, NH_4^{+}, H^{+}, K^{+}, PO_4^{-3}, Cl^{-1}, SO_4^{-2}, and NO_3^{-} are the most common cations and anions located on clay surfaces [51]

1.8 Bentonite clay

Bentonite is a clay formed of highly colloidal and plastic clays composed mainly of montmorillonite, a clay mineral of the smectite group, and is produced by in situ devitrification of volcanic ash. In addition to montmorillonite, bentonite may contain feldspar, cristobalite, and crystalline quartz. The special properties of bentonite are an ability to form thixotrophic gels with water, an ability to absorb large quantities of water, and a high cation exchange capacity. The properties of bentonite are derived from the crystal structure of the smectite group, which is an octahedral alumina sheet between two tetrahedral silica sheets. Variations in interstitial water and exchangeable cations in the interlayer space affect the properties of bentonite and thus the commercial uses of the different types of bentonite. By extension, the term bentonite is applied commercially to any clay with similar properties[51].

Bentonite is an impure form of aluminum phyllosilicate clay consisting 98% of montmorillonite and the chemical composition of the unit cell has been represented as $[(Si_{8.0})(Al_{3\cdot02}Mg_{0.50}Ca_{0\cdot06}Fe_{0.18}Ti_{0.02}Na_{0.22})O_{20}(OH)_4]$. It is a versatile mineral due to its platelet structure. The platelet consisting of a tetrahedral silicon oxide layer in which some silicon replaced by trivalent cations sandwiched between two octahedral aluminum oxide layers in which aluminum replaced by divalent cations. The hydroxide group is present on the edge of each platelet results in thixotropic nature[50] . The different types of bentonite are found based on their respective dominant element, such as potassium (K), sodium (Na), calcium (Ca), and aluminum (Al). For industrial purposes, three main classes of bentonite exist: sodium, calcium and potassium bentonite[52].

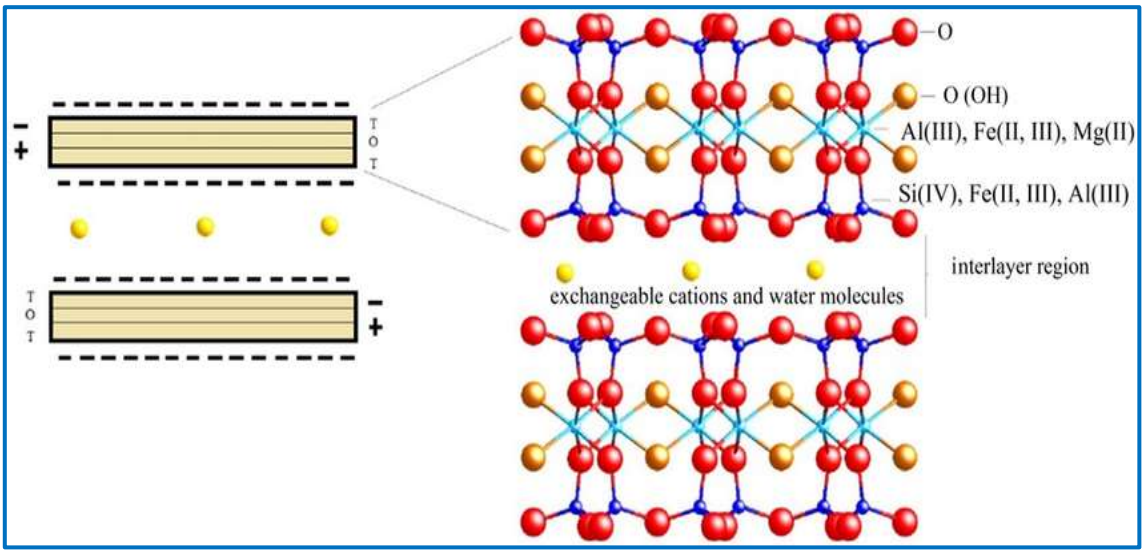

Figure 1-4: Layer structure of bentonite clay[53]

1.8.1 Calcium bentonite

Majority bentonite occurring worldwide is of the calcium type. Calcium-bentonite or non-activated bentonite is type that is predominantly occupied by Ca^{2+} or Mg^{2+}ions in the intermediate layers. This Ca-bentonite has lower swelling when

compared to that of Na-bentonite. It is used as an adsorbent in cooking oil industries, and lubricant oil recycling, as a catalyst, adsorber, filler, etc.[54].

1.9 Chitosan

Chitosan is a natural polysaccharide obtained from partial or full deacetylation of chitin[55]. Chitin, the source material for chitosan, is the most naturally abundant polysaccharide after cellulose[56]. Chitin is an important component of the cell wall of fungi, the exoskeleton of crustaceans, and insects. Chitosan is the N-deacetylated derivative of chitin, a linear and semicrystalline polysaccharide composed of glucosamine and N-acetyl glucosamine units linked by β-(1→4) glycosidic bonds [57]. When the fraction of glucosamine units is greater than 50%, the Polymer is commonly called chitosan and the number of glucosamine units is termed degree of deacetylation (DDA). Chitosan is the only polycation in nature and its charge density depends on the degree of acetylation

and pH of the media. The solubility of the polymer depends on the acetylation degree and molecular weight[58]. Chitosan oligomers are soluble over a wide pH range, from acidic to basic ones (i.e., physiological pH 7.4). On the contrary, chitosan samples with higher Mw are only soluble in acidic aqueous media even at high deacetylation degrees. This lack of solubility at neutral and basic pH has hindered the use of chitosan in some applications under neutral physiological conditions (i.e., pH 7.4). This is the reason why a great number of chitosan derivatives with enhanced solubility have been synthetized[59].

1.9.1 Technological Chitosan Properties

a) Solubility

Chitosan is produced by deacetylation of chitin; in this process, some N-acetyl glucosamine moieties are converted into glucosamine units. The presence of large amounts of protonated -NH_2 groups on the chitosan structure accounts for its solubility in acid aqueous media since its pKa value is approximately 6.5. When around 50% of all amino groups are protonated, chitosan becomes soluble. Chitosan solubility depends on different factors such as polymer molecular weight, degree of acetylation, pH, temperature, and polymer crystallinity[60].

b) Viscosity

The viscosity of polymers is a parametre of great interest from the technological point of view since highly viscous solutions are difficult to manage. Moreover, viscometry is a powerful tool for determining chitosan's molecular weight, as it is a simple and rapid method even though it is not an absolute method. Chitosan viscosity depends on the molecular weight of the polymer and deacetylation degree and decreases as the molecular weight of chitosan is reduced. In fact, viscosity can be used to determine the stability of the polymer in solution, as a reduction is observed during polymer storage due to polymer degradation[61].

1.9.2 Chemistry of Chitosan

As seen in Figure 1-5 , the reactive groups found in chitosan are a primary amino group (C2) and primary and secondary hydroxyl groups (C6, C3). Glycosidic bonds and the acetamide group can also be considered functional groups. These functional groups allow for a great number of modifications, producing polymers with new properties and behaviours[62].

Chitosan is insoluble in aqueous solution above pH 7, in its crystalline form. However, in dilute acids (pH < 6), the protonated free amino groups on glucosamine facilitate solubility of the polymeric molecule[61]. A polyelectrolyte is a polymer carrying either positively or negatively charged ionizable groups. Solubilization occurs by protonation of the $–NH_2$ group on the C-2 position of the d-glucosamine repeat unit.

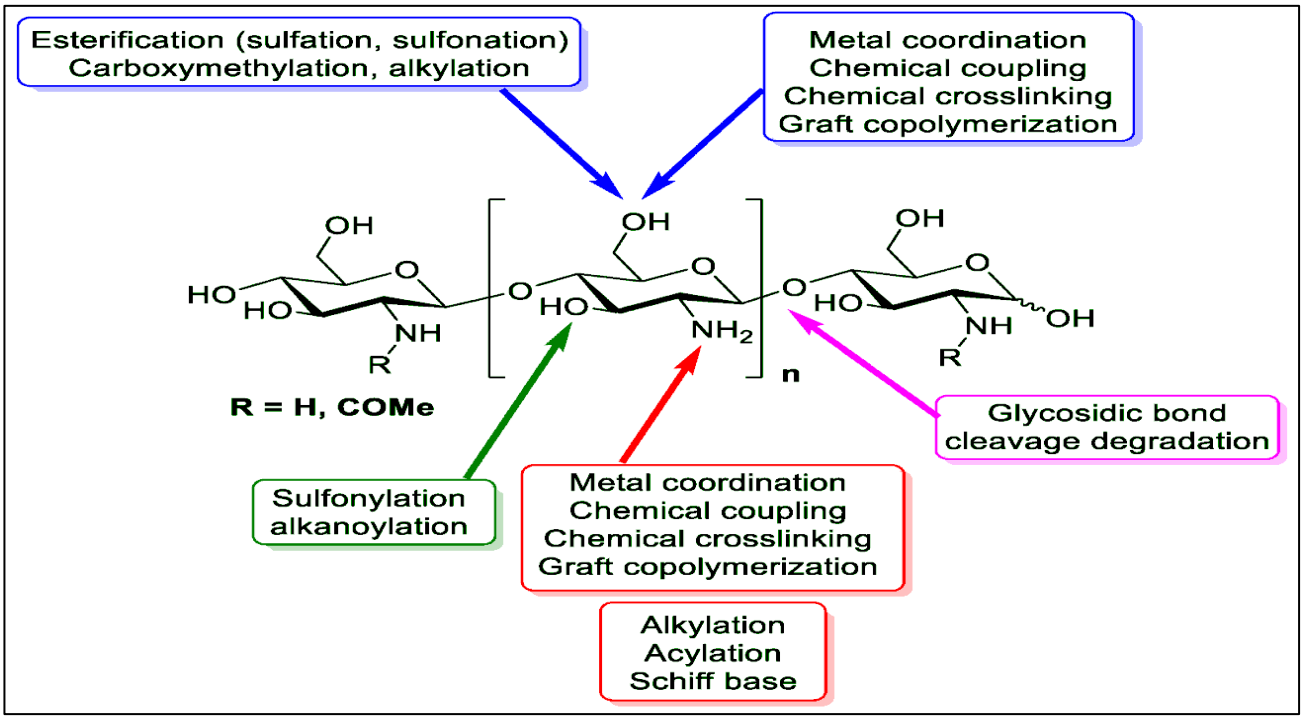

Figure 1-5: Functional groups in chitosan's structure[61]

Chitosan is a white to light red solid powder depending on processing conditions and levels of residual pigments. Its physiological functions include decreasing cholesterol, decreasing high blood pressure, inhibition of fat absorption, and improvement of intestinal microflora/environment. It has long

been included in food and food additives due to its safety in humans, animals, and microbes[63].

Chitosan has several key properties that make it one of the most promising natural substances for application in medical and pharmaceutical fields.

1.10Atomic spectroscopy

Spectroscopy is the study of interactions between matter and different forms of electromagnetic radiation; when practiced to quantitative analysis, the term spectrometry is used.

Atomic spectroscopy includes a number of analytical techniques used to determine the elemental composition of a sample (it can be gas, liquid, or solid) by observing its electromagnetic spectrum or its mass spectrum. Element concentrations of a millionth (ppm) or one billionth part (ppb) of the sample can be detected[64].

Atomic spectroscopy includes the techniques of atomic absorption spectroscopy (AAS), atomic emission spectroscopy (AES), atomic fluorescence spectroscopy (AFS), X-ray fluorescence (XRF), and inorganic mass spectroscopy (MS). AAS, AES, and AFS exploit interactions between UV-visible light and the valence electrons of free gaseous atoms. Formation of the atomic vapor i.e. atomization is the major principle of emission, absorption, and fluorescence techniques. The most critical component of instruments used in atomic spectroscopy is the atomization sources and sample introduction devices with an associated spectrometer for wavelength selection and detection of light. Atomization involves the several key (the basic) steps: solvent removal, separation from anion and other elements of the matrix, and reduction of ions to the ground state atom[65].

Analytical methods of atomic spectroscopy have been used for elemental analysis identification, and quantitation in varieties of samples. Recently, most all

of the spectroscopic techniques available are used in the analysis of metals and trace elements in samples of industrial and environmental origin[66].

1.10.1 Atomic Absorption Spectrometry (AAS)

Atomic Absorption Spectrometry (AAS) is a technique for measuring quantities of chemical elements present in environmental samples by measuring the absorbed radiation by the chemical element of interest. This is done by reading the spectra produced when the sample is excited by radiation. The atoms absorb ultraviolet or visible light and make transitions to higher energy levels. Atomic absorption methods measure the amount of energy in the form of photons of light that are absorbed by the sample. A detector measures the wavelengths of light transmitted by the sample, and compares them to the wavelengths which originally passed through the sample[67]. A signal processor then integrates the changes in wavelength absorbed, which appear in the readout as peaks of energy absorption at discrete wavelengths. The energy required for an electron to leave an atom is known as ionization energy and is specific to each chemical element. When an electron moves from one energy level to another within the atom, a photon is emitted with energy E. Atoms of an element emit a characteristic spectral line. Every atom has its own distinct pattern of wavelengths at which it will absorb energy, due to the unique configuration of electrons in its outer shell. This enables the qualitative analysis of a sample[68]. The concentration is calculated based on the Beer-Lambert law. Absorbance is directly proportional to the concentration of the analyte absorbed for the existing set of conditions. The concentration is usually determined from a calibration curve, obtained using standards of known concentration. However, applying the Beer-Lambert law directly in AAS is difficult due to: variations in atomization efficiency from the sample matrix, non-uniformity of concentration and path length of analyte atoms (in graphite furnace AA).

The chemical methods used are based on matter interactions, i.e. chemical reactions. For a long period of time these methods were essentially empirical,

involving, in most cases, great experimental skills. In analytical chemistry, AAS is a technique used mostly for determining the concentration of a particular metal element within a sample. AAS can be used to analyze the concentration of over 62 different metals in a solution. Typically, the technique makes use of a flame to atomize the sample, but other atomizers, such as a graphite furnace, are also used. Three steps are involved in turning a liquid sample into an atomic gas:

1. Desolvation – the liquid solvent is evaporated, and the dry sample remains.
2. Vaporization – the solid sample vaporizes to a gas.
3. Volatilization – the compounds that compose the sample are broken into free atoms[67].

To measure how much of a given element is present in a sample, one must first establish a basis for comparison using known quantities of that element to produce a calibration curve. To generate this curve, a specific wavelength is selected, and the detector is set to measure only the energy transmitted at that wavelength. As the concentration of the target atom in the sample increases, the absorption will also increase proportionally. A series of samples containing known concentrations of the compound of interest are analyzed, and the corresponding absorbance, which is the inverse percentage of light transmitted, is recorded. The measured absorption at each concentration is then plotted, so that a straight line can then be drawn between the resulting points. From this line, the concentration of the substance under investigation is extrapolated from the substance's absorbance. The use of special light sources and the selection of specific wavelengths allow for the quantitative determination of individual components in a multielement mixture. [69].

1.10.2Basic instrumentation

Every atomic absorption spectrometer presents the same basic components; however, each manufacturer differentiates the configuration due to the analytical demand and according to technological advance. Figure 1-6 shows

the main components of an atomic absorption spectrometer, typical atomic absorption spectrometer consists of four main components:

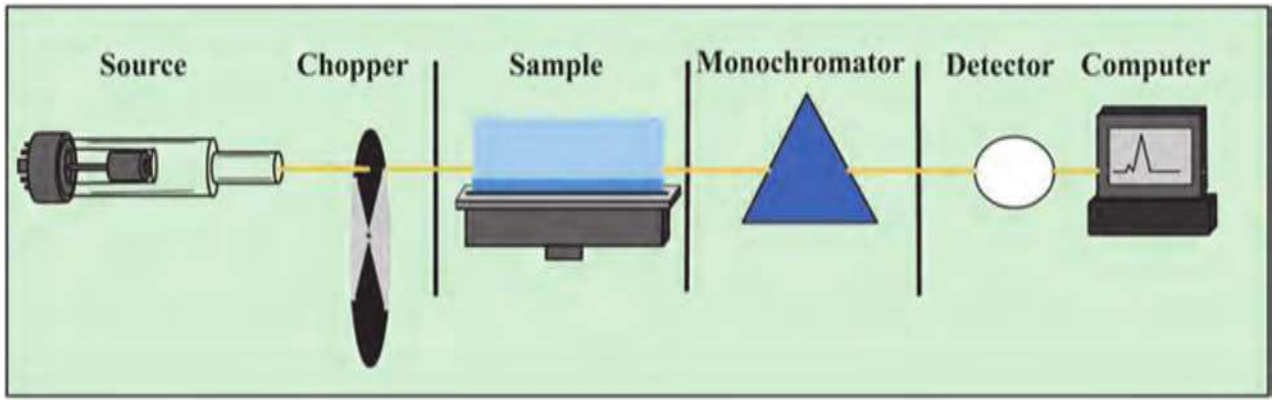

Figure 1-6: main components in atomic absorption spectroscopy instrumentation[69]

1. The light source :

An atom absorbs light at discrete wavelengths. In order to measure this narrow light absorption with maximum sensitivity, it is necessary to use a line source, which emits the specific wavelengths which can be absorbed by the atom. Narrow line sources not only provide high sensitivity, but also make atomic absorption a very specific analytical technique with few spectral interferences. The two most common line sources used in atomic absorption are the ‘‘hollow cathode lamp’’ and the ‘‘electrodeless discharge lamp[70].

2. The atomization system

AA spectroscopy requires that the analyte atoms be in the gas phase. Ions or atoms in a sample must undergo desolvation and vaporization in a high-temperature source such as a flame or graphite furnace. The following atomization methods are known: a) Flame atomization, b) Graphite furnace atomization and c) Mercury hydride atomization[71]. Figure 1-7 shows several steps that occur during the atomization process of any element M, initially in solution of ionic M^{+}. The nebulizer and the chamber of nebulizer are responsible for transferring part of a flask solution to the burner, in continuous flow of very

small droplets. When getting to the flame, the solvent dries fast and a solid MA compound is formed where A is an anion present in the solution.

The heat is enough to liquefy, vaporize and break the bond of compound MA, releasing gaseous atomic specie M^o in the ground state. This species absorbs a specific wavelength radiation emitted by the lamp. If the temperature were high enough, M^o could be excited to M* or lose an electron and passed to M^+.

The temperature is the variable that most influences the atomization process. The best way to control this variable is through a critical choice of fuel and oxidants gases, and varying the percentage to a fine adjustment among them. As examples of fuel gases, we can cite propane, hydrogen and acetylene. As examples of oxidant gases, we can cite are air, oxygen and nitrous oxide[72].

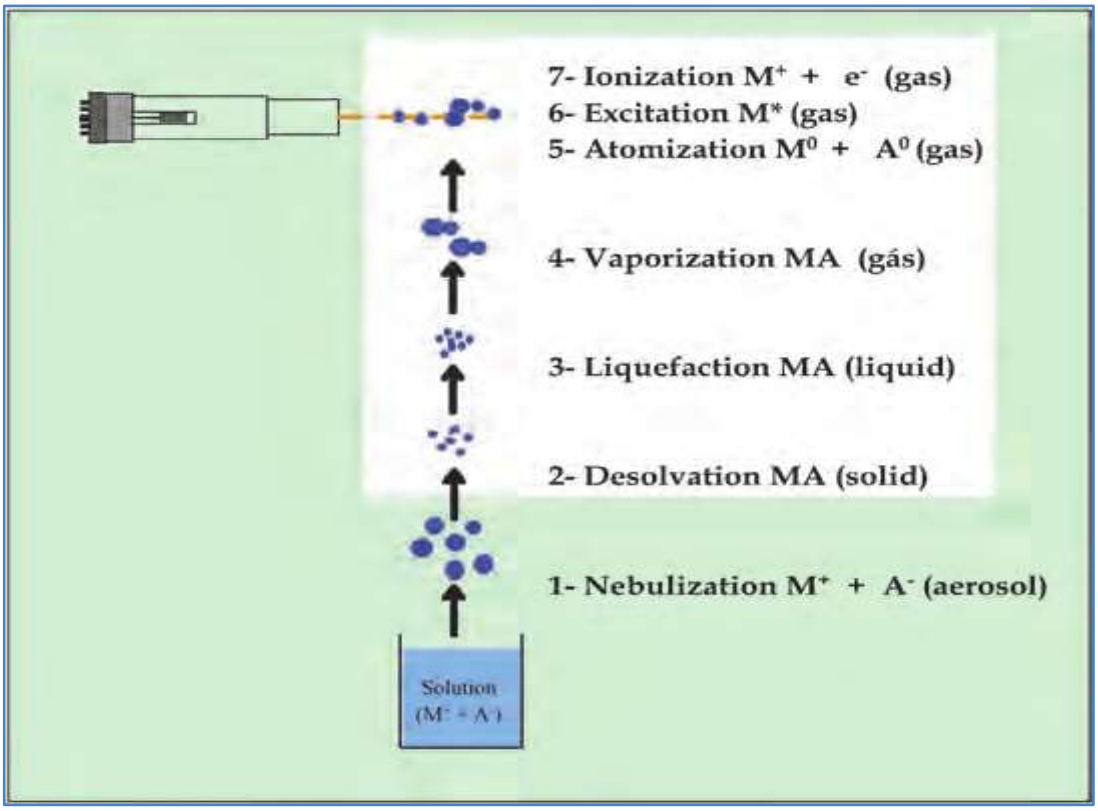

Figure 1-7: Scheme of atomization mechanism[72].

3. **The monochromator :** The monochromator is responsible for selecting the appropriate wavelength for analysis. It is a hermetical closed box with entrance and exit slits of 0.2 to 2nm, lenses and mirrors to focus the

radiation and a dispersed element that can be a prism or a diffraction grating or a combination of them. It is filled up with inert gas to avoid ultraviolet radiation absorption by the air and normally has the walls painted in matte black to avoid reflection and scattered radiation.

The polychromatic radiation enters through the entrance slit, it is separated and only the chosen wavelength of radiation reaches the exit slit and goes on to the detector[73].

4. **The detection system**

The detector is placed in front of the exit slit and receives the determined photons by the monochromator. It transforms lightning energy in an electrical signal, that is amplified and measured. Detectors mostly used in old equipments are photo-multiplier valves. With modern equipments, they are being substituted by a system based on solid-state detectors type CCD (charge coupled device). They are similar to digital cameras sensors with a set of sensitive pixels to electromagnetic radiation in the UV regions and visible that transforms the energy of photons coming from the monochromator into a digital signal[67].

1.10.3 Advantages of Atomic Absorption Spectroscopy (AAS)

- **High Sensitivity**: AAS can detect elements at very low concentrations, often down to parts per billion (ppb)[74]
- **Accuracy:** Provides precise measurements with minimal deviation from true values, typically within a 0.5-5% range[67].
- **Elemental Specificity:** Capable of analyzing over 70 different elements without interference from other components in the sample.
- **Low Sample Volume:** Requires only a small amount of sample for analysis
- **Rapid Analysis:** Offers quick detection and quantification of elements[70]

1.11 Literature Studies

Several studies (Table 1-2) have investigated the adsorption behavior of heavy metal ions such as Pb(II) and Cr(III) ions on natural and modified bentonite surfaces. These studies provide insights into the thermodynamic aspects of the adsorption process, highlighting changes in Gibbs free energy, enthalpy, and entropy. The comparison between natural calcium bentonite and chitosan modified bentonite reveals significant improvements in adsorption performance due to surface modification.

The Table 1-2: key findings from selected recent publications:

Sno.	Adsorbents	Heavy metal	Maximum adsorption	Isotherm models	Reference
1	Montmorillonite	Pb(II)	91.08	Langmuir	[75]
2	Acidified Bentonite	Pb(II)	15.3846	Langmuir	[76]
3	activated bentonite	Pb(II)	13 ± 0.04	Langmuir	[77]
4	bentonite-chitosan	Pb(II)	325mg/g	Langmuir, Freundlich	[78]
5	bentonite-chitosan	Pb(II)	177	Freundlich	[79]
6	Bentonite	Cr(III)	6.44	Langmuir, Freundlich	[80]
7	Illitic-Kaolinite	Cr(III)	14.27	Freundlich	[81]
8	modified bentonite	Cr(III)	3.72	Langmuir	[82]
9	bentonite-chitosan	Cr(III)	23.5	Langmuir	[83]
10	SDS-chitosan	Cr(III)	3.42	Langmuir	[84]

1.12 Aims of Study

The study has the following aims:

1- Modification natural calcium bentonite with chitosan to enhance its adsorption properties.

2 - Compare the adsorption efficiency of natural and modified bentonite for Pb(II) and Cr(III) ions.

3- Investigation of the effect of contact time, adsorbent dosage, PH, and temperature on adsorption behavior.

4- Determination of the thermodynamic parameters ($\Delta G°$, $\Delta H°$, $\Delta S°$) of the adsorption process.

5- Identification of the most suitable isotherm model describing the adsorption mechanism.

Chapter Two

(Experimental Work)

2.1 Instruments Analysis

Table (2-1): The instruments and their manufactures which are used in this study.

No.	Instruments	Company, Source	Places
1	Atomic Absorption Spectrophotometer (AAS)	Sens AA Dual,GBC Scientific Equipment- Malaysia	Marine Science Center, Basrah university
2	Fourier Transform Infrared (FTIR)	8400s ,Shimadzu- Japan	University of Kerbala, Science college
3	Field-emission Scanning Electron Microscopy (FESEM-EDX)	EM620 Eco ,KYKY-China	Buali Sina Scientific and Cultural Foundation, Hamadan - Iran
4	X-Ray Diffraction	Lab X- XRD 6000,Shimadzu-Japan	College of Engineering, University of Kufa.
5	Thermo stated shaker	BS-11,230 VAC -50 Hz , Lab tech- Korea	Marine Science Center, Basrah university
6	Electric Balance	BL 210S ,Germany	Marine Science Center, Basrah university
7	Oven	Memort LDO- 080+N , Labtech- Korea	Marine Science Center, Basrah university
8	pH Meter	AD101, Romania	Marine Science Center, Basrah university
9	Magnetic Hot Plate Stirrer	GmbH, MS-H280-pro , Germany	Marine Science Center, Basrah university
10	Centrifuge	Z200a Hermie,6000 rpm , Universal II- Germany	Marine Science Center, Basrah university
11	sieve	(75µm),(no.200, Germany	University of Kerbala, Science college

2.2. Chemical Materials

The study used specific chemicals which are shown with their suppliers in Table (2-2).

Table (2-2): Materials and their suppliers.

No.	Chemicals	Formula	Purity (%)	Molecular mass(g/mol)	Company
1	Acetic acid	CH_3COOH	99%	60.050	BDH
2	Chromium nitrate Non hydrate	$Cr(NO_3)_3$	97%	238.011	Merk
3	Lead Nitrate	$Pb(NO_3)_2$	99.9%.	331.230	BDH
4	Sodium hydroxide	NaOH	99%	40.000	SDFCL
5	Hydrochloric acid	HCl	37%	36.640	BDH
6	Chitosan	$[C_6H_{11}NO_4]n$	Density: 0.03g/ml	Particle size: ≤ 80	Rongsheng Biotechnology

2.3. Adsorbent surface

Calcium bentonite clay rock (Figure 2-1), used in this project was provided by the General Company for Geological Survey and Mining (GSMGC), Baghdad, Iraq. Table 2-3 presents the chemical composition of this clay.

Figure 2-1: Ca- bentonite clay[85]

Table (2-3): The chemical composition of Ca-bentonite [85]

L.O.I	K_2O	Na_2O	MgO	CaO	Fe_2O_3	Al_2O_3	SiO_2
9.5%	0.6%	1.1%	3.4%	4.5%	5.1%	15.7%	56.7%

2.3.1. Preparation of clay powder

The natural clay was grind and then soaked in deionized water and allowed to dry at 343K for 7 hours. At room temperature (298 K), the natural clay was left to cool. The clay has been crushed and sieved using a sieve of size (no.200) (75 μm) and kept in a closed container[86].

Figure2-2: The natural clay powder

2.3.2 Preparation of Ca-Bentonite Chitosan Composite

The modified clay was prepared using a procedure reported in literature[86] with modification. The composite Ca-bentonite-chitosan was prepared by the following steps:-

1. 1g of chitosan dissolved in a 2% (v:v) acetic acid: water solution at 313 K for 1 hour.
2. 9g of natural clay was dispersed and stirring in 100ml deionized water for 1hour at 298k.
3. The clay suspension added slowly to chitosan solution and stirring at 298k for 4 hours.
4. After ensuring that the clay suspension is mixed with the chitosan solution, the pH is measured.
5. (1M) NaOH solution was added dropwise in to mixture under continuous stirring at 180 rpm. The pH of mixture measured and recorded after each addition of NaOH solution until its neutralization (pH 7-7.8), and the polymer precipitated from solution.
6. The composites Ca-Bt-CS were separated from aqueous phase by simple filtration and allowed to dry at 328 K.
7. The composites were manually ground to pass through 75μm mesh sieves.

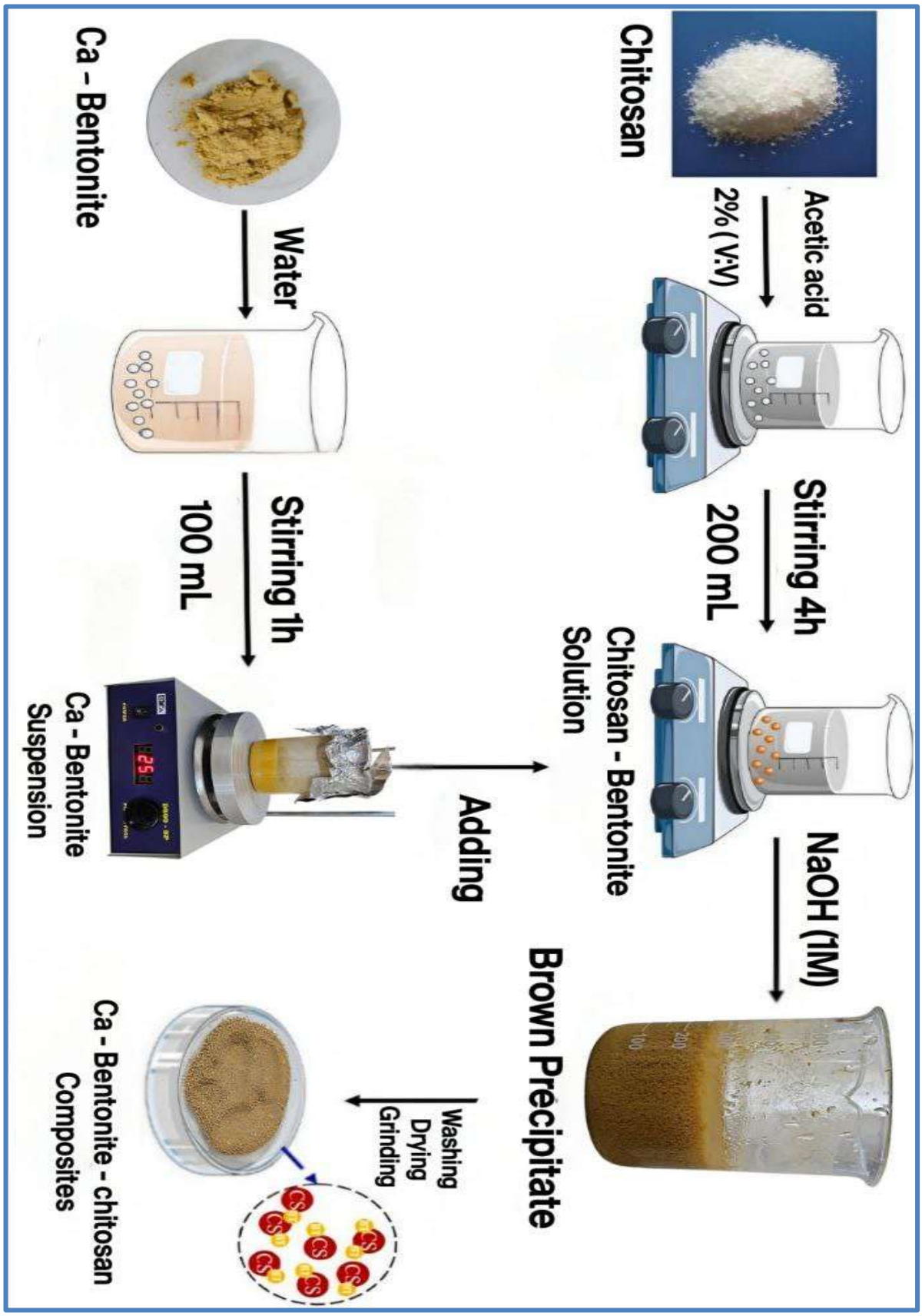

Figure 2-3: Schematic diagram of Preparation of (Ca-Bt-CS) composites.

Figure2-4: The modified clay

2.4.Characterization of adsorbents

2.4.1. Fourier Transform Infrared Spectroscopy (FT-IR)

Fourier Transform Infrared spectra for Iraqi natural and modified clay were recorded as (KBr) discs by using Shimadzu (FT-IR) spectrophotometer in the range (400-4000) cm^{-1}. The representation of the functional groups on the surfaces can be known through the FT-IR spectrum.

2.4.2. Field Emission Scanning Electron Microscopy (FE-SEM) Analysis

The surface morphology of the natural and modified clay were studies by using Field emission scanning electron microscopy (FE-SEM) technique type EM620 Eco.

2.4.3. Energy Dispersive X-ray Analysis (EDX-Elemental)

This technique is used to gives information about the composition of element .As a result of passing electrons beam through the atoms of sample an image of each

element obtained .This technique correlates with scanning electron microscope[87].

2.4.4. X-Ray Diffraction Spectroscopy (XRD)

X-ray diffraction (XRD) data were analyzed by Lab X, XRD 6000 instrument equipped. This instrument was employing CuKα 1as a target source (wave length1.54060 A°, at 30 mA and 40 KV) 2θ range from 16 to 80°.

2.5.Preparation of solutions used in adsorption process

2.5.1 Standard stock solution of Pb (II) ions (1000mg/L)

The standard stock solution is made by dissolving 1.590gm of (Pb $(NO_3)_2$ in 1L of deionized water, a standard stock solution of Pb (II) (1000 mg/L) ions was prepared. The solutions (5.000-80.000 mg/L) were prepared by diluting the stock solution with deionized water.

2.5.2 Standard stock solution of Cr (III) ions (1000mg/L)

The standard stock solution is made by dissolving 4.570gm of $Cr(NO_3)_3$ in 1 L of deionized water, a standard stock solution of Cr (III) (1000 mg/L) ions was prepared. The solutions (5.000-80.000 mg/L) were prepared by diluting the stock solution with deionized water.

Figure2-5: The Standard stock solutions of Cr(III) and Pb(II)

2.6 Batch adsorption process optimization (single system)

The natural bentonite's capacity to adsorb pb(II) and Cr(III) from aqueous solution was studied under number of optimized pH, adsorbent dosage, and contact time circumstances. The adsorption process was examined separately. The concentration of Pb (II) and Cr (III) ions solutions was analyzed using atomic absorption spectrophotometer (AAS). The absorbance of the solutions was determined at (λ_{max} = 217.0) nm for lead and (λmax = 357.9) nm for Chromium.

Figure 2-6: Atomic absorption spectroscopy instrument used in this study

2.6.1. Effect of contact time

The period that is adequate for adsorption system to reach equilibrium was done according to the procedures in which a volume of (25mL) of an initial concentration (50.0000 mg/L) of each Pb (II) and Cr (III), solutions were shaken with (0.1000 g) of adsorbents surface at a temperature (298K), shaking speed was (180) rpm. For Pb (II) adsorption on to natural and modified clay, the time ranged from (10 to 90min). To adsorp Cr (III) ions on to natural clay and modified clay, the time ranged from (5 to 60min).

2.6.2. Effect of clay mass

At a specific temperature (298 K), 25 mL of a constant concentration (50.0000 mg/L) of each Pb (II) and Cr (III) ions solutions with varying weights of Ca-bentonite and modified clay a (0.0500- 0.9000 g) were used in this project to examine the effect of clay dosage change on adsorption. The shaking speed was (180) rpm and the contact time of pb (II), Cr (III) on Ca-bentonite were (50, 35) minutes. The contact time of pb (II) and Cr (III) on the modified clay was (45, 15) minutes.

2.6.3. Effect of pH:

The effect of changing the acidity function on the percentage of removal and the adsorption process was studied by using concentrations of 50.0000 mg/L of each pb(II) and Cr(III), tested in various pH medium. NaOH (0.1 N) and HCl (0.1 N) were used to adjust the pH within the range of (2–7), and then the identical steps as in (2.6.1) were carried out. Using a pH-meter, the pH of the two systems at the adsorption concentration was determined, where the pH of the Pb(II) solution before adsorption was 5, while that of the Cr(III) solution was 3.

2.6.4 Temperature

To determine the fundamental thermodynamic functions, adsorption experiments were conducted at temperatures (298, 308, and 318 K) in the same way as described in Section 2.6.1.

2.7 Adsorption isotherms study

In order to demonstrate adsorption isotherms for Pb (II) and Cr (III) ions solutions on natural and modified clay, volumetric flasks containing (0.1000, 0.3000) g of natural clay and (0.0700, 0.1000) g of modified clay were used with 25 mL of metal ion solutions. Initial concentrations (5-80) mg/L. At three different

temperatures (298, 308 and 318). The pH = 5for natural and modified clay respectively. The flasks were agitated by a thermostatically controlled stirrer at (180) rpm for the required equilibrium time. The quantity of Pb (II) and Cr (III) ions adsorbed was measured from the initial and final concentrations andvolume of the solution, according to the following equation[88].

$$qe = \frac{(C_0 - C_e) * V}{m} \qquad (2.1)$$

Where:

qe: represents adsorbed amount of adsorbate per weight of adsorbent (mg/g)

C_0: Initial concentration (mg/L).

C_e: solute concentration at equilibrium (mg/L),

V: volume of solution (L)

m: weight of clay (g).

The percentage removal of the adsorbate (%R) was computed using the formula follow [81].

$$\%R = \frac{C_0 - Ce}{C_0} \times 100 \qquad (2.2)$$

Chapter Three

(Results & Discussion)

3. Characterization of Adsorbents

3.1Fourier Transform Infrared Spectroscopy (FT-IR) analysis

For further characterization of natural clay and modified clay, the important peaks observed in the FTIR spectrum and the structural units inferred with the help of available literature such as[89]. are recorded in Figures 3-1, 3-2, 3-3 and Table (3-1).

3.1.1 FT-IR analysis for Ca-bentonite clay

The FT-IR spectrum of Ca – bentonite clay recorded in the range 400 to 4000 cm^{-1} is shown in Figure 3-1

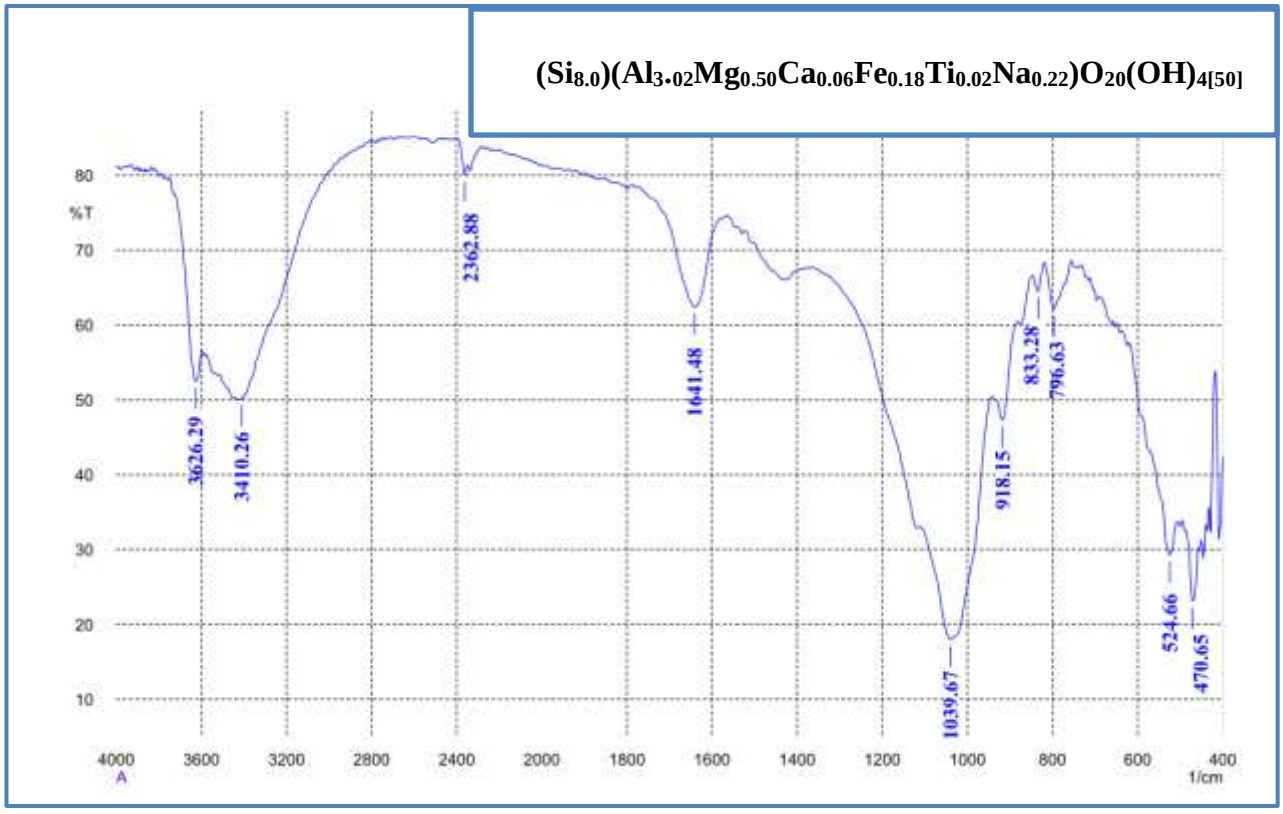

Figure 3-1: FT-IR Spectrum of Ca-bentonite clay

A sharp band observed at 3626.29 cm^{-1} represents the stretching vibration of (Al–Al–OH) in the mineral. At 918.15 cm^{-1},the band which less intense shows bending vibration of (Al–Al-OH)[90]. The water's stretching and bending vibrations at 3410.26, 1641.48 cm^{-1}, respectively. FTIR spectrum of Ca – bentonite shows the peaks (strong band at 1039.67, 542.66, 470.65 cm^{-1}), the first related to the stretching vibration of Si–O groups but another beaks indicated to bending mode.

The bands observed at 833.28, 796.63 cm^{-1} corresponding to bending vibrations of Al–Fe–OH and Al–Mg –OH respectively. Low intensity of these bands shows low content of Fe and Mg in clay[91].

3.1.2 FT-IR for Chitosan

The FT-IR test was used to assess the functional groups present in the chitosan. In Figure 3-2, we can observe the infrared spectrum of chitosan. A strong band in the region 3383.26 cm^{-1} corresponds to N-H and O-H stretching, as well as the intramolecular hydrogen bonds.

The absorption bands at around 2875.96 cm^{-1} can be attributed to C-H stretching. This band is characteristics typical of polysaccharide and are found in other polysaccharide spectra, such as xylan[92].

The presence of residual N-acetyl groups was confirmed by the bands at around 1654.98 cm^{-1} (C=O stretching of amide) and 1319.35 cm^{-1} (C-N stretching of amine), respectively. The band at 1599.04 cm^{-1} corresponds to the N-H bending of the primary amine[93].

The CH_2 bending and CH_3 symmetrical deformations were confirmed by the presence of bands at around 1421.58 and 1379.15 cm^{-1}, respectively. The absorption band at 1157 cm^{-1} can be attributed to asymmetric stretching of the C-

O-C bridge. The bands at 1599.04 (N-H) bending and 1078.24 cm^{-1} correspond to C-O stretching[94].

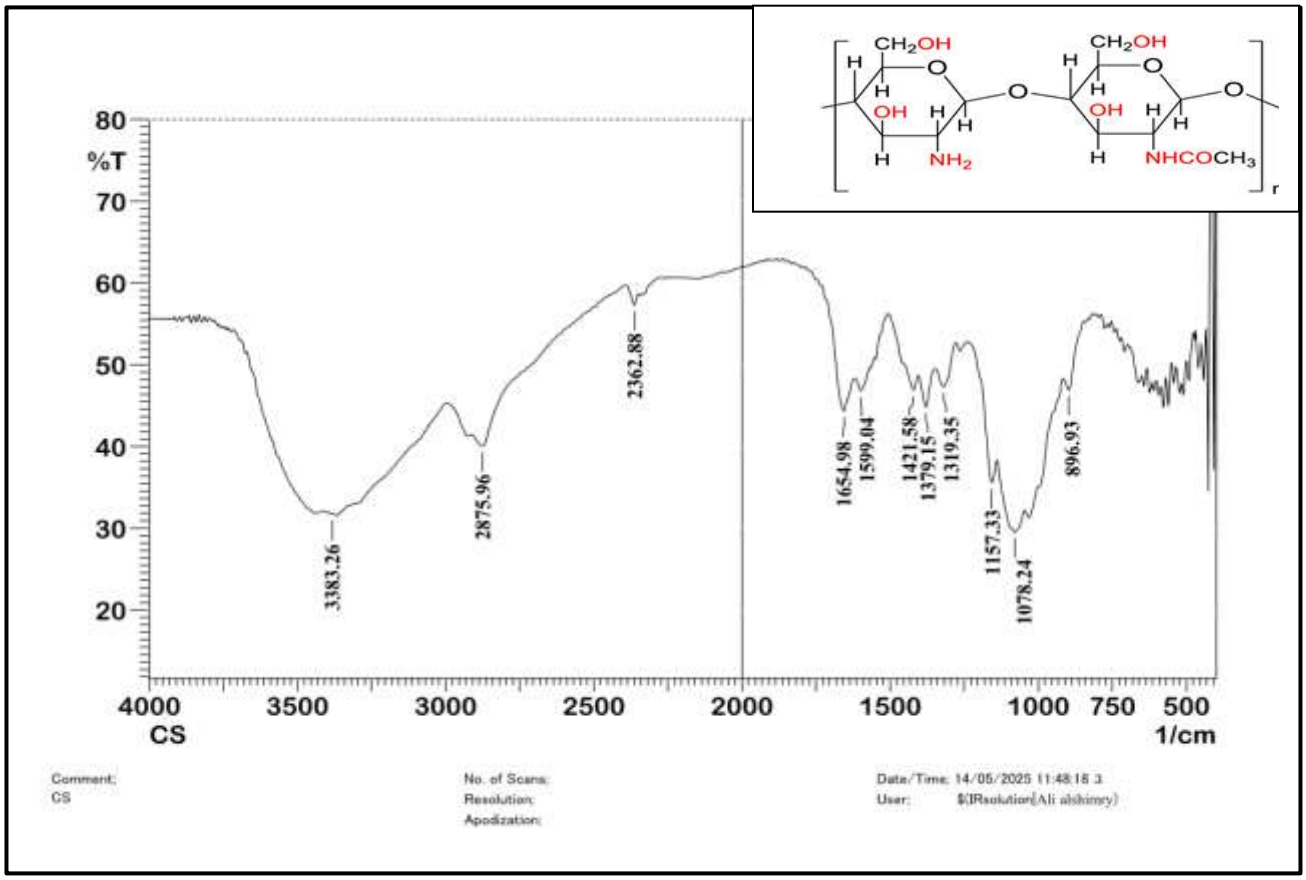

Figure 3-2: FT-IR Spectrum of Chitosan

3.1.3 FT-IR for Ca-bentonite-chitosan composite

Figure 3-3 present the FT-IR spectrum of Ca – bentonite – chitosan. From the spectrum, a sharp band at 3618.58 cm^{-1} was observed. It shows the present of hydroxyl group which is coordinated with octahedral cations like Al^{+3}. The absorption bands of O-H groups which appeared at 3423.76 cm^{-1} overlapped with N-H amine because O-H and N-H stretching vibration at similar frequencies. The peak of amine also appeared at 1548.89 cm^{-1}. The peak at 2929.97 cm^{-1} is attributed to C-H of the polymer and clarified the existence of bending vibration at 1425.44 cm^{-1} [95]. The bands at 1016.52 , 430.14 cm^{-1} were represented the Si-O

stretching and bending vibration which confirmed the presence of montmorillonite.Typical montmorillonite also observed at peak 920.08 cm^{-1} which indicate to the bending vibration of Al-O-Al.

Other peaks at 840.99 and 798.56 cm^{-1} correspond to vibrations of octahedral Al-O. From the FT-IR spectrum, it show the appearance of peak 2929.97 cm^{-1} , the peak at 1016.52 cm^{-1} becomes broader and a gradual decrease in the intensity of the hydroxyl groups is observed. According to the results, the chitosan was successfully loaded on clay without changing the basic structure of the clay and this agreement with[96] .

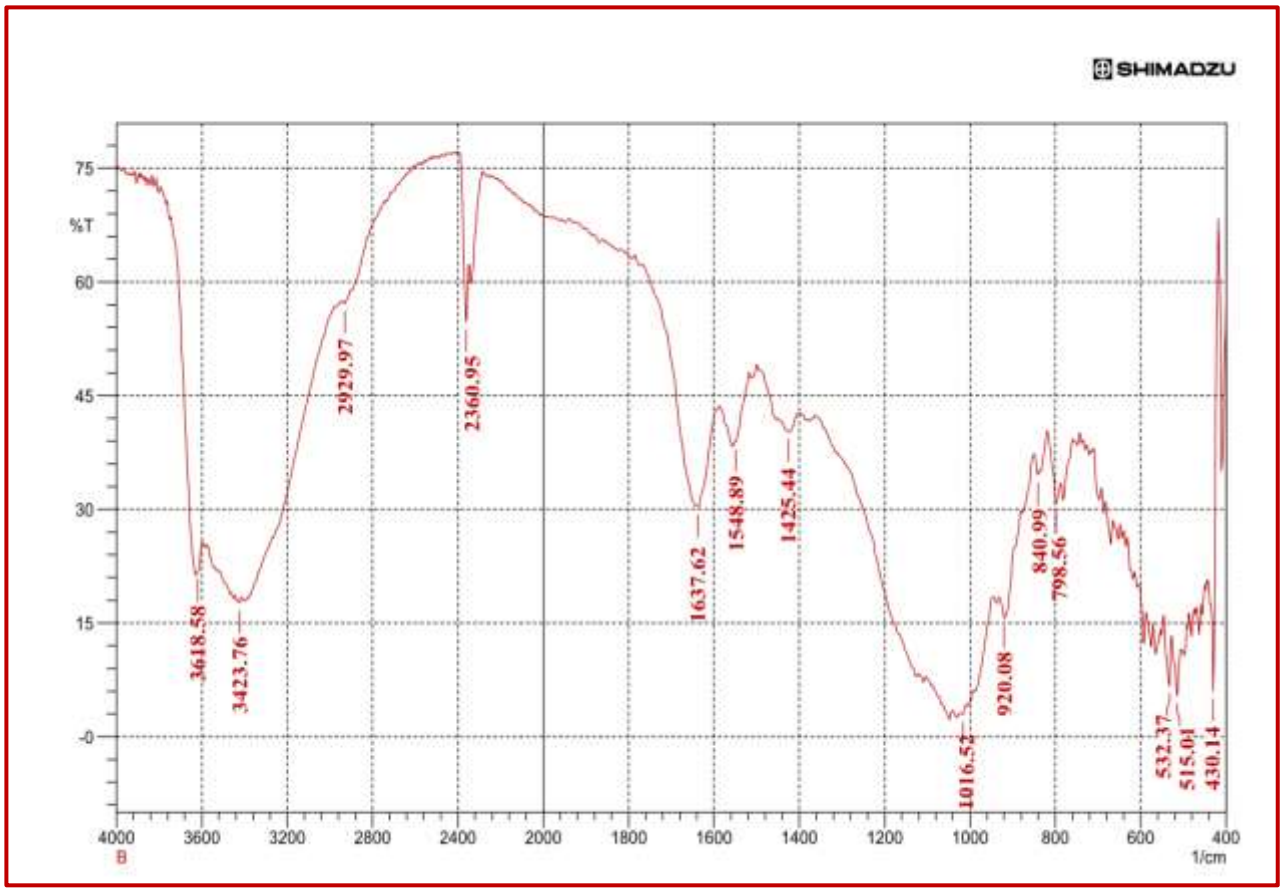

Figure 3-3: FT-IR Spectrum of Ca-bentonite-chitosan composite

Table (3-1): Characteristic of FT-IR absorption band (cm^{-1}) of the natural and modified clays

	Ca-bentonite	Ca-bentonite-chitosan	
No.	**Wave number cm^{-1}**	**Wave number cm^{-1}**	**Assignment**
1.	**3626.29**	**3618.58**	**Stretching vibration of (Al–Al–OH)**
2.	**3410.26**	**-**	**water's stretching vibration**
3.		**3423.76**	**O-H groups overlapped with N-H amine**
4.	**-**	**2929.97**	**C-H of the polymer stretching vibration**
5.	**1641.48**	**1637.62**	**water's bending vibrations**
6.	**-**	**1548.89**	**Amine bending**
7.	**-**	**1425.44**	**C-H of the polymer bending vibration**
8.	**1039.67**	**1016.52**	**Stretching vibration of Si–O groups**
9.	**918.15**	**920.08**	**Bending vibration of (Al–Al-OH)**
10.	**833.28**	**840.99**	**Bending vibrations of Al–Fe–OH**
11	**796.63**	**798.56**	**Bending vibrations of Al–Mg –OH**
1.	**542.66**	**532.37**	**Si–O groups bending vibration**
13	**470.65**	**430.14**	**Si–O groups bending vibration**

3.2 Field Emission Scanning Electron Microscopy FE-SEM Analysis for adsorbents

The FE-SEM images of the Ca-bentonite and Ca-bentonite–chitosan composite are presented in Figure 3-4(A, B).The FESEM image Figure 3-4A of natural clay reveals a combination of acicular and plate structure, which are

characteristic of natural bentonite. Some of regions of sample are displayed elongated, rod–like structures. The majority of mineral consists of thin closely packed layers, which align with the typical layered silicate structure of bentonite[97].

The dense staking of layers and needle – like structure limits surface accessibility and reduces a available adsorption sites and low surface area in its raw form. The FESEM image Figure 3-4.B of modified clay exposes significant structural changes compared to raw bentonite, suggesting that chitosan has successfully intercalated between layers, increasing the available surface area for adsorption[98].

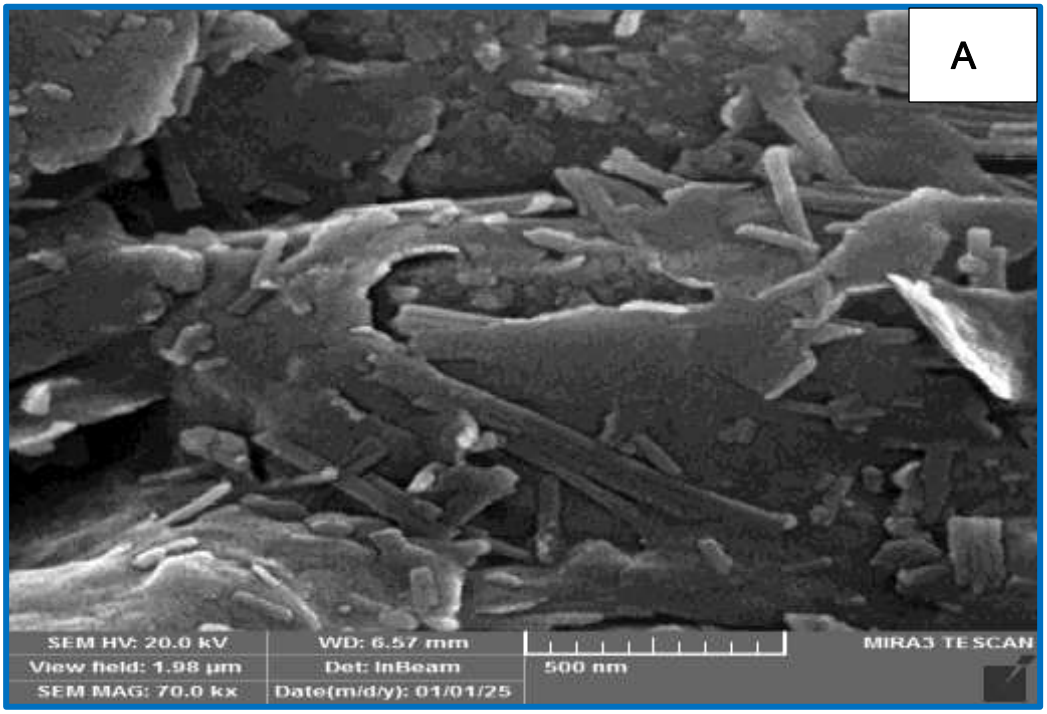

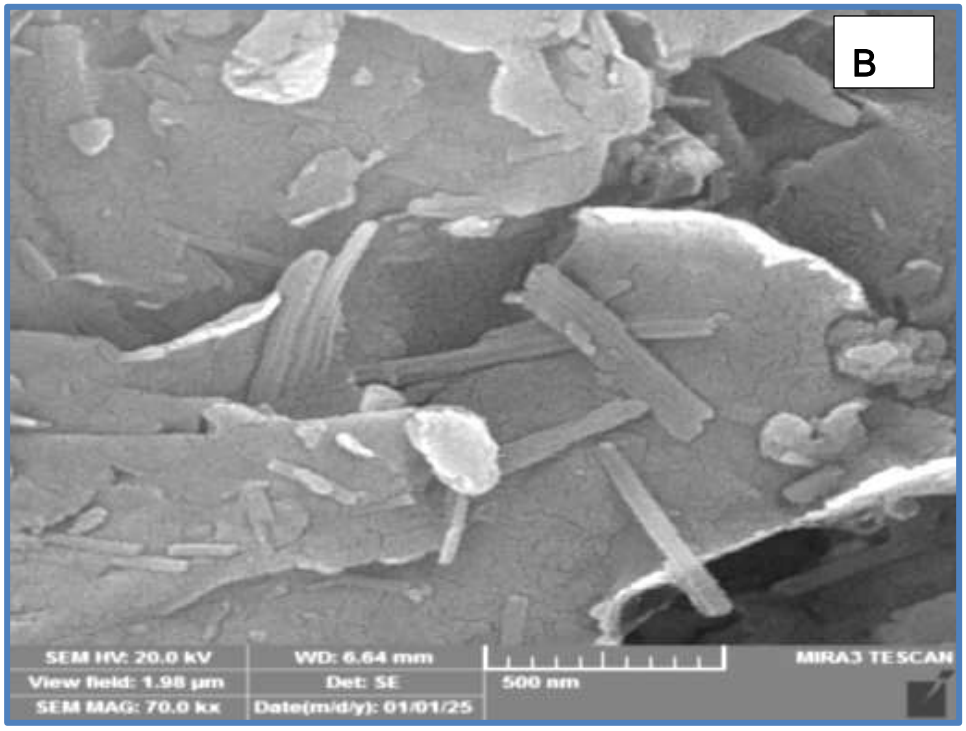

Figure 3-4: FE-SEM images (A) Ca-bentonite clay, (B) Ca-bentonite-chitosan composite

3.3 Energy-Dispersive X-ray Spectroscopy EDX analysis for adsorbents

Energy-dispersive X-ray spectroscopy (EDX) provides critical insights into the elemental composition of raw Ca-bentonite and its modified composite. When an electron beam strikes the sample, it generates characteristic X-rays, which are analyzed to identify and quantify the present elements[99].Qualitative analysis pinpoints the positions of elemental peaks (e.g., Si, Al, and Ca for Ca-bentonite; additional C and N for the composite), while quantitative analysis measures their relative abundances based on peak intensities[100][1]. As illustrated in Figure 3-5(A, B, C) and Table (3-2), EDX results confirmed the successful functionalization of Ca-bentonite with chitosan, demonstrated by the emergence of carbon and nitrogen signals

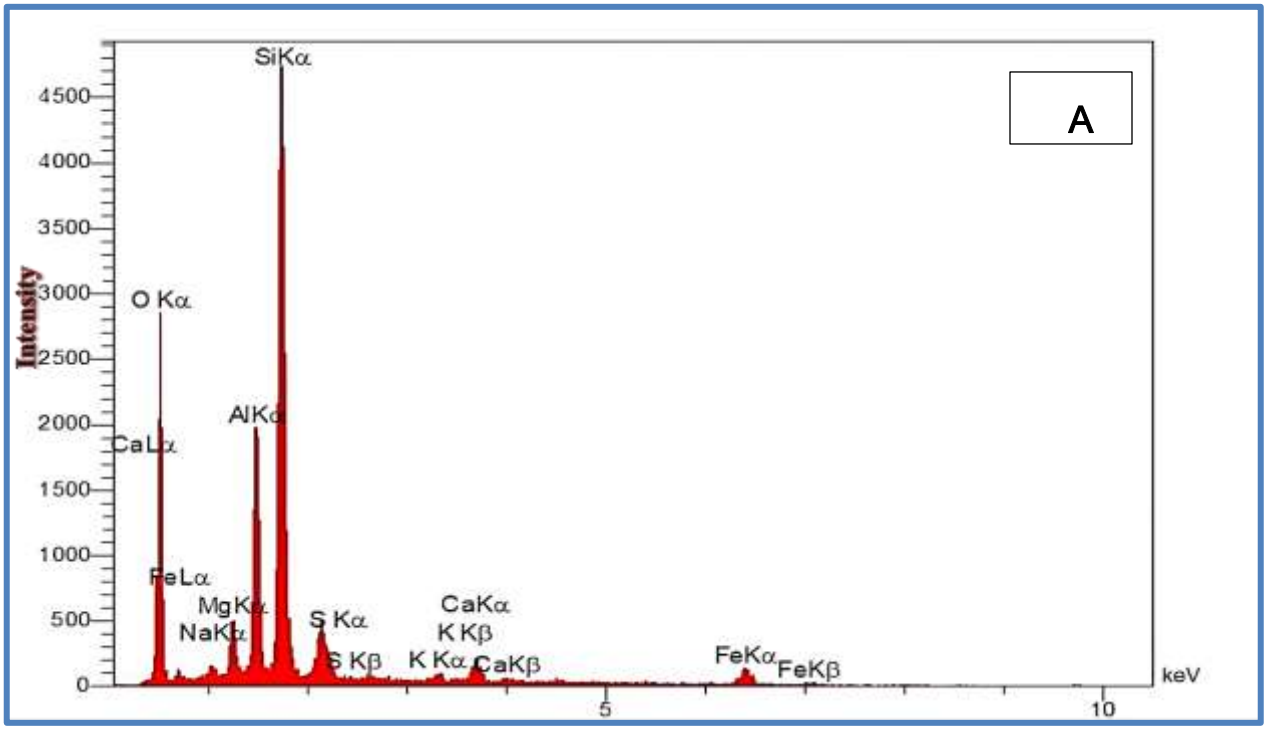
A
Intensity
SiKα
O Kα
AlKα
CaLα
FeLα
MgKα
NaKα
S Kα
S Kβ
CaKα
K Kβ
K Kα
CaKβ
FeKα
FeKβ
keV
4500
4000
3500
3000
2500
2000
1500
1000
500
0
5
10

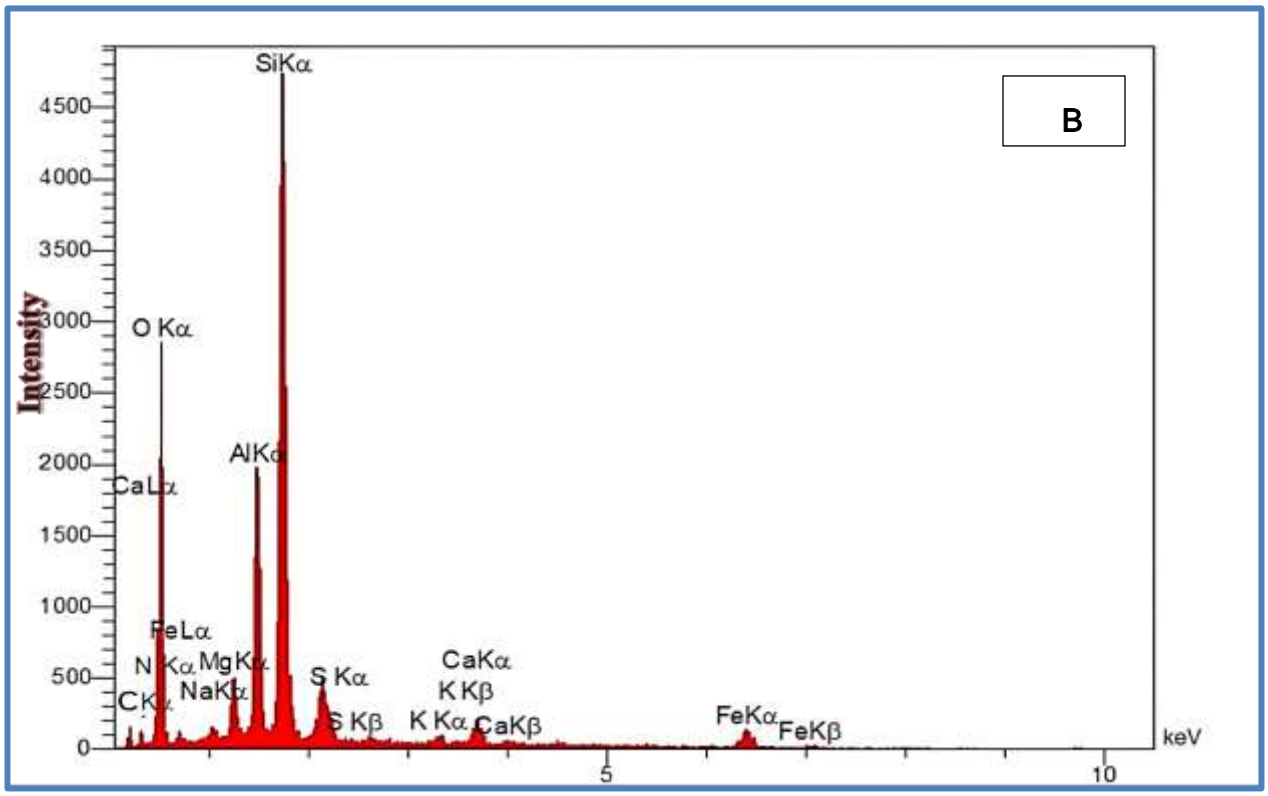
B
Intensity
SiKα
O Kα
AlKα
CaLα
FeLα
NKα
MgKα
NaKα
CKα
S Kα
S Kβ
CaKα
K Kβ
K Kα
CaKβ
FeKα
FeKβ
keV
4500
4000
3500
3000
2500
2000
1500
1000
500
0
5
10

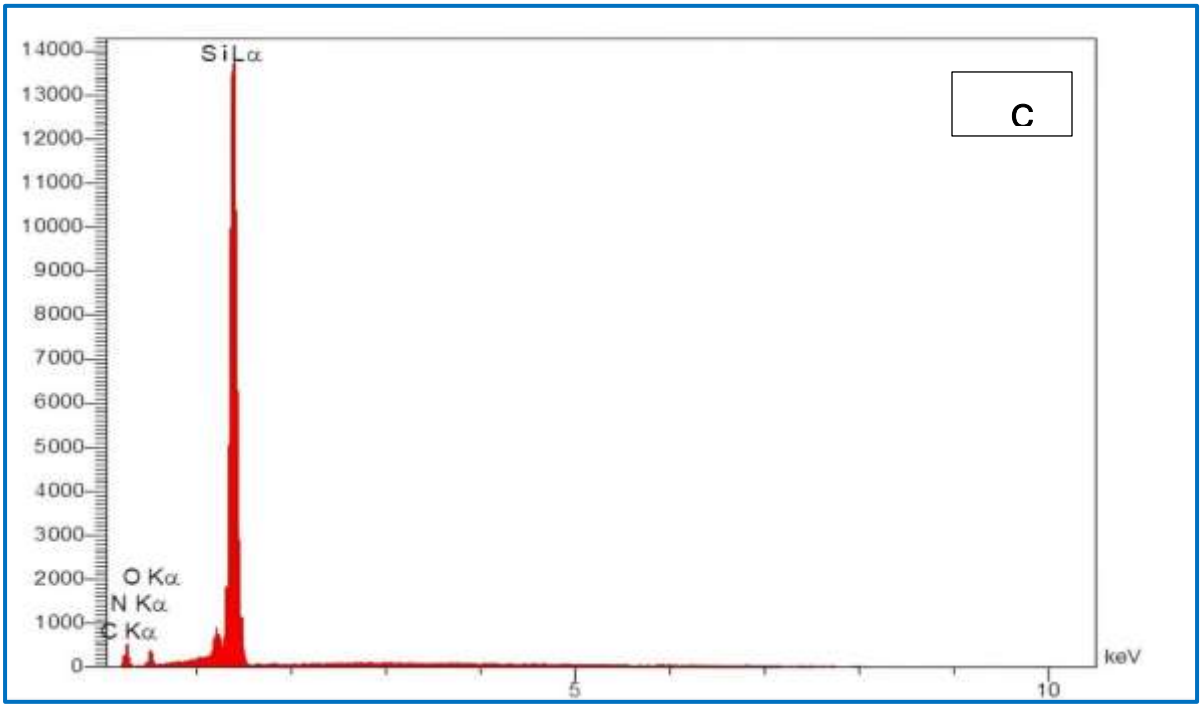

Figure 3-5: EDX images (A) Ca-bentonite clay (B) Ca-bentonite-chitosan composite (C) magnified EDX image of Ca-bentonite-chitosan composite

The EDX analysis reveals distinct differences between natural and modified bentonite. The presence of carbon (25.91 wt. %) and nitrogen (2.78 wt. %) in the modified sample confirms the successful modification and incorporation of chitosan onto the clay surface. The increase in oxygen content (from 50.40% to 53.95%) further supports surface modification.

Meanwhile, the relatively stable levels of key structural elements such as silicon and calcium suggest that the clay's fundamental structure remained intact after modification. These compositional changes reflect improvements in surface chemistry that may enhance the adsorption efficiency. Decreased Na (0.63→0.32 wt%) and Ca (2.16→2.00 wt%) suggest ion exchange between metal cations and protonated amino groups ($-NH_3^+$) of chitosan. Reduced Al (9.86→8.13 wt%) and Fe (5.26→4.86 wt%) percentages indicate possible surface masking by chitosan layers[101].

Table (3-2): Result of EDX elemental identification of natural clay and modified clay

No.	Elements	Natural clay Int	Natural clay(% w)	Natural clay(% A)	Modified clay Int	Modified clay (% w)	Modified clay(%A)
1	C	-	-	-	136.1	25.91	59.98
2	N	-	-	-	10.8	2.78	5.51
3	O	724.6	50.40	65.43	779.4	53.95	68.62
4	Na	26.1	0.63	0.57	12.5	0.32	0.28
5	Ca	90.0	2.16	1.12	101.7	2.00	1.68
6	Mg	132.8	2.25	1.92	113.3	2.52	1.28
7	Al	670.8	9.86	7.59	532.6	8.13	6.13
8	Si	1781.3	26.13	19.32	1770.4	26.55	19.24
9	Fe	82.9	5.26	1.96	74.0	4.86	1.77
10	S	150.9	2.82	1.83	57.7	1.11	0.71

%W: The mass of each element relative to the total mass of the sample.

%A: The ratio of atoms of a given element to the total number of atoms in the sample

Int: Signal intensity

3.4 X-Ray Diffraction Spectroscopy (XRD)

The X-ray diffraction (XRD) patterns was used to investigate the mineral composition of Ca-bentonite before and after modification with chitosan (figures 3-6, 3-7 and Table 3-3). The key mineral phases were identified:

1- The peak at 2θ =20.920° (d = 4.434 A°) indicate the presence of the montmorillonite mineral in natural clay[102]. After modification, the XRD pattern of modified clay shows the characteristic crystalline peak at 2θ = 19.874°(d = 4.464A°). This shift of reflection of natural clay to lower angle indicating a slight expansion (Δd=+0.031A°), due to chitosan intercalation [95].

2- Slight variations in quartz peaks where the peaks changed from 26.77°(d = 3.32A°), 39.53°(d = 2.27A°) for natural clay to 26.59°(d = 3.34A°) and 39.41°(d = 2.28A°) for modified clay, indicating that quartz crystals are not affected by the process[103].

3- The XRD difractogram of natural clay shows peak at 29.48° (d =3.02A°) corresponding calcite. The low intensity and slight decreasing of this peak to 28.27° (d = 3.15A°), which may indicate a slight interaction between chitosan and carbonates in the modified clay[98], and with surface Ca^{+2} ions[104].

Table 3-3: Comparative XRD analysis of Ca-Bentonite clay and Ca-Bentonite-Chitosan composite

Ca- Bentonite clay					**Ca- Bentonite- Chitosan composite**				
2-θ	**d**	**Height**	**I %**	**FWHM**	**2-Theta**	**d**	**Height**	**I %**	**FWHM**
20.92	**4.433**	**65**	**32.7**	**0.414**	**19.874**	**4.464**	**100**	**32.9**	**0.227**
26.77	**3.327**	**199**	**100**	**0.356**	**26.599**	**3.348**	**419**	**100**	**0.238**
39.53	**2.277**	**65**	**32.7**	**0.381**	**39.416**	**2.284**	**69**	**16.5**	**0.286**
29.489	**3.026**	**104**	**52.3**	**0.377**	**28.272**	**3.154**	**128**	**23.2**	**0.224**

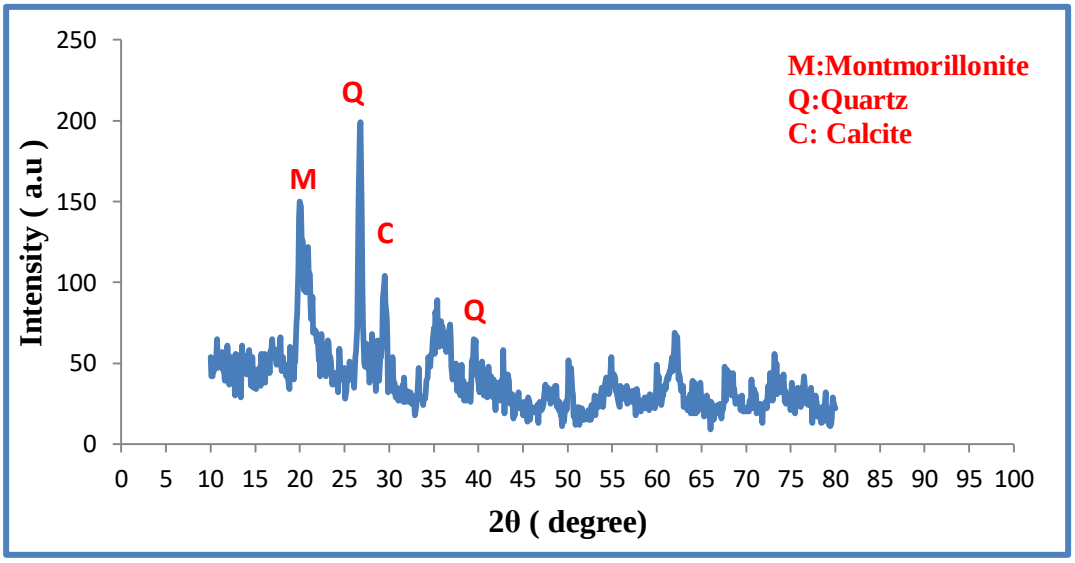

Figure 3-6 XRD spectra of Ca-bentonite clay

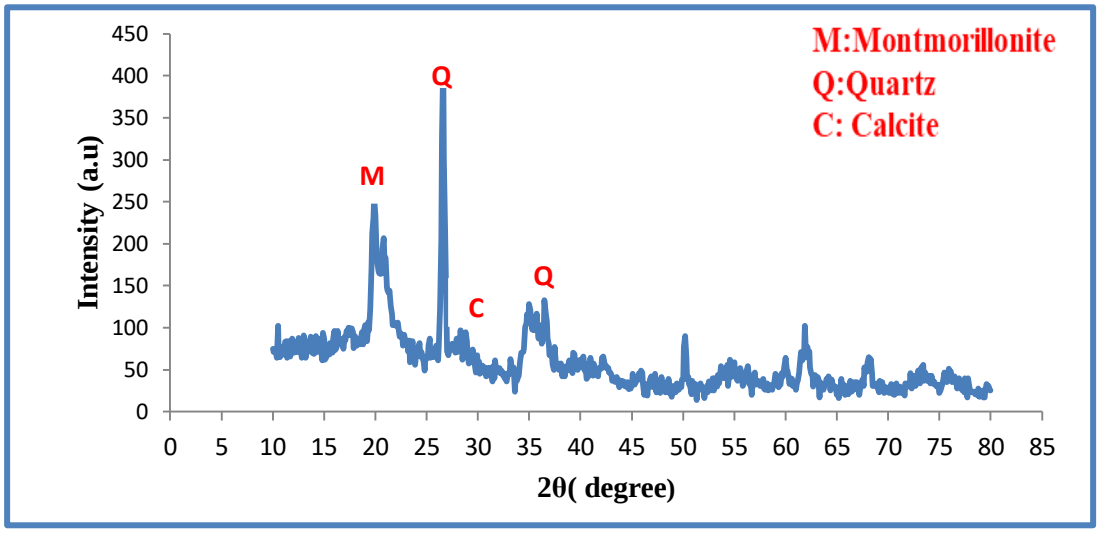

Figure 3-7: XRD spectra of Ca-bentonite-chitosan composite

3.5 Study of factors affecting on adsorption process

3.5.1 Contact time effect

The effect of contact time on adsorption of pb (II), Cr (III) ions from their aqueous solutions in mono-system onto Calcium bentonite and calcium bentonite Chitosan clays at 298K were studied using a fixed initial concentration (C_0 = 50

mg/L), fixed weight (0.1) g, agitation speed 180 rpm, and tested at various periods (10 - 90) min. for Pb (II) adsorption on to natural and modified clays.

To adsorb Cr (III) ions on to natural and modified clays, the time ranged from (5 to 60min). The investigations were carried out in accordance with the procedures described in (section 2.6.1). Table (3-4) indicates the experimental data for the natural and modified clay. The plots of R% vs time are shown in Figures 3-8, 3-9, 3-10 and 3-11. The time required for pb (II), Cr (III) ions on Calcium bentonite and calcium bentonite Chitosan to achieve equilibrium was (50, 35) minutes and (45, 15) minutes respectively. The results showed that adsorption removals for pb (II), Cr (III) ions on natural and modified clay were rapidly increased for the first 10 minutes and continued gradually to increase to a certain time and then stabilized.

The initial quick adsorption was most likely caused by initial concentration slope between amount of vacant sites available and adsorbate in solution on the natural surface. The steady increase in adsorption and, as a result, the achievement of equilibrium adsorption can be explained by the transfer of mass of adsorbate particles from bulk liquid to outer surfaces of natural clay[105] .The adsorption of two ions on modified clay, the dramatically increase of Pb(II) and Cr(III) removal rate in the first 10 mins is due to the higher concentration of metal ions in solution, providing a strong driving force for Pb(II) and Cr(III) ions to interact with the adsorbent. In addition, there were relatively higher free adsorption vacancies on the surface of modified clay, where a strong adsorption affinity to Pb(II) and Cr(III) was generated. As time went on, the Pb(II) ions gradually occupied the adsorption sites from modified clay until the equilibrium was finally reached between adsorption and desorption[106] .

Table (3-4): Contact time effect on adsorption removal of pb(II),and Cr(III) ions onto Ca-bentonite and Ca- bentonite-chitosan composite

Clays									
Metal ions	Ca- bentonite					Ca-bentonite-chitosan composite			
	Time (min)	C_0(mg/L) Pb(II)	Ce(mg/L) Pb(II)	R%	Contact time	Time(min)	Ce(mg/L) Pb(II)	R%	Contact time
Pb(II)	10	50.0000	30.5172	38.9654	50	10	29.7532	40.4936	45
	20	50.0000	25.1875	49.6250		20	12.5415	74.9170	
	30	50.0000	19.2845	61.4308		30	5.2431	89.5138	
	45	50.0000	10.6143	78.7712		45	0.8370	98.3260	
	50	50.0000	3.5172	92.9654		60	0.7837	98.4326	
	60	50.0000	3.5072	92.9854		75	0.7459	98.5082	
	75	50.0000	3.6284	92.7431		90	0.7513	98.4974	
	90	50.0000	3.7362	92.5276					
	Time (min)	C_0(mg/L) Cr(III)	Ce(mg/L) Cr(III)	R %	Contact time	Time (min)	C_0(mg/L) Cr(III)	Ce(mg/L) Cr(III)	Contact time
Cr(III)	5	50.0000	21.3200	57.3600	35	5	17.751	64.498	15
	10	50.0000	20.5430	58.9140		10	10.5767	78.8466	
	15	50.0000	18.4000	63.200		15	2.3750	95.2500	
	25	50.0000	15.5040	68.9920		25	2.7660	94.4680	
	35	50.0000	9.8080	80.3840		35	2.7600	94.4800	
	45	50.0000	9.9100	80.8100		45	2.7000	94.6000	
	60	50.0000	9.7100	80.5800		60	2.7000	94.6000	

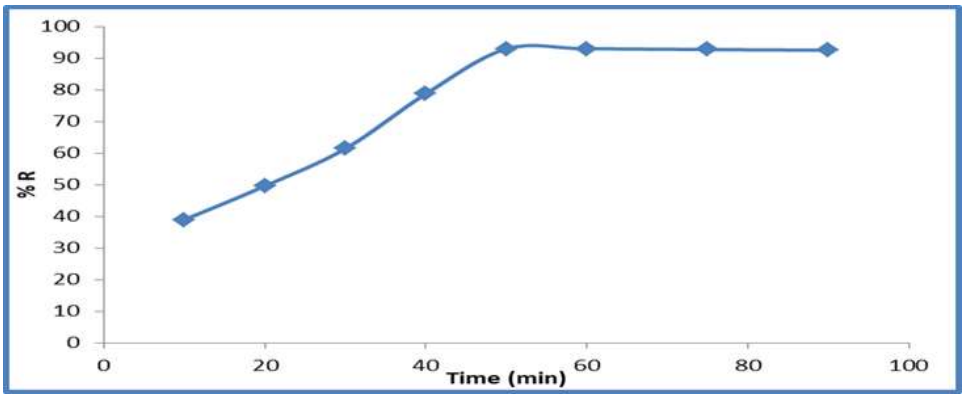

Figure 3-8: Contact time effect on adsorption percentage of pb (II) ions on Ca-bentonite clay

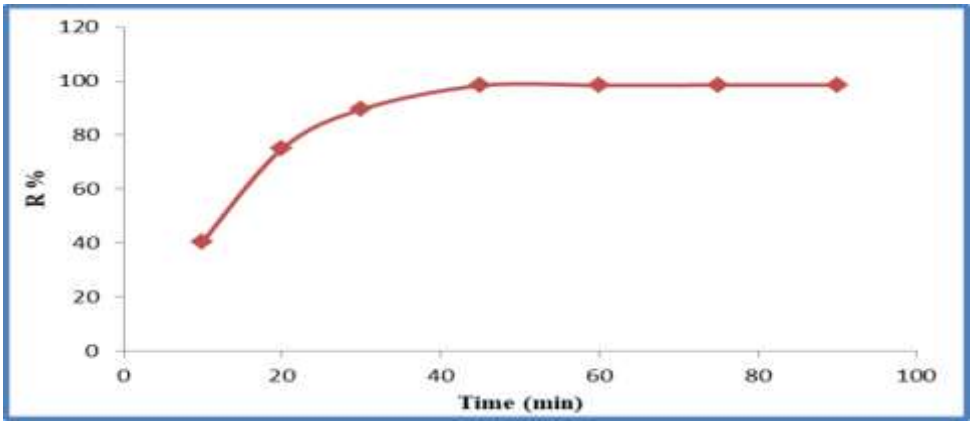

Figure 3- 9: Contact time effect on adsorption percentage of pb (II) ions on of Ca-bentonite-chitosan composite

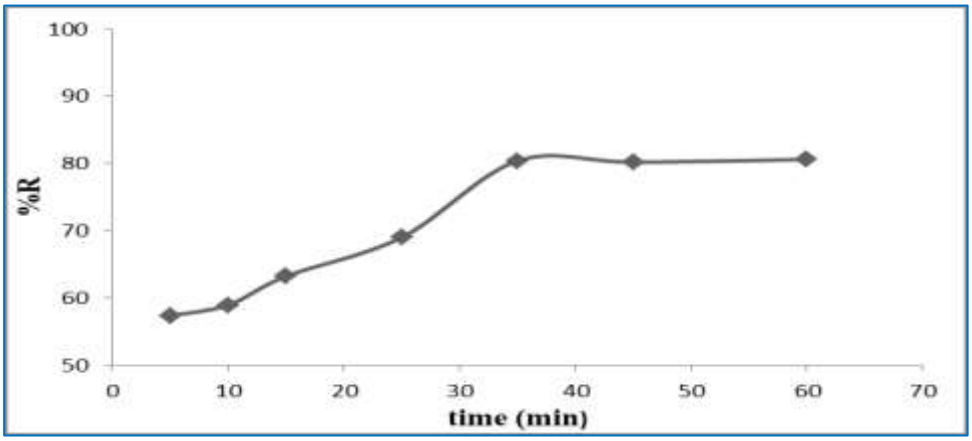

Figure 3-10: Contact time effect on adsorption percentage of Cr (III) on Ca-bentonite clay

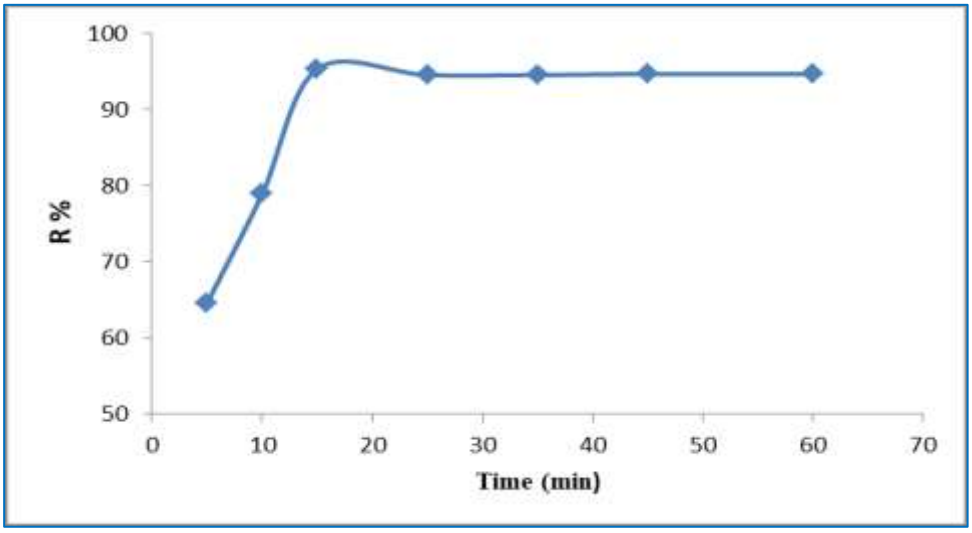

Figure 3-11: Contact time effect on adsorption percentage of Cr (III) on Ca-bentonite-chitosan composite

3.5.2 Adsorbent mass effect

The effect of the adsorbent mass that was used to adsorb pb(II) and Cr(III) ions from their aqueous solutions in a single system was studied at 298 K, with a solution volume of 25mL and a fixed initial concentration of 50 mg/L for both ions. Different masses of the two surfaces were tested according to the procedures mentioned in section (2.6.2). The results of the study on the effect of adsorbent mass for pb (II) and Cr(III) ions are shown in Tables(3-5) and Figures 3-12, 3-13, 3-14,and 3-15. Through the results of the experiment, it was noted that the ideal mass of the adsorbents were 0.1, 0.3 g for natural clay when adsorbed pb(II) and Cr(III) ions respectively, while for modified clay it were 0.07 and 0.1 g for adsorbe both ions.

The experimental results indicated that as the amount of adsorbent increased, the removal of adsorption increased until the optimum mass for the adsorbent was reached, where the removal percentage remained stable without significant change regardless of the amount of adsorbent used.

Table (3-5): Adsorbent mass effect on adsorption removal of pb(II), and Cr(III) ions onto Ca- bentonite caly and Ca- bentonite-chitosan composite

Clays									
Metal ions	Ca- bentonite					Ca-bentonite-chitosan composite			
	Mass(g) adsorbent	C_0(mg/L) Pb(II)	Ce(mg/L) Pb(II)	R%	Optimum mass	Mass(g) adsorbent	Ce(mg/L) Pb(II)	R%	Optimum mass
pb(II)	0.0500	50.0000	7.6580	84.6840	0.1000 g	0.0500	1.8820	96.2362	0.0700 g
	0.0700	50.0000	4.4930	91.0140		0.0700	0.6570	98.6869	
	0.1000	50.0000	3.6181	92.1637		0.1000	0.7580	98.4835	
	0.3000	50.0000	3.5270	92.9460		0.3000	0.7890	98.4216	
	0.5000	50.0000	3.5440	92.9120		0.5000	0.7850	98.4303	
	0.7000	50.0000	3.5980	92.8040		0.7000	0.7870	98.4260	
	0.9000	50.0000	3.5880	92.8240		0.9000	0.7910	98.4180	
	Mass(g) adsorbent	C_0(mg/L) Cr(III)	Ce(mg/L) Cr(III)	R %	Optimum mass	Mass(g) adsorbent	C_e(mg/L) Cr(III)	R %	Optimum mass
Cr(III)	0.0500	50.0000	23.214	53.57	0.3000	0.0500	1.757	96.48	0.1000
	0.0700	50.0000	13.428	73.14		0.0700	1.042	97.91	
	0.1000	50.0000	9.7485	80.5030		0.1000	0.9	98.2	
	0.3000	50.0000	7.5714	84.8571		0.3000	0.758	98.48	
	0.5000	50.0000	7.5421	84.9158		0.5000	0.614	98.77	
	0.7000	50.0000	7.5410	84.9180		0.7000	0.543	98.91	
	0.9000	50.0000	7.6380	84.7240		0.9000	0.5712	98.85	

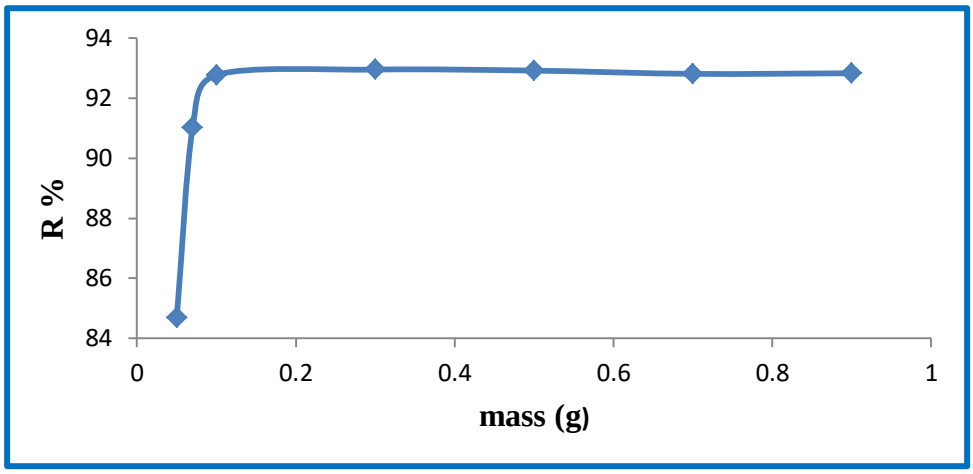

Figure 3-12: Adsorbent mass effect on adsorption percentage of pb (II) ions onCa-bentonite clay

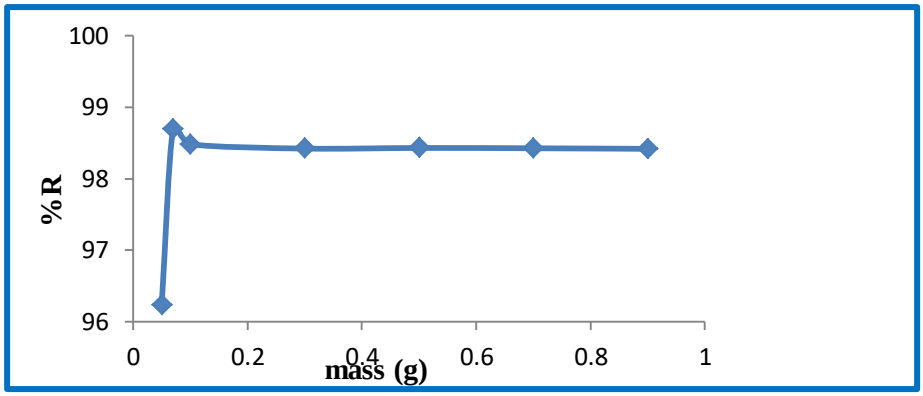

Figure 3-13: Adsorbent mass effect on adsorption percentage of pb (II) ions on Ca-bentonite-chitosan composite

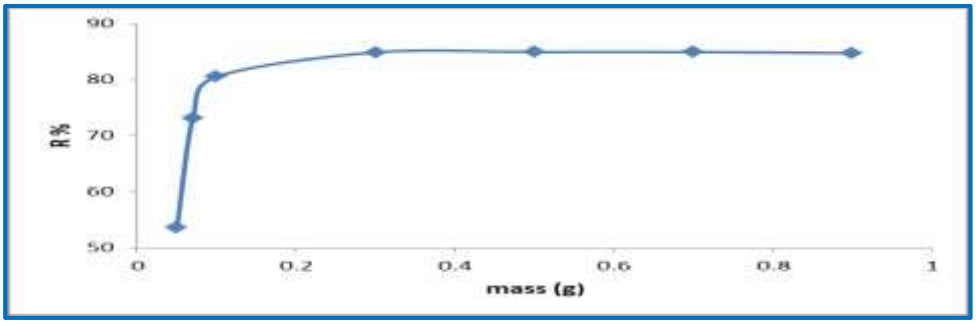

Figure 3-14: Adsorbent mass effect on adsorption percentage of Cr(III) ions on Ca-bentonite clay

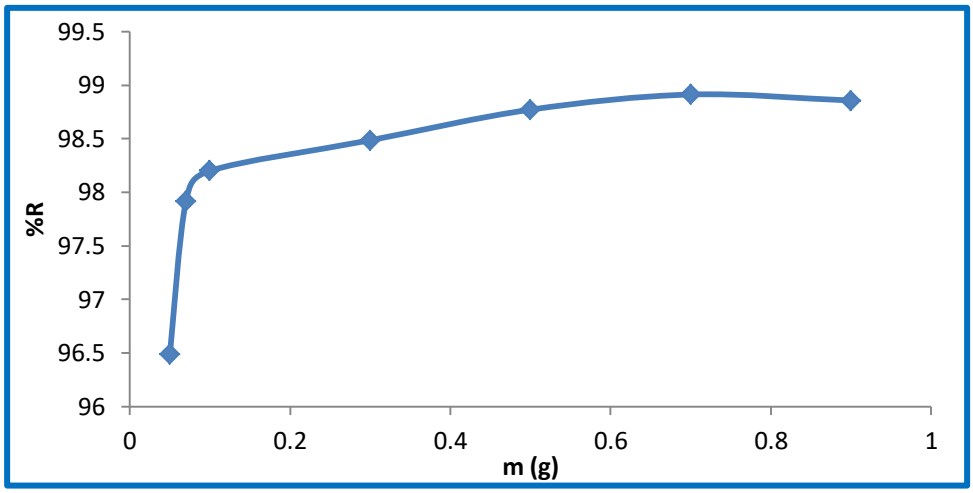

Figure 3-15: Adsorbent mass effect on adsorption percentage of Cr(III) ions on Ca-bentonite-chitosan composite

These results can be explained based on the following reasons:

1. At the beginning of the adsorption process (the first stage), more active adsorption sites become available as the adsorbent dose increases, increasing the chances of collisions between ions and the adsorption sites[107].

2. The stabilization stage (the removal percentage remains stable without significant change) is due to the aggregation of adsorbent molecules, which reduces the effective surface area[108].

3. The active sites become saturated, so increasing the amount of adsorbent does not make a significant difference[105].

4. The concentration of residual ions in the solution required for adsorption decreases[109]. The role of modifying bentonite with chitosan, increasing functional density: The addition of chitosan adds functional groups (-NH_2, -OH) that increase the surface affinity for ions, improving removal even at low doses[95]

3.5.3 pH effect

The pH of the aqueous solution is an important variable governing metal adsorption. Hence, it is obvious that this is partly due to the fact that the competition between hydrogen ions and the solution of pH affect the chemical composition as well as the ionization of the functional groups onto the adsorbent surface .Different PH values (2-7) of the two surfaces were tested according to the procedures mentioned in section (2.6.3), where the pH of the Pb(II) solution before adsorption was 5, while that of the Cr(III) solution was 3.

The results of the study on the effect of pH for pb (II) and Cr(III) ions are shown in Tables(3-6) and Figures 3-16, 3-17, 3-18,and 3-19. Through the results of the experiment, it was noted that the ideal pH of the adsorption of two ions on natural and modified clays was 5. The experimental results indicated that at low pH (high acidity conditions), hydronium ions compete with metal ions on the surface of natural clay, hindering the access of metal ions due to charge repulsion on the surface active sites. As pH increases, [H_3O^+] concentration decreases, allowing metal ions to reach the clay surface and increasing the removal percentage[110], where for pb(II) 93.44% and Cr(III) 98.34%at pH = 5.

From Figures 3-14 and 3-17, due to the high pH value, the removal percentage of both metal ions increases when they are adsorbed onto the modified clay at pH = 5. The main reason for this phenomenon is that the $–NH_2$ group in chitosan binds to [H^+] in the solution, forming a $–NH_3^+$, which binds to the negatively charged bentonite surface[95].

When pH decreases (hydronium ions increase), they compete with chitosan to bind to the clay surface, thus decreasing the removal percentage at low pH.

The removal efficiency increases when the PH is higher than 6 because metals ions precipitate from the solution as hydroxides[111].

Table (3-6): pH effect on adsorption removal of pb(II), and Cr(III) ions onto Calcium bentonite clay and calcium bentonite Chitosan composite

Metal ions	Clays								
	Ca- bentonite					Ca-bentonite-chitosan composite			
Pb(II)	pH	C_0(mg/L) Pb(II)	Ce(mg/L) Pb(II)	R%	Optimum PH	pH	Ce(mg/L) Pb(II)	R%	Optimum pH
	2	50.0000	25.3200	49.3600	5	2	27.4200	45.1600	5
	3	50.0000	24.4700	51.0600		3	14.7220	70.5560	
	5	50.0000	3.2780	93.4440		5	0.9831	98.0338	
	6.5	50.0000	3.0720	93.8560		6.5	0.9599	98.0801	
	7	50.0000	-	-		7	-	-	
	pH	C_0(mg/L) Cr(III)	Ce(mg/L) Cr(III)	R %		pH	Ce(mg/L) Cr(III)	R %	
Cr(III)	2	50.0000	13.4320	73.1360	5	2	14.3714	71.2571	5
	3	50.0000	10.8760	78.2480		3	5.3285	89.3428	
	5	50.0000	0.8285	98.3429		5	0.47145	99.0571	
	6	50.0000	0.4714	99.0571		6	0.4285	99.1428	
	6.5	50.0000	0.4714	99.0571		6.5	0.4714	99.0571	
	7	50.0000	-	-		7	-	-	

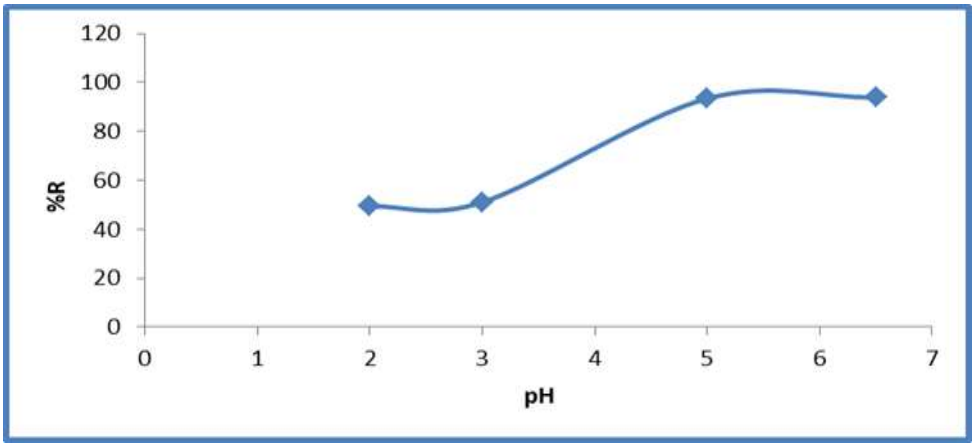

Figure 3-16: Effect of pH for adsorption percentage of pb(II) onto Ca-bentonite clay

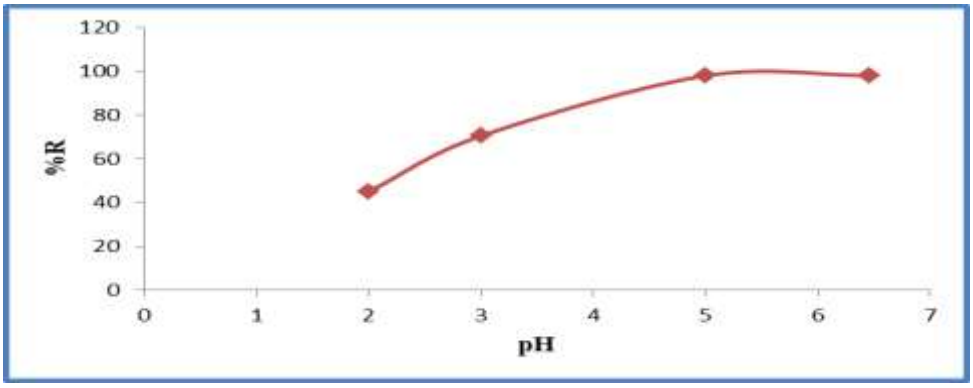

Figure 3-17: Effect of pH for adsorption percentage of pb(II) onto Ca-bentonite-chitosan composite

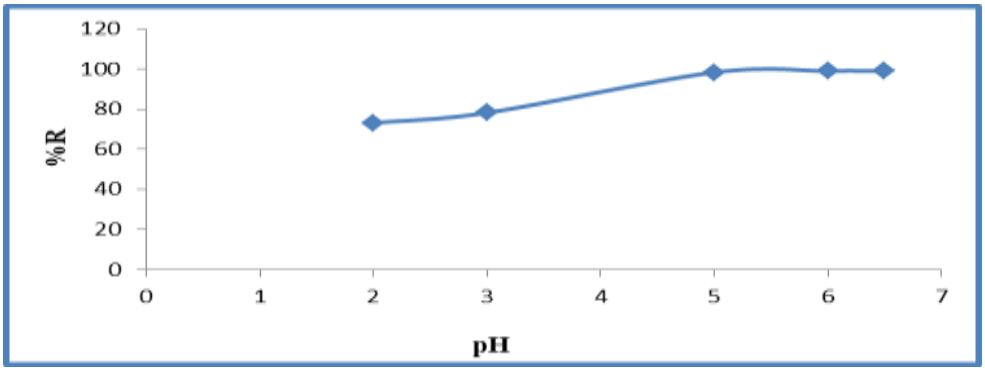

Figure 3-18: Effect of pH for adsorption percentage of Cr(III) onto Ca-bentonite clay

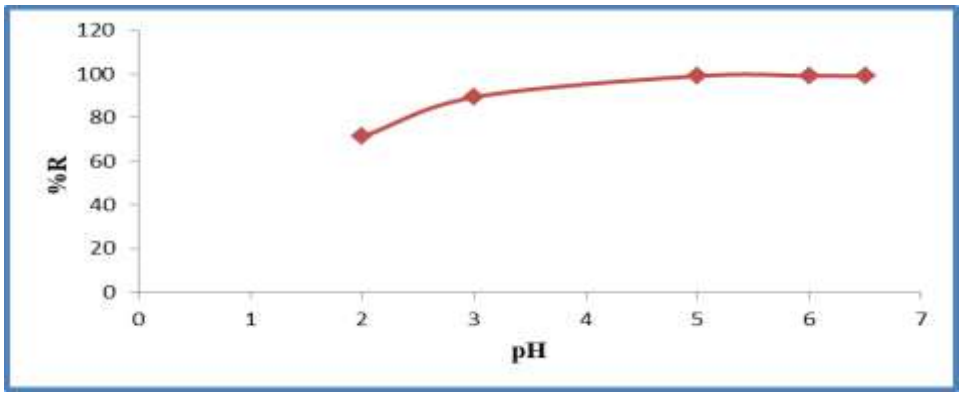

Figure 3-19: Effect of pH for adsorption percentage of Cr(III) onto Ca-bentonite-chitosan composite

3.5.4 Temperature effect

In order to understand the possible adsorption mechanism involved in the removal process, thermodynamic functions for the system, including changes in Gibbs free energy (ΔG), change in enthalpy of adsorption(ΔH) and changes in entropy of adsorption(ΔS), were calculated using the following equations[112] .Adsorption thermodynamic procedure yields great insights about bond strength magnitude, spontaneity, and randomness in the adsorption process The assessment of heat effects associated with adsorption is among the most important jobs of adsorption thermodynamics[113].

$$\mathbf{K_{eq} = \frac{q_e\, M}{C_e\, V}} \qquad \textbf{(3-1)}$$

K_{eq} = Each temperature's equilibrium constant for the adsorption process.

qe (mg/g) = amount of metal ions adsorbed at equilibrium (adsorption capacity), Ce(mg/L)= the concentration of metal ions e at quilibrium.

V = the volume of the solution (L).

M = the adsorbent mass (gm.).

$$\Delta G = -RT\ln K_{eq} \quad (3\text{-}2)$$

ΔG = Gibbs energy change (kJ/mol)

R = the ideal gas constant (8.314 J/mol. K)

T = the absolute temperature (K)

$$\ln K_{eq} = \frac{\Delta S}{R} - \frac{\Delta H}{RT} \quad (3\text{-}3)$$

$$\Delta S = \frac{\Delta H - \Delta G}{T} \quad (3\text{-}4)$$

ΔH = Enthalpy (KJ mol^{-1}) , ΔS = Entropy (J/ mol. K).

The relationship (Van't Hoff plots), $\ln K_{eq}$ vs. 1/T result in a straight line with slope = (ΔH / R-) and intercept=ΔS/R respectively, as seen in Table (3-7) and Figures 3-20, 3-21, 3-22 and 3-23.

Table (3-7): Thermodynamic functions for adsorption of pb (II) and Cr (III) ions on Ca-bentonite clay and Ca-bentonite-chitosan composite

Clays	Metals	Temp. (K)	1/T	K_{eq}	lnK_{eq}	ΔG KJ/mol	ΔH KJ/mol	ΔS J/mol.K
Ca-bentonite	Pb^{2+}	298	0.0033	7.6653	2.0367	-5.0461	20.187	84.578
		308	0.0032	9.6414	2.2660	-5.8027		
		318	0.0031	12.8063	2.5499	-6.7416		
Ca-bentonite – chitosan composite		298	0.0033	12.5221	2.5274	-6.2620	46.218	175.957
		308	0.0032	21.7169	3.0780	-7.8821		
		318	0.0031	40.5260	3.7019	-9.7873		
Ca-bentonite	Cr^{3+}	298	0.0033	13.8638	2.6292	-6.5142	16.282	76.563
		308	0.0032	17.5672	2.8660	-7.3390		
		318	0.0031	20.9495	3.0421	-8.0429		
Ca-bentonite - chitosan composite		298	0.0033	6.1505	1.8165	-4.5006	60.470	218.217
		308	0.0032	14.5759	2.6793	-6.8610		
		318	0.0031	28.5040	3.3500	-8.8570		

For natural and modified clays, the fixed concentration of Pb (II) and Cr(III) at 50 mg/L, all values the enthalpy changes in adsorption were positive, which indicates that adsorption is an endothermic process. Although not very high, these values of

$\Delta H°$can be interpreted on the basis of considerably strong interaction between metal ions and natural clay surface. This result also supports the suggestion that the adsorption capacity of adsorbent for Pb (II) and Cr(III) increase with increasing temperature[114].

The ΔH values significantly increased in the modified clay (46.218 kJ/mol for Pb(II) and 60.470 kJ/mol for Cr(III)) compared to the natural clay (20.187 kJ/mol for Pb(II) and 16.282 kJ/mol for Cr(III)), confirming enhanced endothermic adsorption efficiency due to strengthened surface interactions such as chemisorption or ion exchange.

Table 3-7 also shows that the ΔS value was positive. This occurs as a result of redistribution of energy between the adsorbate and the adsorbent. Before adsorption occurs, the heavy metal ions near the surface of the adsorbent will be more ordered than in the subsequent adsorbed state and the ratio of free heavy metal ions to ions interacting with the adsorbent will be higher than in the adsorbed state. As a result, the distribution of rotational and translational energy among a small number of molecules will increase with increasing adsorption by producing a positive value of ΔS and randomness will increase at the solid–solution interface during the process of adsorption[115].

Adsorption is thus likely to occur spontaneously at normal and high temperatures because ΔH > 0, and ΔS > 0. The Gibbs free energy is negative values indicating that the adsorption reaction is a spontaneous process and that the degree of spontaneity of the reaction increases with increasing temperature[116]. A temperature increase can activate adsorption sites on the surface of bentonite, thus increasing the number of adsorption sites while decreasing the activation energy of the reaction. These conditions are beneficial to the formation of chemical bonds and chemical adsorption[117].

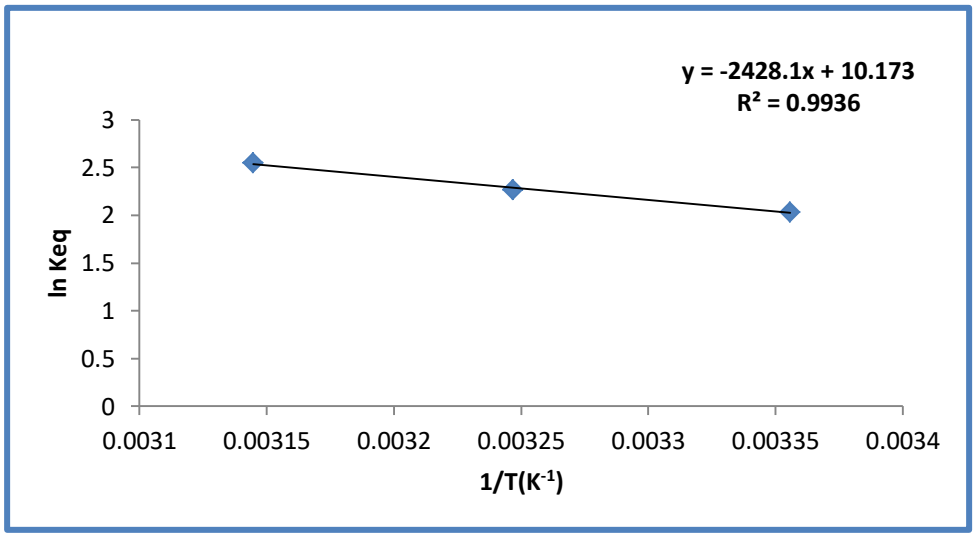

Figure 3-20: Plot ln Keq Versus 1/T of pb(II) ions on the adsorption Surface for Ca-bentonite.

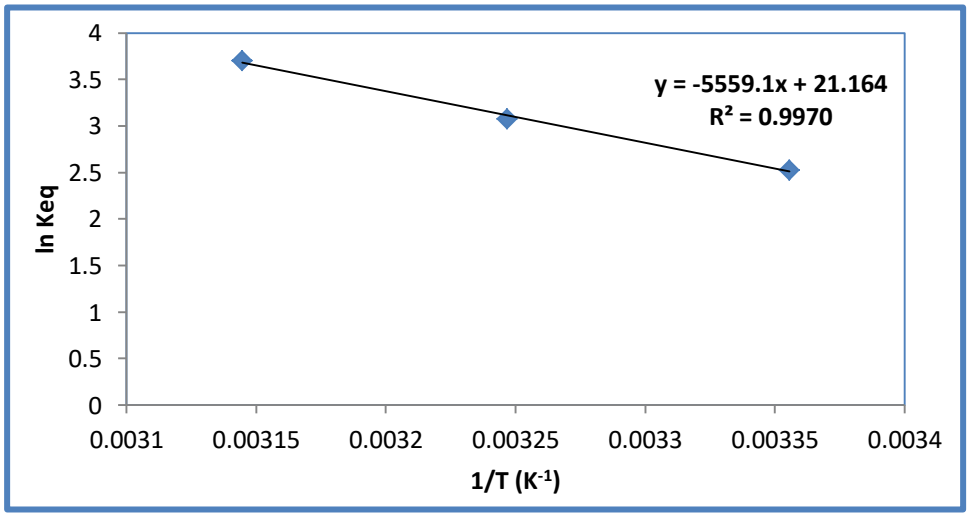

Figure 3-21: Plot ln Keq Versus 1/T of pb(II) ions on the adsorption Surface for Ca-bentonite-chitosan composite.

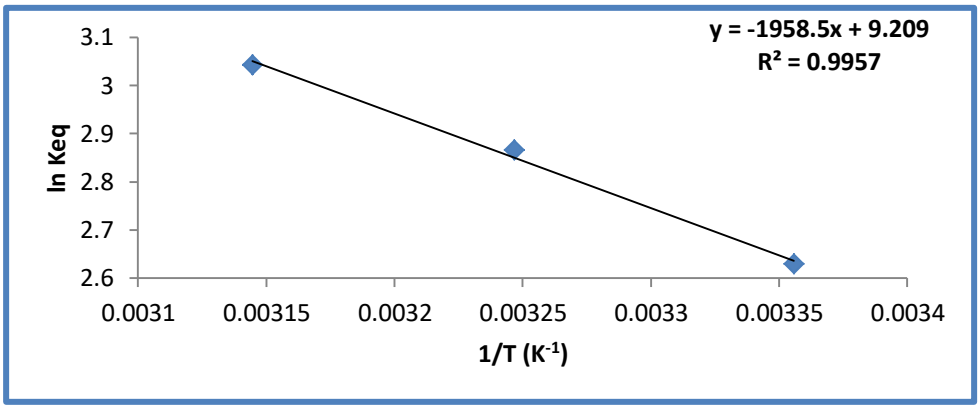

Figure 3-22: Plot ln Keq Versus 1/T of Cr (III) ions on the adsorption Surface for Ca-bentonite.

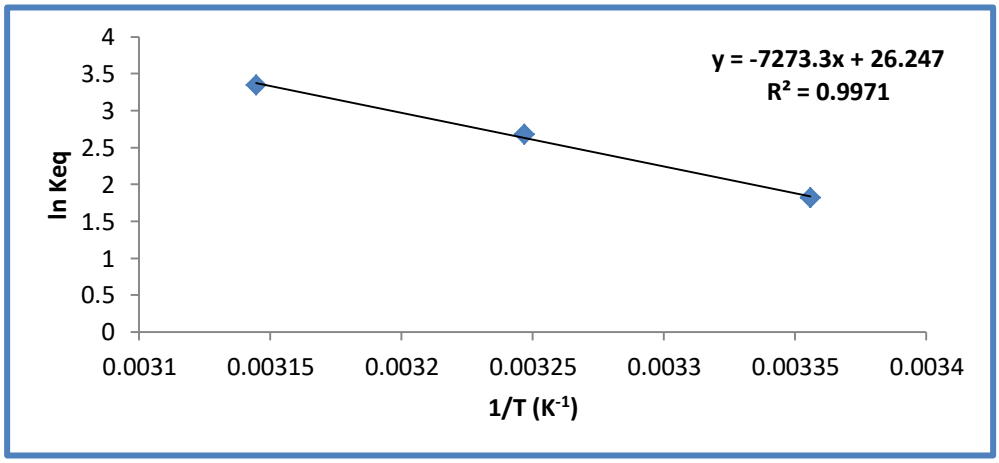

Figure 3-23: Plot ln Keq Versus 1/T of Cr(III) ions on the adsorption Surface for Ca-bentonite-chitosan composite.

3.6 Adsorption Isotherms

Equilibrium adsorption is generally defined by an isotherm equation which the surface properties and attraction of the adsorbent expressed by its parameters. The experimental results of the adsorption isotherm curves were obtained by plotting the weight of the metal adsorbed per unit weight of the adsorbent against the equilibrium concentration of the solute (metal). The adsorption isotherm experiments for pb(II) and Cr(III) ions were conducted as described in Section (2-

7). They were carried out at three temperatures: 298, 308, and 318 K. The shaking time was 50, 35 minutes for natural clay and 45, 15 minutes for modified clay. The shaking speed was 180 rpm, and the adsorbent masses for pb(II) and Cr(III) ions adsorption were (0. 1 and 0.3) g for natural clay and (0.07 and 0. 1) g for modified clay. The volume used for the adsorption isotherm experiments was 25 ml, and the range concentrations were 5- 80 mg/L.

The results are listed in Table (3-8), (3-9), (3-10) and (3-11), and Figures 3-24, 2-25, 3-26 and 3-27. The isotherms obtained from experiments were identical to S – curve in form at Gile's discretion when using the natural clay as adsorbent, indicating that the adsorbent is possibly mesoporous. This type is also represents the adsorption process when the solid has a high affinity for the solvent[118].

The isotherms identical to L – curve in form at Gile's discretion if the adsorbent was modified clay. In this type of isotherm, the initial part provides information about the availability of the active sites to the adsorbate and the plateau indicate the monolayer formation.

The initial curvature indicates that a large amount of metal ions is adsorbed at a lower concentration as more active sites of adsorbent are available. As the concentration increases, it becomes difficult for a adsorbates molecules to find unoccupied sites, and so monolayer formation occurs[119] .Adsorption data explain the performance of adsorbent and adsorption isotherms and the equilibrium distribution of a solute between adsorbent and solution, will provide the ability to estimate the adsorbent efficiency and costs. Two most common isotherm equations namely, Langmuir and Freundlich isotherms were tested in this work.

Table (3-8): Values of Ce and qe for the adsorption of pb(II) ions on natural clay at 298k, 308k, and318k.

Metal ions	Ca- Bentonite clay						
	C_0(mg/L) Pb(II)	298 k		308 k		318 k	
		Ce (mg/L) Pb(II)	q_e(mg/g)	Ce (mg/L) Pb(II)	q_e(mg/g)	Ce (mg/L) Pb(II)	q_e(mg/g)
Pb(II)	5.0000	1.3628	0.9092	1.2180	0.9454	0.8691	1.0327
	10.0000	1.3067	2.1733	1.2957	2.1760	1.1223	2.2194
	20.0000	6.7245	3.3188	3.8187	4.0453	2.9852	4.2536
	30.0000	10.5727	4.8568	9.6783	5.0804	8.5991	5.3502
	40.0000	11.1518	7.2120	9.4521	7.6369	8.7932	7.8016
	50.0000	12.5400	9.3649	11.7857	9.5535	9.0215	10.2446
	60.0000	13.2236	11.6940	12.5124	11.8718	11.5907	12.1023
	70.0000	25.8101	11.0474	17.3811	13.1547	11.7890	14.5527
	80.0000	29.4092	12.6476	25.5458	13.6135	19.6543	15.0864

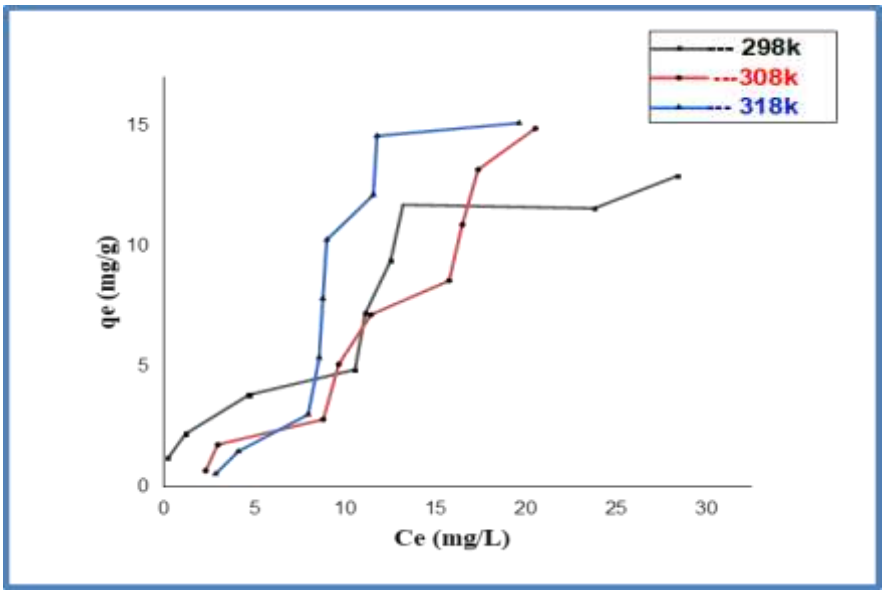

Figure 3-24: Isotherm adsorption for pb(II) ions from aqueous solution using Ca-bentonite clay.

Table (3-9): Values of Ce and qe for the adsorption of pb(II) ions on modified clay at 298k,308k,and 318k

Metal ions	Ca- Bentonite – chitosan composite						
	C_0(mg/L)	298 k		308 k		318 k	
Pb(II)		Ce (mg/L)	q_e(mg/g)	Ce(mg/L)	q_e(mg/g)	Ce (mg/L)	q_e(mg/g)
	5.0000	0.5390	1.5931	0.5080	1.6042	0.1292	1.7395
	10.0000	0.9863	3.2191	1.1061	3.1763	0.1236	3.5272
	20.0000	2.5489	6.2325	2.1940	6.3592	0.3080	7.0328
	30.0000	4.9430	8.9489	3.9050	9.3196	0.5345	10.5233
	40.0000	7.4388	11.6289	5.5098	12.3179	0.8565	13.9798
	50.0000	10.0687	14.2611	7.2083	15.2827	1.2040	17.4271
	60.0000	13.3012	16.6781	9.4840	18.0414	1.6160	20.8514
	70.0000	16.9101	18.9606	12.2278	20.6329	3.6835	23.6844
	80.0000	22.0840	20.6842	15.0685	23.1897	6.5670	26.2261

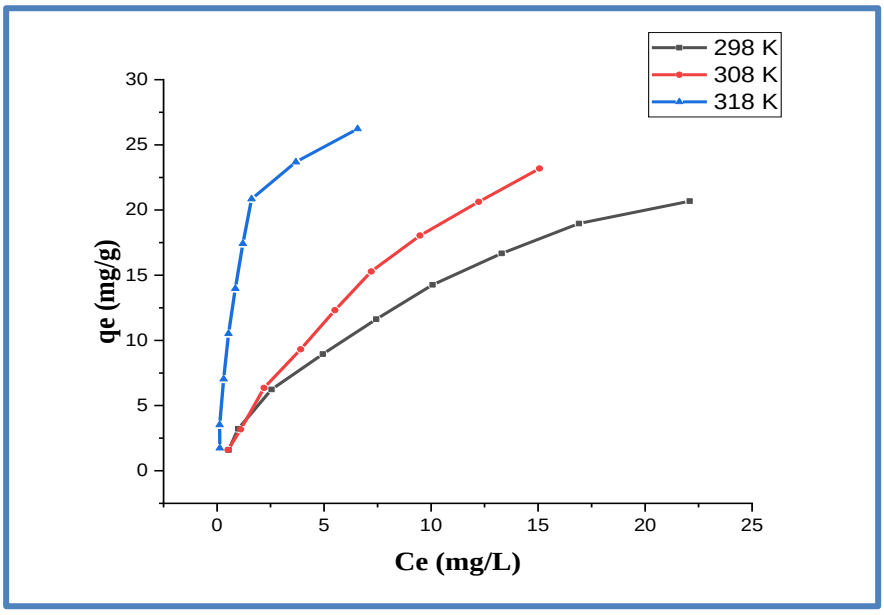

Figure 3-25: Isotherm adsorption for pb(II) ions from aqueous solution using Ca-bentonite-chitosan composite

Table (3.10): Values of Ce and qe for the adsorption of Cr(III) ions on natural clay at 298k, 308k, and318k

Metal ions	Ca- Bentonite clay						
	C_0(mg/L)	298 k		308 k		318 k	
		Ce (mg/L)	q_e(mg/g)	Ce (mg/L)	q_e(mg/g)	Ce(mg/L)	q_e(mg/g)
Cr(III)	5.0000	1.9527	0.2539	0.6921	0.3589	0.4454	0.3795
	10.0000	2.7165	0.6069	2.4566	0.6286	1.5204	0.7066
	20.0000	4.4015	1.2998	5.3779	1.2185	4.2653	1.3112
	30.0000	9.3228	1.7231	10.0630	1.6614	4.5929	2.1172
	40.0000	18.3178	1.8068	16.6142	1.9488	4.8592	2.9283
	50.0000	22.9339	2.2555	17.6929	2.6922	5.2779	3.7268
	60.0000	28.8504	2.5958	18.0157	3.4986	5.6929	4.5255
	70.0000	35.8504	2.8458	20.0079	4.1660	7.1544	5.2371
	80.0000	39.8453	3.3462	26.6929	4.4422	14.7141	5.4404

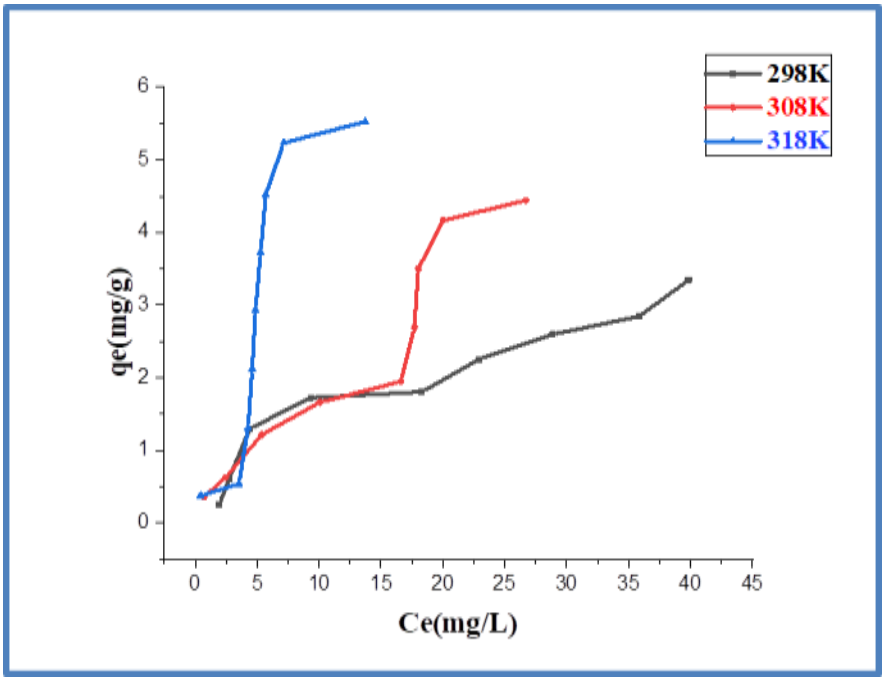

Figure 3-26: Isotherm adsorption for Cr(III) ions from aqueous solution using Ca-bentonite clay

Table (3-11): Values of Ce and qe for the adsorption of Cr(III) ions on modified clay at 298k, 308k, and318k

Metal ions	Ca- Bentonite – Chitosan composite						
	C_0(mg/L)	298 k		308 k		318 k	
Cr(III)		Ce(mg/L)	q_e(mg/g)	Ce (mg/L)	q_e(mg/g)	Ce (mg/L)	q_e(mg/g)
	5.0000	0.9157	1.0210	0.6779	1.0805	0.7454	1.0636
	10.0000	0.9921	2.2519	1.1854	2.2036	0.9204	2.2698
	20.0000	1.7155	4.5711	2.2629	4.4342	2.6753	4.3311
	30.0000	3.1141	6.7214	3.8566	6.5358	3.8929	6.5267
	40.0000	6.2204	8.4448	6.2157	8.4460	6.8792	8.2801
	50.0000	12.6705	9.3323	10.0079	9.9980	9.5779	10.1055
	60.0000	23.0155	9.2461	14.2292	11.4427	12.3929	11.9017
	70.0000	31.8504	9.5370	19.0866	12.7283	17.3544	13.1613
	80.0000	39.3779	10.1555	25.4567	13.6358	27.6141	13.0964

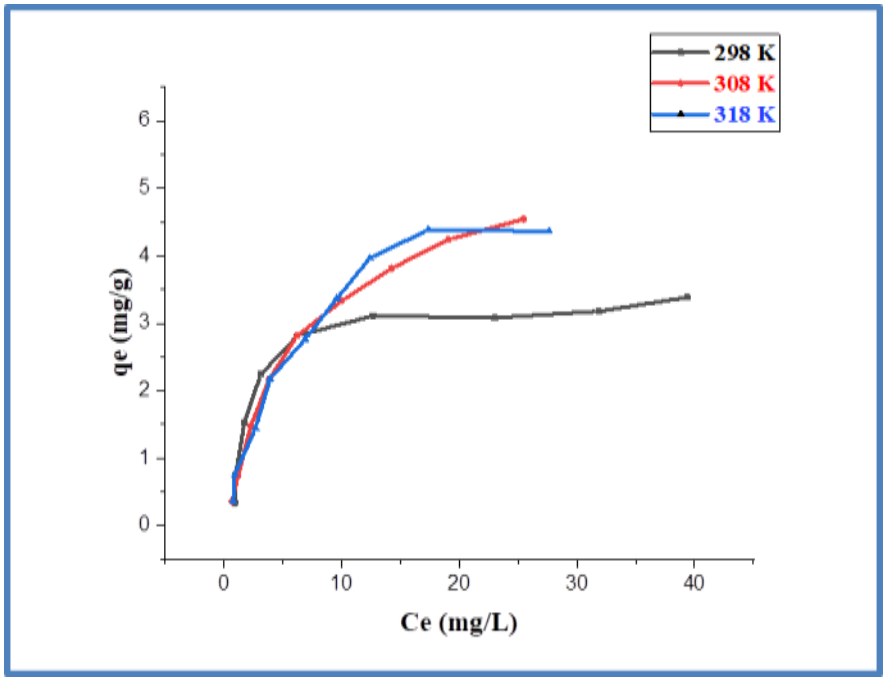

Figure 3-27: Isotherm adsorption for Cr(III) ions from aqueous solution using Ca-bentonite-chitosan composite

3.6.1 Adsorption Isotherm Models

The adsorption isotherm models are significantly important because they can help to investigate the way an adsorbate interacts with a sorbent. The most commonly used models are Langmuir (section 1.4.4.1) and Freundlich (section 1.4.4.2). These two models are presented in this study. The linearized forms (1.1) and (1.3) are used for Langmuir, Freundlich respectively.

The plots for Langmuir, Freundlich equations for adsorption of pb (II) and Cr (III) ions on Ca- bentonite and Ca- bentonite-chitosan clays are shown in Tables (3-12) , (3-13), (3-14) and (3-15) and Figures from 3-28 to 3-35 respectively. The values of K_L and qmax (Langmuir model), K_F and n (Freundlich model) for adsorption were calculated from intercept and slope of each linear plot. Table (3-18) lists values for all systems. According to the values of the correlation coefficient (R^2), seen in Table (3-18), for Pb(II) on modified clay, both the Langmuir and Freundlich models show good fit ($R^2 > 0.90$), indicating a hybrid adsorption process . In contrast, Cr(III) on modified clay exclusively follows the Langmuir model. Freundlich isotherm seems to be a better fit ($R^2 > 0.95$) for all systems on natural clay. The magnitude of the exponent (n) gives an indication of the favourability and Kf the capacity of the adsorbent/adsorbate. The values of 1/n , less than unity represent favourable adsorption and values of $1/n>1$ indicate unfavourable adsorption. The results for metal ions adsorption systems of this study are favourable[120].

Table (3-12): The calculations for pb (II) adsorption onto Ca-bentonite clay using the Langmuir and Freundlich models after applying experimental data.

Pb(II)							
Clay	**Temp.(K)**	**C_0(mg/L)**	**C_e (mg/L)**	**q_e(mg/g)**	**C_e/q_e**	**logC_e**	**logq_e**
Ca – bentonite	298	5	1.3628	0.9092	1.4988	0.1344	-0.0413
		10	1.3067	2.1733	0.6012	0.1161	0.3371
		20	6.7245	3.3188	2.0261	0.8276	0.5209
		30	10.5727	4.8568	2.1769	1.0241	0.6863
		40	11.1518	7.2120	1.5462	1.0473	0.8580
		50	12.5400	9.3649	1.3390	1.0983	0.9715
		60	13.2236	11.6940	1.1307	1.1213	1.0679
		70	25.8101	11.0474	2.3362	1.4117	1.0432
		80	29.4092	12.6476	2.3252	1.4684	1.1020
	308	5	1.2180	0.9454	1.2882	0.0856	-0.0243
		10	1.2957	2.1760	0.5954	0.1125	0.3376
		20	3.8187	4.0453	0.9440	0.5819	0.6069
		30	9.6783	5.0804	1.9050	0.9858	0.7058
		40	9.4521	7.6369	1.2376	0.9755	0.8829
		50	11.7857	9.5535	1.2336	1.0713	0.9801
		60	12.5124	11.8718	1.0539	1.0973	1.0745
		70	17.3811	13.1547	1.3212	1.2400	1.1190
		80	25.5458	13.6135	1.8765	1.4073	1.1339
	318	5	0.8691	1.0327	0.8416	-0.0608	0.01397
		10	1.1223	2.2194	0.5057	0.05013	0.34623
		20	2.9852	4.2536	0.7018	0.47498	0.62876
		30	8.5991	5.3502	1.6072	0.9344	0.72837
		40	8.7932	7.8016	1.1270	0.9441	0.89218
		50	9.0215	10.2446	0.8806	0.9552	1.0104
		60	11.5907	12.1023	0.9577	1.0641	1.0828
		70	11.7890	14.5527	0.8100	1.0714	1.1629
		80	19.6543	15.0864	1.3027	1.2934	1.1785

Table (3-13): The calculations for pb (II) adsorption onto Ca-bentonite- chitosan composite using the Langmuir and Freundlich models after applying experimental data.

		Pb(II)					
Clay	Temp.(K)	C_0(mg/L)	C_e (mg/L)	q_e(mg/g)	C_e/q_e(g/L)	logC_e	logq_e
Ca – bentonite – chitosan composite	298	5	0.539043	1.593199	0.33834	-0.26838	0.20227
		10	0.98634	3.219164	0.3063969	-0.00597	0.507743
		20	2.548945	6.23252	0.408975	0.40636	0.794664
		30	4.943038	8.948915	0.552362	0.693994	0.95177
		40	7.438819	11.62899	0.639679	0.871504	1.065542
		50	10.06878	14.26115	0.706028	1.002977	1.154155
		60	13.30127	16.67812	0.797528	1.123893	1.222147
		70	16.91013	18.96067	0.891853	1.228147	1.277854
		80	22.08401	20.68428	1.067671	1.344078	1.31564
	308	5	0.508017	1.60428	0.316664	-0.29412	0.20528
		10	1.10617	3.176368	0.34825	0.043822	0.501931
		20	2.194093	6.359253	0.345024	0.341255	0.803406
		30	3.905021	9.319635	0.41901	0.591623	0.969399
		40	5.509831	12.31792	0.447302	0.741138	1.090537
		50	7.2083101	15.28275	0.471663	0.857833	1.184201
		60	9.484	18.04143	0.525679	0.976992	1.256271
		70	12.22785	20.63291	0.592638	1.08735	1.314561
		80	15.06859	23.18979	0.649794	1.178073	1.365297
	318	5	0.129241	1.739557	0.074295	-0.8886	0.240439
		10	0.123628	3.527276	0.035049	-0.90788	0.547439
		20	0.308017	7.032851	0.043797	-0.51143	0.847131
		30	0.534599	10.52336	0.050801	-0.27197	1.022154
		40	0.85654	13.97981	0.06127	-0.06725	1.145501
		50	1.204063	17.42712	0.069091	0.080649	1.241226
		60	1.616034	20.85142	0.077502	0.20845	1.319136
		70	3.683544	23.68445	0.155526	0.566266	1.374463
		80	4.0671	27.11889	0.149973	0.609285	1.433272

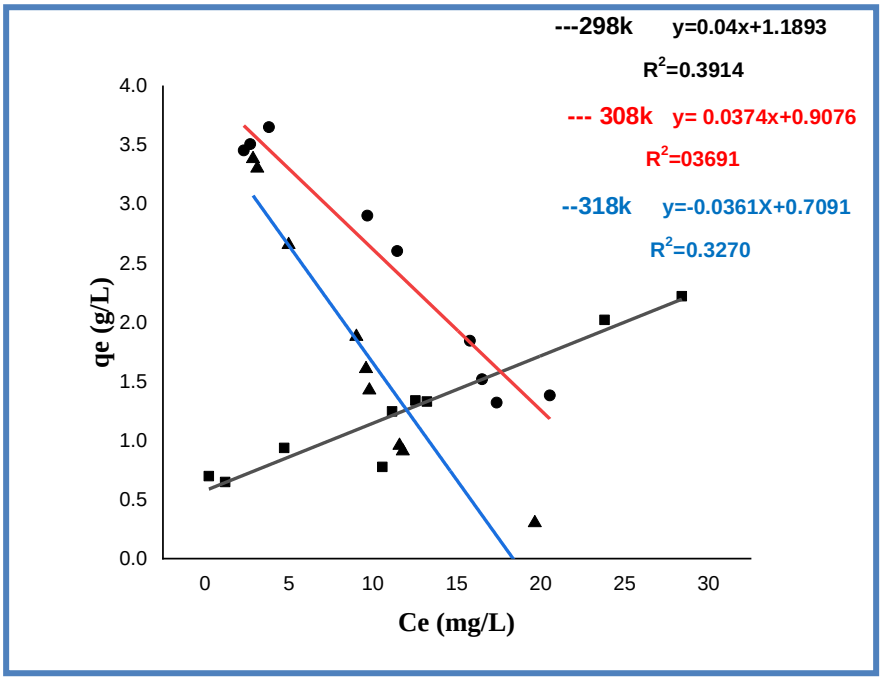

Figure 3-28: Linear forms of Langmuir isotherms for adsorption of pb (II) ions on Ca-bentonite clay

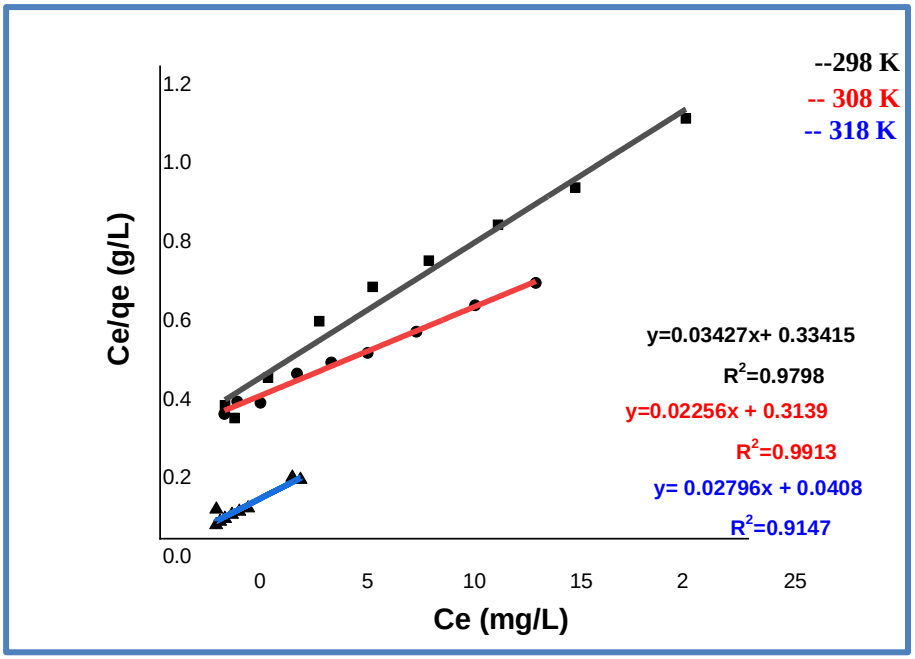

Figure 3-29: Linear forms of Langmuir isotherms for adsorption of pb (II) ions on Ca-bentonite - chitosan composite

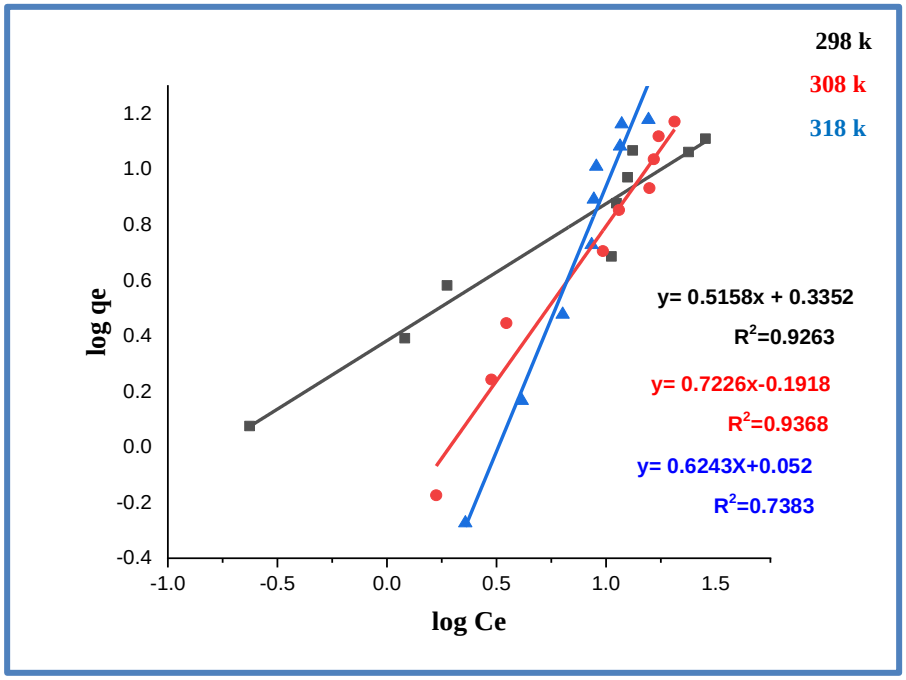

Figure 3-30: Linear forms of Freundlich isotherms for adsorption of pb (II) ions on Ca-bentonite clay

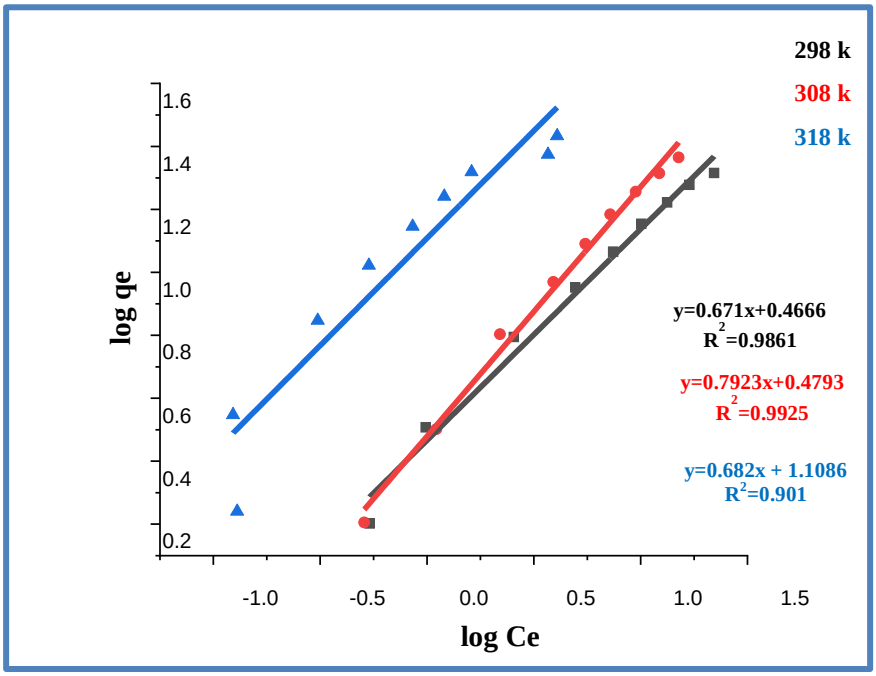

Figure 3-31: Linear forms of Freundlich isotherms for adsorption of pb (II) ions on Ca-bentonite - chitosan composite

Table (3-14) : The calculations for Cr (III) adsorption onto Ca-bentonite clay using the Langmuir and Freundlich models after applying experimental data

Cr(III)							
Clay	**Temp.(K)**	**C_0(mg/L)**	**C_e (mg/L)**	**q_e(mg/g)**	**C_e/q_e**	**logC_e**	**logq_e**
Ca – bentonite	**298**	**5**	**1.952756**	**0.253937**	**7.689922**	**0.290648**	**-0.59527**
		10	**2.716535**	**0.606955**	**4.475676**	**0.434015**	**-0.21684**
		20	**4.401575**	**1.2998689**	**3.386169**	**0.643608**	**0.1139**
		30	**9.322835**	**1.723097**	**5.41051**	**0.969548**	**0.23631**
		40	**18.31778**	**1.80685**	**10.13797**	**1.262873**	**0.256922**
		50	**22.93386**	**2.255512**	**10.16792**	**1.360477**	**0.353245**
		60	**28.85039**	**2.595801**	**11.11426**	**1.460152**	**0.414271**
		70	**35.85039**	**2.845801**	**12.59765**	**1.554494**	**0.454204**
		80	**39.8453**	**3.346225**	**11.90754**	**1.600377**	**0.524555**
	308	**5**	**0.692126**	**0.35899**	**1.927984**	**-0.15981**	**-0.44492**
		10	**2.456693**	**0.628609**	**3.908142**	**0.390351**	**-0.20162**
		20	**5.377953**	**1.218504**	**4.41357**	**0.730617**	**0.085827**
		30	**10.06299**	**1.661417**	**6.056872**	**1.002727**	**0.220479**
		40	**16.61417**	**1.948819**	**8.525253**	**1.220479**	**0.289771**
		50	**17.69291**	**2.692257**	**6.571777**	**1.247799**	**0.430117**
		60	**18.01575**	**3.498688**	**5.149287**	**1.255652**	**0.543905**
		70	**20.00787**	**4.16601**	**4.802646**	**1.301201**	**0.61972**
		80	**26.69291**	**4.442257**	**6.008863**	**1.426396**	**0.647604**
	318	**5**	**0.445433**	**0.3795**	**11.1735**	**-0.351217**	**-0.420734**
		10	**1.520472**	**0.7066**	**2.1517**	**0.546601**	**-0.150809**
		20	**4.265354**	**1.31122**	**3.252965**	**0.629955**	**0.117676**
		30	**4.592913**	**2.117257**	**2.169275**	**0.662088**	**0.325774**
		40	**4.859213**	**2.928399**	**1.659341**	**0.686566**	**0.46663**
		50	**5.277953**	**3.726837**	**1.416202**	**0.722465**	**0.57134**
		60	**5.692913**	**4.525591**	**1.257938**	**0.755335**	**0.655675**
		70	**7.154488**	**5.237126**	**1.36611**	**0.854579**	**0.719093**
		80	**14.71417**	**5.4404**	**2.7045**	**1.13717**	**0.73563**

Table (3-15): The calculations for Cr (III) adsorption onto Ca-bentonite-chitosan composite using the Langmuir and Freundlich models after applying experimental data.

Cr(III)							
Clay	**Temp.(K)**	**C_0(mg/L)**	**C_e (mg/L)**	**q_e(mg/g)**	**C_e/q_e**	**logC_e**	**logq_e**
Ca – bentonite – chitosan composite	**298**	**5**	**0.91575**	**1.0210**	**0.89686**	**-0.0382230**	**0.00905**
		10	**0.992126**	**2.2519**	**0.44055**	**-0.0034331**	**0.35256**
		20	**1.7155**	**4.5711**	**0.37529**	**0.2343907**	**0.66002**
		30	**3.114173**	**6.7214**	**0.46331**	**0.4933427**	**0.82746**
		40	**6.220472**	**8.4448**	**0.73659**	**0.793823**	**0.92659**
		50	**12.67047**	**9.3323**	**1.35768**	**1.102792**	**0.96999**
		60	**23.01557**	**9.2461**	**2.48921**	**1.3620**	**0.96595**
		70	**31.85039**	**9.5370**	**3.33952**	**1.5031**	**0.97943**
		80	**39.37795**	**10.1555**	**3.87749**	**1.5952**	**1.00670**
	308	**5**	**0.677953**	**1.08051181**	**0.62743**	**-0.16880057**	**0.033629**
		10	**1.18544**	**2.20364**	**0.537946**	**0.073879577**	**0.343140**
		20	**2.262913**	**4.43427165**	**0.510323**	**0.354667931**	**0.646822**
		30	**3.856693**	**6.53582677**	**0.590084**	**0.58621506**	**0.815300**
		40	**6.215748**	**8.44606299**	**0.735934**	**0.793493401**	**0.926654**
		50	**10.00787**	**9.99803149**	**1.000984**	**1.00034183**	**0.999914**
		60	**14.22921**	**11.4426968**	**1.243519**	**1.153180868**	**1.058528**
		70	**19.08661**	**12.7283464**	**1.499536**	**1.280728895**	**1.104771**
		80	**25.45669**	**13.6358267**	**1.866897**	**1.405801984**	**1.134681**
	318	**5**	**0.745433**	**1.06364173**	**0.700830**	**-0.127591344**	**0.026795**
		10	**0.920472**	**2.26988189**	**0.405515**	**-0.03598921**	**0.356003**
		20	**2.675354**	**4.33116141**	**0.617699**	**0.427381309**	**0.636604**
		30	**3.892913**	**6.52677165**	**0.596453**	**0.590274741**	**0.814698**
		40	**6.879213**	**8.28019685**	**0.830803**	**0.837538731**	**0.918040**
		50	**9.577953**	**10.1055118**	**0.947794**	**0.981272691**	**1.004558**
		60	**12.39291**	**11.9017716**	**1.041266**	**1.093173414**	**1.075611**
		70	**17.35449**	**13.1613779**	**1.3185920**	**1.23941181**	**1.119301**
		80	**27.61417**	**13.0964566**	**2.1085224**	**1.441132045**	**1.117153**

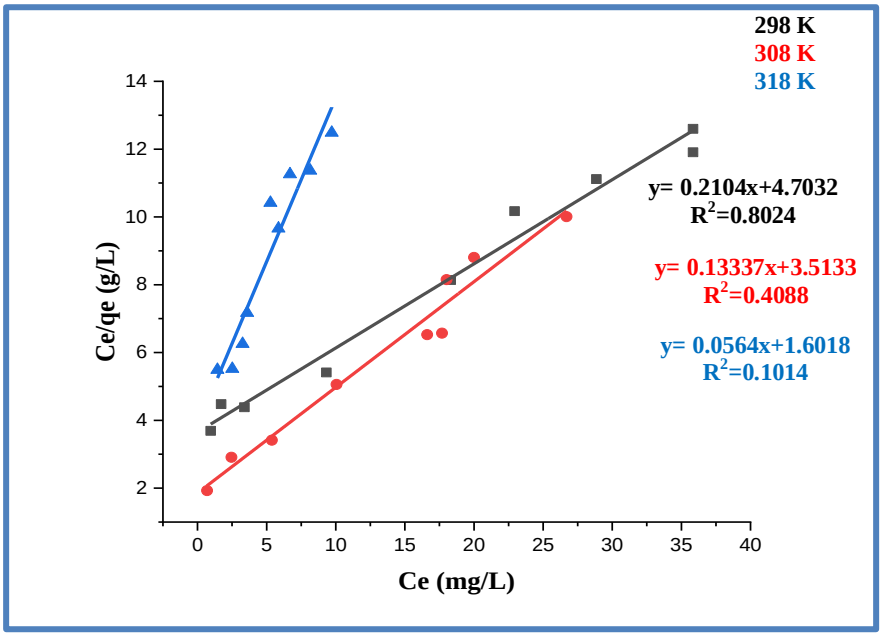

Figure 3-32: Linear forms of Langmuir isotherms for adsorption of Cr (III) ions on Ca-bentonite clay

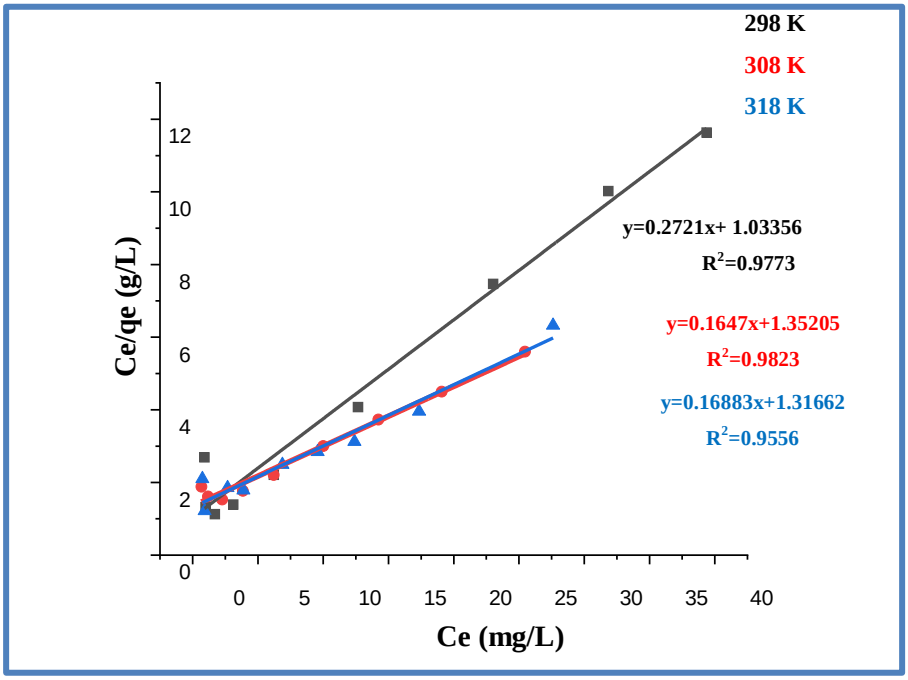

Figure 3-33: Linear forms of Langmuir isotherms for adsorption of Cr (III) ions on Ca-bentonite - chitosan composite

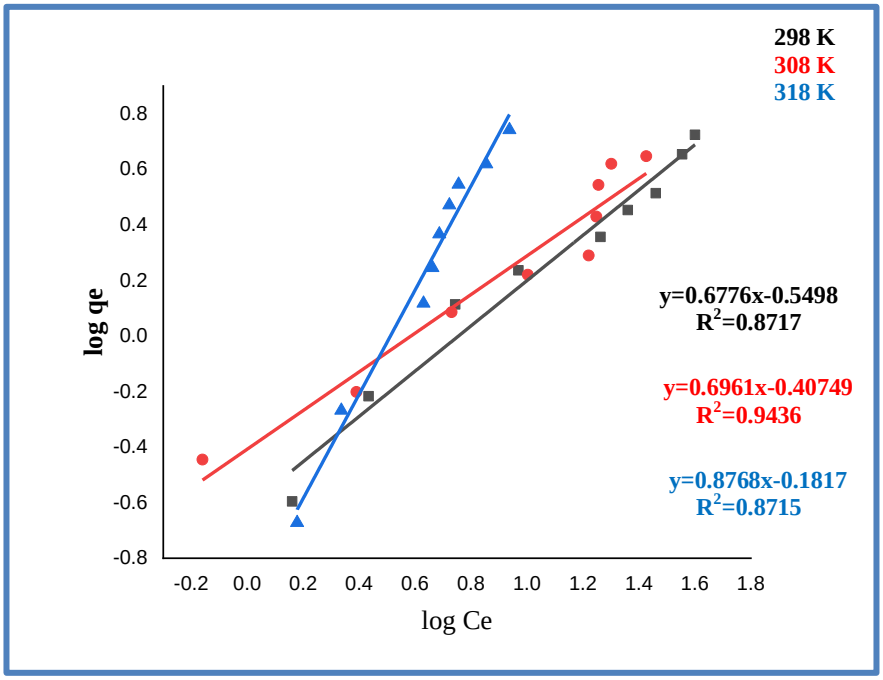

Figure 3-34: Linear forms of Freundlich isotherms for adsorption of Cr (III) ions on Ca-bentonite clay

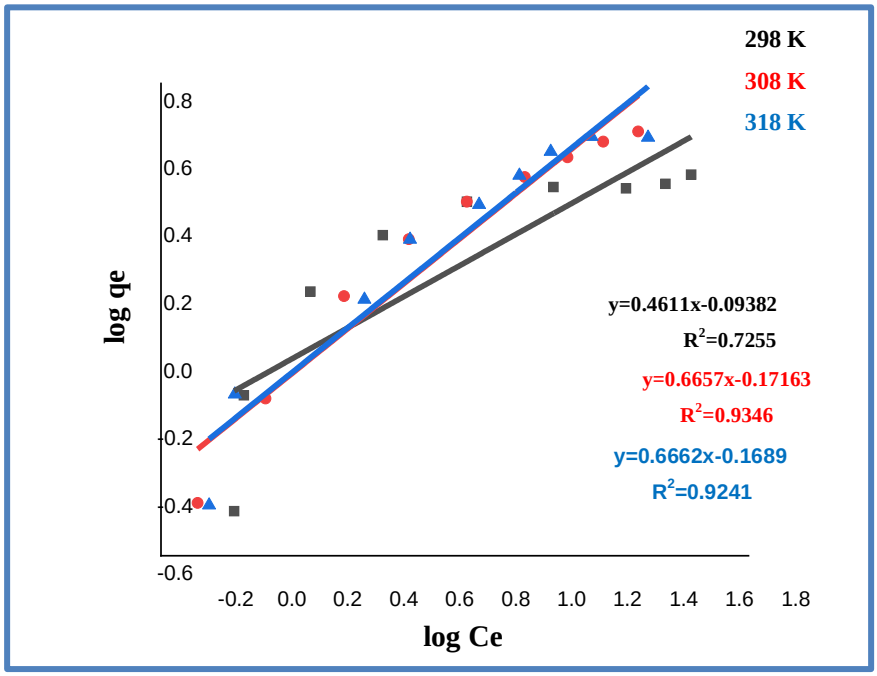

Figure 3-35: Linear forms of Freundlich isotherms for adsorption of Cr (III) ions on Ca-bentonite-chitosan composite

Table (3-16): Langmuir and Freundlich isotherms factors for adsorption of pb (II) and Cr (III) ions on Ca-bentonite and Ca-bentonite-chitosan clays

Clays				Langmauir			Freundlich		
	Metals	Temp. K	q_{max} mg/g	K_L L/mg	R_L	R^2	n	K_F L/g	R^2
Ca-bentonite	Pb(II)	298	25	0.0475	0.2959	0.3914	1.3458	1.1124	0.8658
		308	26.7379	0.0339	0.3707	0.3691	1.2588	1.2311	0.9111
		318	31.6455	0.0224	0.4716	0.3270	1.2554	1.5395	0.9209
Ca-bentonite-chitosan composite		298	29.154	0.1026	0.1630	0.9798	1.490	2.9281	0.9861
		308	44.247	0.07199	0.2173	0.9913	1.262	3.01508	0.9925
		318	35.714	0.6862	0.0283	0.9147	1.4662	12.841	0.901
Ca-bentonite	Cr^{+3}	298	4.7505	0.0447	0.3088	0.8025	1.4755	0.2819	0.8717
		308	7.4682	0.0381	0.3441	0.4088	1.4365	0.931	0.9436
		318	17.7304	0.0352	0.3622	0.1014	1.1405	0.65811	0.8715
Ca-bentonite-chitosan composite		298	11.025	0.2633	0.0706	0.9773	2.1682	2.4171	0.7255
		308	18.2149	0.1218	0.1410	0.9824	1.5019	2.0206	0.9347
		318	17.761	0.1282	0.1349	0.955	1.5010	2.033	0.9241

3.6.2 Comparison of maximum sorption capacity for Pb(II) and Cr(III) of different adsorbents

The maximum sorption capacities of various adsorbents for lead (II)and Cr(III) are listed in Table (3-17).Compared with other adsorbents, the maximum adsorption capacities of both Pb(II) and Cr(III) obtained in this study are considered reasonable. The results indicate that the modified clay is very efficient in removing lead (II) from solutions.

Table (3-17): Comparison of the maximum adsorption capacity of Pb(II) and Cr(III) ions on some natural and synthetic adsorbents from aqueous solution

Sno.	Adsorbents	Heavy metal	Maximum adsorption	Reference
1	Montmorillonite	Pb(II)	49.54	[121][2]
2	Castor plant-chitosan- Fe_3O_4	Pb(II)	48.64	[122]
3	activated bentonite	Pb(II)	22.76	[123]
4	Ca-bentonite	Pb(II)	16.4203	Present work
5	Ca-bentonite-chitosan composite	Pb(II)	44.247	Present work
6	organobentonite	Cr(III)	10.020	[124]
7	Algerian kaolinite	Cr(III)	8.422	[125]
8	modified bentonite	Cr(III)	3.72	[126]
9	Ca-bentonite	Cr(III)	7.4682	Present work
10	Ca-bentonite-chitosan composite	Cr(III)	18.2149	Present work

3.7 Conclusions

The study has concluded the following**:**

1- Characterization techniques such as Fourier-transform infrared spectroscopy (FTIR), X-ray diffraction (XRD), scanning electron microscopy (FE-SEM), and energy-dispersive X-ray spectroscopy (EDX) confirmed the successful modification of calcium bentonite with 10% (w/w) chitosan.

2- The chitosan modification enhanced the adsorption capacity of calcium bentonite for both Pb(II) and Cr(III) ions. The adsorption removal percentage of modified clay greater than that of natural clay.

3- The study identified distinct optimum adsorption conditions for Pb(II) and Cr(III) ions, which varied between the natural and modified bentonite surfaces. These conditions were influenced by factors such as contact time, adsorbent dosage, and solution pH, with pH 5 found to be ideal for both ions

4- The isotherm analysis revealed that Pb(II) adsorption onto natural bentonite fits the Freundlich model, indicating a heterogeneous surface. In contrast, the modified bentonite fits both Langmuir and Freundlich models, suggesting a more complex adsorption mechanism. For Cr(III), the adsorption on natural bentonite follows the Freundlich model, while the modified surface fits the Langmuir model, reflecting a shift toward monolayer adsorption behavior due to surface modification.

5- For Cr(III), natural bentonite follows Freundlich, whereas modified bentonite follows Langmuir, suggesting monolayer adsorption after modification.".

3.8 Recommendations

1- A study can be conducted to investigate the effect of higher chitosan loading on bentonite surface modification and adsorption efficiency.

2- Evaluate the modified clay's performance in multi-metal systems.

3- Testing the adsorbent efficiency on real industrial wastewater.

4- Incorporate nanomaterials with modified clay to enhance adsorption performance can be done.

5- Expanding the study to include other heavy metals such as cadmium or zinc.

References

References

[1] H. Xu, Y. Jia, Z. Sun, J. Su, Q. S. Liu, Q. Zhou, and G. Jiang, “Environmental pollution, a hidden culprit for health issues,” Eco-Environment & Health, vol. 1, no. 1, pp. 31-45, 2022.

[2] S. Khasanova, E. Alieva, and A. Shemilkhanova, "Environmental pollution: types, causes and consequences." p. 07014, 2023

[3] A. Siddiqua, J. N. Hahladakis, and W. A. K. Al-Attiya, “An overview of the environmental pollution and health effects associated with waste landfilling and open dumping,” Environmental Science and Pollution Research, vol. 29, no. 39, pp. 58514-58536, 2022.

[4] H. C. Josh "Environmental Pollution and Health" pp. 2, Haldwani Uttarakhand Open University, Haldwani, Nainital – 263139, 2022.

[5] R. A. Mir, A. Mantoo, Z. A. Sofi, D. Bhat, A. Bashir, and S. Bashir, "Types of Environmental Pollution and Its Effects on the Environment and Society," pp. 1-31, 2023.

[6] R. Marci, Environment impact on reproductive health: a translational approach: Springer Nature, PP.241, 2023.

[7] P. Verma, and J. K. Ratan, “Assessment of the negative effects of various inorganic water pollutants on the biosphere—an overview,” Inorganic Pollutants in Water, pp. 73-96, 2020.

[8] M. Jayasiri, S. Yadav, N. Dayawansa, C. R. Propper, V. Kumar, and G. R. Singleton, “Spatio-temporal analysis of water quality for pesticides and other agricultural pollutants in Deduru Oya river basin of Sri Lanka,” Journal of Cleaner Production, vol. 330, pp. 129897, 2022.

[9] E. R. Weiner, Applications of environmental chemistry: a practical guide for environmental professionals: CRC press, 2010.

[10] S.AL-Taai, H. Hadi "Water pollution causesd and effects" IOP conference series: Earth and Enviromental Science ,Vol.790.No.1, 2021

[11] H. Ali, E. Khan, and I. Ilahi, “Environmental chemistry and ecotoxicology of

hazardous heavy metals: environmental persistence, toxicity, and bioaccumulation," Journal of chemistry, vol. 2019, no. 1, pp. 6730305, 2019.

[12] G. Crini, and E. Lichtfouse, "Wastewater Treatment: An Overview," Green Adsorbents for Pollutant Removal: Fundamentals and Design, G. Crini and E. Lichtfouse, eds., pp. 1-21, Cham: Springer International Publishing, 2018.

[13] T. AL talhi, and A. AL rooqi, Handbook of water pollution, Newark: John Wiley and Sons 2024.

[14] G. N.-E. Abdel-Rahman, "Heavy metals, definition, sources of food contamination, incidence, impacts and remediation: A literature review with recent updates," Egyptian Journal of Chemistry, vol. 65, no. 1, pp. 419-437, 2022.

[15] J. P. Chen, Decontamination of heavy metals: processes, mechanisms, and applications: Crc Press, 2012.

[16] A. Maftouh, O. El Fatni, S. El Hajjaji, M. W. Jawish, and M. Sillanpää, "Comparative review of different adsorption techniques used in heavy metals removal in water.", 2023

[17] A. A. El-Kady, and M. A. Abdel-Wahhab, "Occurrence of trace metals in foodstuffs and their health impact," Trends in food science & technology, vol. 75, pp. 36-45, 2018.

[18] M. Shahid, S. Khalid, G. Abbas, N. Shahid, M. Nadeem, M. Sabir, M. Aslam, and C. Dumat, "Heavy metal stress and crop productivity," Crop production and global environmental issues, pp. 1-25: Springer, 2015.

[19] L. Wei, Q. Ding, H. Guo, W. Xiu, and Z. Guo, "Forms and mobility of heavy metals/metalloids in sewage-irrigated soils in the North China Plain," Journal of Soils and Sediments, vol. 21, no. 1, pp. 215-234, 2021.

[20] J. E. Gall, R. S. Boyd, and N. Rajakaruna, "Transfer of heavy metals through terrestrial food webs: a review," Environmental monitoring and assessment, vol. 187, no. 4, pp. 201, 2015.

[21] M. M. Islam, A. A. Mohana, M. A. Rahman, M. Rahman, R. Naidu, and M. M.

Rahman, “A comprehensive review of the current progress of chromium removal methods from aqueous solution,” Toxics, vol. 11, no. 3, pp. 252, 2023.

[22] Y. Hao, H. Ma, Q. Wang, C. Zhu, and A. He, “Complexation behaviour and removal of organic-Cr (III) complexes from the environment: A review,” Ecotoxicology and Environmental Safety, vol. 240, pp. 113676, 2022.

[23] T. Pavesi, and J. C. Moreira, “Mechanisms and individuality in chromium toxicity in humans,” Journal of applied toxicology, vol. 40, no. 9, pp. 1183-1197, 2020.

[24] R. Rashid, I. Shafiq, P. Akhter, M. J. Iqbal, and M. Hussain, “A state-of-the-art review on wastewater treatment techniques: the effectiveness of adsorption method,” Environmental Science and Pollution Research, vol. 28, no. 8, pp. 9050-9066, 2021.

[25] S. Faizan, S. Miyazaki, T. Saha, and A. Ali “Recent updates on the adsorption capacities of adsorbent-adsorbate pairs for heat transformation applications,” Renewable and Sustainable Energy Reviews, vol. 109630, pp. 119, 2020.

[26] W. J., and G. X., “Adsorption kinetic models: Physical meanings, applications, and solving methods,” Journal of Hazardous Materials,, vol. 390, pp. 122 - 156, 2020.

[27] O. P. Dalby, S. Abbott, N. Matubayasi, and S. Shimizu, “Cooperative sorption on heterogeneous surfaces,” Langmuir, vol. 38, no. 43, pp. 13084-13092, 2022.

[28] H. Hu, and K. Xu, "Physicochemical technologies for HRPs and risk control," High-risk pollutants in wastewater, pp. 169-207: Elsevier, 2020.

[29] N. M. Aljamali, R. Khdur, and I. O. Alfatlawi, “Physical and chemical adsorption and its applications,” International Journal of Thermodynamics and Chemical Kinetics, vol. 7, no. 2, pp. 1-8, 2021.

[30] A. Khedri, D. Jafari, and M. Esfandyari, “Adsorption of nickel (II) ions from synthetic wastewater using activated carbon prepared from Mespilus germanica leaf,” Arabian Journal for Science and Engineering, vol. 47, no. 5, pp. 6155-6166, 2022.

[31] C. T. Chiou, Partition and adsorption of organic contaminants in environmental systems: John Wiley & Sons, 2003.

[32] J. Aktar, "Batch adsorption process in water treatment," Intelligent environmental data monitoring for pollution management, pp. 1-24: Elsevier, 2021.

[33] M. Ghaedi, Adsorption: fundamental processes and applications: Academic press, 2021.

[34] N. Mistry, V. Patel, P. Parekh, P. Naik, N. S. Kumar, R. Vekariya, and M. Khimani, "Adsorbent materials," Materials from Natural Sources, pp. 20-45: CRC Press, 2024.

[35] H. M. Hamadeen, E. A. Elkhatib, and M. L. Moharem, “Optimization and mechanisms of rapid adsorptive removal of chromium (VI) from wastewater using industrial waste derived nanoparticles,” Scientific reports, vol. 12, no. 1, pp. 14174, 2022.

[36] H. A. T. Amer, “Removal of lead from industrial wastewater using a low cost waste material,” 2015.

[37] S. N. S. Jaafar, “Adsorption study-dye removal using clay,” Kuktem, 2006.

[38] M. Jain, M. Yadav, and S. Chaudhry, “Copper oxide nanoparticles for the removal of divalent nickel ions from aqueous solution,” Toxin Reviews, vol. 40, no. 4, pp. 872-885, 2021.

[39] H. Kuhn, D. H. Waldeck, and H.-D. Försterling, Principles of physical chemistry: John Wiley & Sons, 2024.

[40] S. A. Obaid, "Langmuir, Freundlich and Tamkin adsorption isotherms and kinetics for the removal aartichoke tournefortii straw from agricultural waste." p. 012011, 2020

[41] S. Azizian, and S. Eris, "Adsorption isotherms and kinetics," Interface science and technology, pp. 445-509: Elsevier, 2021.

[42] C. Buttersack, “General cluster sorption isotherm,” Microporous and Mesoporous Materials, vol. 316, pp. 110909, 2021.

[43] R. R. Prasath, P. Muthirulan, and N. Kannan, “Agricultural wastes as a low cost adsorbents for the removal of Acid Blue 92 dye: A comparative study with commercial

activated carbon," IOSR Journal of Agriculture and Veterinary Science, vol. 7, no. 2, pp. 19-32, 2014.

[44] S. Shimizu, and N. Matubayasi, "Understanding sorption mechanisms directly from isotherms," Langmuir, vol. 39, no. 17, pp. 6113-6125, 2023.

[45] M. Musah, J. Yisa, M. T. Suleiman, M. Abdullahi, and E. Y. Shaba, "Study of isotherm models for the adsorption of cr (vi) ion from aqueous solution onto Bombax buonopozense calyx activated carbon," 2018.

[46] H. A. Qasim, Enhancing the adsorption capacity of Iraqi clay for removal dyes effluent using nano-materials, Iraq: M.Sc. thesis, the College of Science University of Baghdad, 2020.

[47] S. A. Khit, A Green Synthesis of Copper Oxide Nanoparticles And Study Their Effects On Water Pollutants Removal And Blood Hemolysis Karbala: university of Karbala, 2022.

[48] H. Majiya, F. Clegg, and C. Sammon, "Bentonite-Chitosan composites or beads for lead (Pb) adsorption: Design, preparation, and characterisation," Applied Clay Science, vol. 246, pp. 107180, 2023.

[49] S. M. Malih, Treatment of industry wastewater by adsorption using some Iraqi clays, Diyala: M.S.C.Thesis,College of Science, University of Diyala, 2021.

[50] N. Kumari, and C. Mohan, "Basics of clay minerals and their characteristic properties," Clay Clay Miner, vol. 24, no. 1, pp. 1-29, 2021.

[51] F. Bergaya, and G. Lagaly, Handbook of clay science: Newnes, 2013.

[52] Z. Yaneva, B. Koumanova, and V. Meshko, "Dynamic studies of nitrophenols adsorption on perfil in a fixed-bed column: Application of single and two resistance model," Water Science and Technology, vol. 62, no. 4, pp. 883-891, 2010.

[53] A. A. Abdulabbas, "Clay basics and their physical and chemical properties: Review Paper," Innovative Infrastructure, 2022.

[54] H. H. Murray, "Structure and composition of the clay minerals and their physical and chemical properties," Developments in clay science, vol. 2, pp. 7-31,

2006.

[55] S. Barakan, and V. Aghazadeh, “Separation and Characterization of Montmorillonite from a Low-grade Natural Bentonite: Using a Non-destructive Methods,” Micro & Nano Letters, vol. 14, 05/29, 2019.

[56] T. Ravindra Reddy, S. Kaneko, T. Endo, and S. Lakshmi Reddy, “Spectroscopic characterization of bentonite,” J. Lasers Opt. Photonics, vol. 4, no. 3, 2017.

[57] P. P. Mishra, P. Das, S. Paul, P. Das, S. Manna, P. Basak, N. Das, and A. K. Behera, “Graphene oxide dots-loaded chitin flask: A sustainable adsorbent for separating multiple dyes from water,” Environmental Quality Management, vol. 34, no. 1, pp. e22249, 2024.

[58] A. A. Bazghaleh, M. A. Dogolsar, and J. Barzin, “Preparation and characterization of oxidized pectin/N-succinyl chitosan/graphene oxide hydrogels,” Cellulose, vol. 30, no. 4, pp. 2165-2179, 2023.

[59] M. Rinaudo, "Characterization and properties of some polysaccharides used as biomaterials." pp. 549-557, 2006

[60] V. Ghormade, E. Pathan, and M. Deshpande, “Can fungi compete with marine sources for chitosan production?” International journal of biological macromolecules, vol. 104, pp. 1415-1421, 2017.

[61] M. B. Kaczmarek, K. Struszczyk-Swita, X. Li, M. Szczęsna-Antczak, and M. Daroch, “Enzymatic modifications of chitin, chitosan, and chitooligosaccharides,” Frontiers in bioengineering and biotechnology, vol. 7, pp. 243, 2019.

[62] G. Kayan, and A. Kayan, “Composite of Natural Polymers and Their Adsorbent Properties on the Dyes and Heavy Metal Ions,” Journal of Polymers and the Environment, vol. 29, pp. 1-20, 04/24, 2021.

[63] I. A. Sogias, V. V. Khutoryanskiy, and A. C. Williams, “Exploring the factors affecting the solubility of chitosan in water,” Macromolecular Chemistry and Physics, vol. 211, no. 4, pp. 426-433, 2010.

[64] I. Aranaz, A. R. Alcántara, M. C. Civera, C. Arias, B. Elorza, A. Heras

Caballero, and N. Acosta, “Chitosan: An overview of its properties and applications,” Polymers, vol. 13, no. 19, pp. 3256, 2021.

[65] C. Coquery, C. Negrell, N. Caussé, N. Pébère, and G. David, “Synthesis of new high molecular weight phosphorylated chitosans for improving corrosion protection,” Pure and Applied Chemistry, vol. 91, no. 3, pp. 509-521, 2019.

[66] P. Zou, X. Yang, J. Wang, Y. Li, H. Yu, Y. Zhang, and G. Liu, “Advances in characterisation and biological activities of chitosan and chitosan oligosaccharides,” Food chemistry, vol. 190, pp. 1174-1181, 2016.

[67] J. C. Lindon, G. E. Tranter, and D. Koppenaal, Encyclopedia of spectroscopy and spectrometry: Academic Press, 2016.

[68] D. Sahin, "Atomic spectroscopy," Modern Spectroscopic Techniques and Applications: IntechOpen, 2019.

[69] D. Sahin, "Atomic Spectroscopy," 2019.

[70] R. García, and A. Báez, “Atomic absorption spectrometry (AAS),” Atomic absorption spectroscopy, vol. 1, pp. 1-13, 2012.

[71] A. T. Van Loon, Analytical atomic absorption spectroscopy: selected methods: Elsevier, 2012.

[72] D. Visser, “Atomic absorption spectroscopy, principles and applications,” pp.356829 , 2021.

[73] O. R. Thorat, S. D. Raut, N. R. Kale, and A. Sukhdev, “A Review Of Atomic Absorption Spectroscopy And Method.” Pp.141-152, 2024

[74] S. Chanda, S. Das, B. Paul, P. Singh, and S. Giri, “Mineral Assay in Atomic Absorption Spectroscopy,” The Beats of Natural Sciences, vol. 1, pp. 1-17, 12/01, 2014.

[75] I. Skoog, and D. Gustafson, “Update on hypertension and Alzheimer's disease,” Neurological research, vol. 28, no. 6, pp. 605-611, 2006.

[76] M. S. Kumar, C. A. Kumar, N. P. Pravin, N. Swarnalatha, and A. Nida, “Atomic Absorption Spectroscopy: A Short Review,” Journal For Innovative Development in

Pharmaceutical and Technical Science (JIDPTS), vol. 7, no. 6, 2024.

[77] Q. M. Salih, "Developing an analytical method using atomic absorption spectroscopy to estimate some heavy metals in medicines nutritional supplements and blood," International Journal of Advanced Chemistry Research, vol. 6, no. 1, 2024.

[78] V.-P. Dinh, P.-T. Nguyen, M.-C. Tran, A.-T. Luu, N. Q. Hung, T.-T. Luu, H. T. Kiet, X.-T. Mai, T.-B. Luong, and T.-L. Nguyen, "HTDMA-modified bentonite clay for effective removal of Pb (II) from aqueous solution," Chemosphere, vol. 286, pp. 131766, 2022.

[79] O. Idoko, M. O. Ajana, J. S. Gushit, and A. Jock, "Adsorption of heavy metals (lead ion) from industrial waste water using acidified bentonite CLAY," Int. J. Eng. Appl. Sci. Technol, vol. 4, pp. 394-401, 2019.

[80] M. I. Eleraky, T. M. Razek, I. W. Hasani, and Y. A. Fahim, "Adsorptive removal of lead, copper, and nickel using natural and activated Egyptian calcium bentonite clay," Scientific Reports, vol. 15, no. 1, pp. 13050, 2025.

[81] R. Et-tanteny, B. El Amrani, and M. Benhamou, "Investigation and modeling of physicochemical properties of bentonite-chitosan composites versus the concentration of chitosan added by intercalation," Chemical Physics Impact, vol. 8, pp. 100611, 2024.

[82] E. Radha, T. Gomathi, P. Sudha, S. Latha, A. A. Ghfar, and N. Hossain, "Adsorption studies on removal of Pb (II) and Cd (II) ions using chitosan derived copoymeric blend," Biomass Conversion and Biorefinery, vol. 15, no. 2, pp. 1847-1862, 2025.

[83] J. D. Castro-Castro, N. R. Sanabria-González, and G. I. Giraldo-Gómez, "Experimental data of adsorption of Cr (III) from aqueous solution using a bentonite: optimization by response surface methodology," Data in brief, vol. 28, pp. 105022, 2020.

[84] B. Abbou, I. Lebkiri, and H. Ouaddari, "Evaluation of Illitic-Kaolinite clay as an adsorbent for Cr3+ removal from synthetic aqueous solutions: Isotherm, kinetic, and

thermodynamic analyses," Chemical Physics Impact, vol. 8, pp. 100527, 2024.

[85] F. Zahaf, R. Marouf, and F. Ouadjenia, "Kinetic and thermodynamic studies of the adsorption of Pb(II), Cr(III) and Cu(II) onto modified bentonite," Desalination And Water Treatment, vol. 131, pp. 282-290, 11/01, 2018.

[86] E. Majigsuren, U. Byambasuren, M. Bat-Amgalan, E. Mendsaikhan, N. Kano, H. J. Kim, and G. Yunden, "Adsorption of chromium (III) and chromium (VI) ions from aqueous solution using Chitosan–clay composite materials," Polymers, vol. 16, no. 10, pp. 1399, 2024.

[87] M. Bat-Amgalan, Z. Khashbaatar, D. E. V. Anak, M. N. M. Sari, N. Miyamoto, N. Kano, H.-J. Kim, and G. Yunden, "Adsorption of Cr (III) from an aqueous solution by chitosan beads modified with sodium dodecyl sulfate (SDS)," Journal of Environmental Protection, vol. 12, no. 11, pp. 939-960, 2021.

[88] General Company for Geological Survey and Mining (GSMGC), Baghdad, Iraq "Bentonite Clay Sample Analysis,", https://geosurviraqi.industry.gov.iq/ 2024.

[89] S. Bensalem, B. Hamdi, S. Del Confetto, and R. Calvet, "Characterization of surface properties of chitosan/bentonite composites beads by inverse gas chromatography," International Journal of Biological Macromolecules, vol. 166, pp. 1448-1459, 2021.

[90] M. Scimeca, S. Bischetti, H. K. Lamsira, R. Bonfiglio, and E. Bonanno, "Energy Dispersive X-ray (EDX) microanalysis: A powerful tool in biomedical research and diagnosis," European journal of histochemistry: EJH, vol. 62, no. 1, pp. 2841, 2018.

[91] S. A. Khit, E. T. Kareem, and I. M. Shaheed, "Eco-friendly synthesized of CuO nanoparticles using Anchusa strigosa L. flowers and study its adsorption activity," Baghdad Science Journal, vol. 20, no. 4, pp. 21, 2023.

[92] S. Sharma, and D. G. Sarasan, "Influence of acid activation on natural calcium montmorillonite clay," IOSR J. Appl. Chem, vol. 10, no. 06, pp. 71-77, 2017.

[93] N. A. Raheem, and N. S. Majeed, "Statistical Analysis of Phenol Removal

Using Modified Iraqi Bentonite from Wastewater by Adsorption Process." p. 012006.

[94] K. Bahranowski, A. Klimek, A. Gaweł, Z. Olejniczak, and E. M. Serwicka, "Rehydration driven acid impregnation of thermally pretreated ca-bentonite—evolution of the clay structure," Materials, vol. 15, no. 6, pp. 2067, 2022.

[95] R. F. Melo-Silveira, G. P. Fidelis, M. S. S. P. Costa, C. B. S. Telles, N. Dantas-Santos, S. de Oliveira Elias, V. B. Ribeiro, A. L. Barth, A. J. Macedo, and E. L. Leite, "In vitro antioxidant, anticoagulant and antimicrobial activity and in inhibition of cancer cell proliferation by xylan extracted from corn cobs," International Journal of Molecular Sciences, vol. 13, no. 1, pp. 409-426, 2011.

[96] M. T. Isa, A. Y. Abdulkarim, A. Bello, T. K. Bello, and Y. Adamu, "Synthesis and characterization of chitosan for medical applications: A review," Journal of Biomaterials Applications, vol. 38, no. 10, pp. 1036-1057, 2024.

[97] M. Queiroz, K. Melo, D. Sabry, G. Sassaki, and H. Rocha, "Does the Use of Chitosan Contribute to Oxalate Kidney Stone Formation?," Marine Drugs, vol. 13, pp. 141-158, 12/29, 2014.

[98] T. Yu, C. Qu, D. Fan, and R. Xu, "Effects of bentonite activation methods on chitosan loading capacity," Bulletin of Chemical Reaction Engineering & Catalysis, vol. 13, no. 1, pp. 14-23, 2018.

[99] S. Biswas, T. U. Rashid, T. Debnath, P. Haque, and M. M. Rahman, "Application of chitosan-clay biocomposite beads for removal of heavy metal and dye from industrial effluent," Journal of Composites science, vol. 4, no. 1, pp. 16, 2020.

[100] N. Kahya, B. Sen, D. Berber, and N. Oztekin, "Comparison of dye adsorption of chitosan and polyethylenimine modified bentonite clays: optimization, isotherm, and kinetic studies," ACS omega, vol. 9, no. 8, pp. 9040-9052, 2024.

[101] X. Guo, Z. Wu, Z. Lu, Z. Wang, S. Li, F. Madhau, T. Guo, and R. Huo, "Preparation and characterization of chitosan-modified bentonite hydrogels and application for tetracycline adsorption from aqueous solution," Gels, vol. 10, no. 8, pp. 503, 2024.

[102] N. Sebeia, M. Jabli, and A. Ghith, "Biological synthesis of copper nanoparticles, using Nerium oleander leaves extract: characterization and study of their interaction with organic dyes," Inorganic Chemistry Communications, vol. 105, pp. 36-46, 2019.

[103] B. Varghese, M. Kurian, S. Krishna, and T. Athira, "Biochemical synthesis of copper nanoparticles using Zingiber officinalis and Curcuma longa: Characterization and antibacterial activity study," Materials Today: Proceedings, vol. 25, pp. 302-306, 2020.

[104] A. Abdelnaby, N. M. Abdelaleem, E. Elshewy, A. H. Mansour, and S. S. Ibrahim, "Application of bentonite clay, date pit, and chitosan nanoparticles as promising adsorbents to sequester toxic lead and cadmium from milk," Biological Trace Element Research, vol. 201, no. 5, pp. 2650-2664, 2023.

[105] R. Et-tanteny, B. El Amrani, and M. Benhamou, "Investigation and modeling of physicochemical properties of bentonite-chitosan composites versus the concentration of chitosan added by intercalation," Chemical Physics Impact, vol. 8, pp. 100611, 2024.

[106] A. S. Ibrahim, and M. A. Al-Bidry, "Study the effect of particle sizes and concentration on the rheological properties of Iraqi bentonite for using as drilling fluids," Journal of Engineering, vol. 26, no. 3, pp. 65-76, 2020.

[107] J. S. Al-Jariri, and F. Khalili, "Adsorption of Zn (II), Pb (II), Cr (III) and Mn (II) from water by Jordanian bentonite," Desalination and Water Treatment, vol. 21, no. 1-3, pp. 308-322, 2010.

[108] S. M. Malih, "Treatment of industry wastewater by adsorption using some Iraqi clays," College of Science, Diyala University of Diyala 2021.

[109] Y. Shi, S. Zhong, X. Wang, and C. Feng, "A review of the removal of heavy metal ions in wastewater by modified montmorillonite," Water Policy, vol. 24, no. 10, pp. 1590-1609, 2022.

[110] I. Hamadneh, R. Abu-Zurayk, B. Abu-Irmaileh, A. Bozeya, and A. Al-Dujaili, "Adsorption of Pb (II) on raw and organically modified Jordanian bentonite," Clay

Minerals, vol. 50, no. 4, pp. 485-496, 2015.

[111] A. K. Meena, K. Kadirvelu, G. Mishra, C. Rajagopal, and P. Nagar, "Adsorptive removal of heavy metals from aqueous solution by treated sawdust (Acacia arabica)," Journal of hazardous materials, vol. 150, no. 3, pp. 604-611, 2008.

[112] Z. Melichová, and L. Hromada, "Adsorption of Pb^{2+} and Cu^{2+} Ions from Aqueous Solutions on Natural Bentonite," Polish Journal of Environmental Studies, vol. 22, no. 2, 2013.

[113] Y. S. Chang, P. I. Au, N. M. Mubarak, M. Khalid, P. Jagadish, R. Walvekar, and E. C. Abdullah, "Adsorption of Cu (II) and Ni (II) ions from wastewater onto bentonite and bentonite/GO composite," Environmental Science and Pollution Research, vol. 27, no. 26, pp. 33270-33296, 2020.

[114] S. T. Hussain, and S. A. K. Ali, "Removal of heavy metal by ion exchange using bentonite clay," Journal of Ecological Engineering, vol. 22, no. 1, pp. 104-111, 2021.

[115] M. L. De Castro, M. Abad, D. Sumalinog, R. M. Abarca, P. Paoprasert, and M. D. G. de Luna, "Adsorption of methylene blue dye and Cu (II) ions on EDTA-modified bentonite: isotherm, kinetic and thermodynamic studies," Sustainable Environment Research, vol. 28, no. 5, pp. 197-205, 2018.

[116] R. Gopinathan, A. Bhowal, and C. Garlapati, "Thermodynamic study of some basic dyes adsorption from aqueous solutions on activated carbon and new correlations," The Journal of Chemical Thermodynamics, vol. 107, pp. 182-188, 2017.

[117] J. Hefne, W. Mekhemer, N. Alandis, O. Aldayel, and T. Alajyan, "Kinetic and thermodynamic study of the adsorption of Pb (II) from aqueous solution to the natural and treated bentonite," International journal of physical sciences, vol. 3, no. 11, pp. 281-288, 2008.

[118] P. Saha, and S. Chowdhury, "Insight into adsorption thermodynamics," Thermodynamics, vol. 16, pp. 349-364, 2011.

[119] I. El-Naggar, S. A. Ahmed, N. Shehata, E. Sheneshen, M. Fathy, and A. Shehata, "A novel approach for the removal of lead (II) ion from wastewater using

Kaolinite/Smectite natural composite adsorbent," Applied water science, vol. 9, no. 1, pp. 7, 2019.

[120] X. L. Gang Lia, Jinli Zhangb,*, Jia Liuc, Yiran Yang, "Investigation of the adsorption characteristics of Pb(II) onto natural kaolinite and bentonite clays," Desalination and Water Treatment, pp. 121–136 2022.

[121] J. S. Piccin, T. R. S. A. Cadaval Jr, L. A. A. De Pinto, and G. L. Dotto, "Adsorption isotherms in liquid phase: experimental, modeling, and interpretations," Adsorption processes for water treatment and purification, pp. 19-51: Springer, 2017.

[122] H. a. qasim, "Enhancing the adsorption capacity of iraq clay for removal dyes effluent using nano-materials ", College of Science Baghdad University of Baghdad 2020.

[123] M. Vigdorowitsch, A. Pchelintsev, L. Tsygankova, and E. Tanygina, "Freundlich isotherm: An adsorption model complete framework," Applied Sciences, vol. 11, no. 17, pp. 8078, 2021.

[124] Z. Han, Y. Zhang, S. Zheng, J. Chen, Y. Zhang, and X. Yue, "Pb2+ Removal from Aqueous Solutions Using Montmorillonite and Magnetite-Modified Nanostructures," Water, Air, & Soil Pollution, vol. 236, no. 7, pp. 1-16, 2025.

[125] H. M. Meena, S. Kukreti, P. S. Jassal, and A. K. Kalra, "Novel green magnetite-chitosan adsorbent using Ricinus communis plants to adsorption of lead (II) from wastewater solution: anodic linear sweep voltammetry, isotherms, and kinetics study," Environmental Science and Pollution Research, vol. 32, no. 10, pp. 6198-6220, 2025.

[126] M. Belhadri, A. Mokhtar, S. Meziani, F. Belkhadem, M. Sassi, and A. Bengueddach, "Novel low-cost adsorbent based on economically modified bentonite for lead (II) removal from aqueous solutions," Arabian Journal of Geosciences, vol. 12, no. 3, pp. 88, 2019.

الخلاصـــــــــة

بحثت هذه الدراسة في استخدام الطين العراقي Ca-bentonite والطين المعدل (Ca-bentonite-chitosan) كأسطح ماص رخيص وصديق للبيئة لإزالة أيونات الرصاص (II) والكروم (III) من المحاليل المائية. تمت دراسة تأثير كمية الطين ودرجة الحرارة وزمن التوازن ودرجة حموضة المحلول على امتزاز أيونات الرصاص (II) والكروم (III) على طين Ca-bentonite و Ca-bentonite-chitosan من محاليلها المائية في نظام أحادي باستخدام طريقة الدفعات.

أظهرت النتائج أن كفاءة الإزالة والقدرة القصوى لامتصاص أيونات الرصاص (II) والكروم (III) على الطين المعدل أعلى من الطين الطبيعي. كانت أوقات التلامس 50 و 45 دقيقة لامتزاز أيون الرصاص (II) على الطين الطبيعي والمعدل على التوالي، ولكن عند امتزاز Cr (III)، كانت أوقات التلامس 35 و 15 دقيقة. كانت الجرعات المثلى للطين الطبيعي والمعدل 0.1 و 0.07 جم لامتصاص أيون الرصاص (II)، ولكن عند امتزاز أيون الكروم (III)، كانت الجرعات المثلى 0.3 و 0.1 جم للطين الطبيعي والمعدل على التوالي.

كان للرقم الهيدروجيني تأثير كبير على امتزاز أيونات الرصاص (II) والكروم (III) في كلا النظامين، حيث حدث أفضل امتزاز للأيونين عند الرقم الهيدروجيني = 5. تم تحقيق النتائج التجريبية لامتزاز أيونات الرصاص (II) والكروم (III) على الطين الطبيعي والمعدل باستخدام متساوي الحرارة فروندليش ولانكمويز عند ثلاث درجات حرارة (298 و 308 و 318) كلفن. وقد كانت نتائج عملية امتزاز الايونين متفقة مع نموذج متساوي الحرارة فرويندليش على الطين الطبيعي. اما عند تطبيق نموذجي متساوي الحرارة على الطين المعدل ، فقد وجد ان ايون الرصاص (II) يتفق مع نموذج لانكمويز وفرروندليش ، ولكن أيون الكروم (III) على الطين المعدل، يتناسب مع نموذج متساوي الحرارة لانجمويز فقط.

حُسبت الدوال الديناميكية الحرارية (GΔ، ΔH، وΔ S) من معادلات فانت هوف لامتصاص أيونات الرصاص (II) والكروم (III) على الطين الطبيعي والمُعدَّل. كانت قيم (GΔ) لامتصاص كلا الأيونين على سطحين سالبة، مما يُشير إلى عملية امتزاز تلقائية. كانت قيم المحتوى الحراري (ΔH) لامتصاص أيونات الرصاص (II) والكروم (III) على الطين الطبيعي والمُعدَّل موجبة، مما يُشير إلى عملية امتزاز ماصة للحرارة. كانت قيم الإنتروبيا (SΔ) لامتصاص أيونات الرصاص (II) والكروم (III) على سطحين موجبة، مما يُشير إلى زيادة العشوائية.لحرارة أثناء العملية.

جامعة كربلاء

كلية العلوم

قسم الكيمياء

تحضيرمواد حيوية – طين كمادة مازة فعالة لبعض الايونات المعدنية السامة من المحاليل المائية

رسالة

مقدمة الى مجلس كلية العلوم – جامعة كربلاء كجزء من متطلبات نيل درجة الماجستيرفي علوم الكيمياء

من قبل

رحاب حاتم بريج الشمري

بكالوريوس علوم كيمياء (جامعة ذي قار)

(2004)

باشراف

أ.م.د. احسان مهدي شهيد **أ.د. ايمان طالب كريم**

2025 م **1447 هـ**